INFORMATION TO USERS

This manuscript has been reproduced from the microfilm master. UMI films the text directly from the original or copy submitted. Thus, some thesis and dissertation copies are in typewriter face, while others may be from any type of computer printer.

The quality of this reproduction is dependent upon the quality of the copy submitted. Broken or indistinct print, colored or poor quality illustrations and photographs, print bleedthrough, substandard margins, and improper alignment can adversely affect reproduction.

In the unlikely event that the author did not send UMI a complete manuscript and there are missing pages, these will be noted. Also, if unauthorized copyright material had to be removed, a note will indicate the deletion.

Oversize materials (e.g., maps, drawings, charts) are reproduced by sectioning the original, beginning at the upper left-hand corner and continuing from left to right in equal sections with small overlaps. Each original is also photographed in one exposure and is included in reduced form at the back of the book.

Photographs included in the original manuscript have been reproduced xerographically in this copy. Higher quality 6" x 9" black and white photographic prints are available for any photographs or illustrations appearing in this copy for an additional charge. Contact UMI directly to order.

UMI

A Bell & Howell Information Company
300 North Zeeb Road, Ann Arbor MI 48106-1346 USA
313/761-4700 800/521-0600

.

A

DETERMINATION OF PACLITAXEL AND RELATED TAXANES IN BULK DRUG AND INJECTABLE DOSAGE FORMS BY REVERSED PHASE LIQUID CHROMATOGRAPHY AND MICELLAR ELECTROKINETIC CAPILLARY CHROMATOGRAPHY

by

LILLIAN KUANGJING SHAO

A dissertation submitted to the Graduate Faculty in Chemistry

in partial fulfillment of the requirements for the degree of

Doctor of Philosophy, The City University of New York

1998

This manuscript has been read and accepted by the Graduate Faculty in Chemistry in satisfaction of the dissertation requirement for the degree of Doctor of Philosophy.

12 January 98 — Date
David C. Locke — David C. Locke Chair of Examining Committee

Jan. 13, 1998 — Date
Richard Pizer — Richard Pizer Executive Officer

William F. Berkowitz — William F. Berkowitz Supervisory Committee

David Gosser — David Gosser Supervisory Committee

THE CITY UNIVERSITY OF NEW YORK

Abstract

Determination of Paclitaxel and Related Taxanes in Bulk Drug and Injectable Dosage Forms by Reversed Phase Liquid Chromatography and Micellar Electrokinetic Capillary Chromatography

by

Lillian Kuangjing Shao

Advisor: Professor David C. Locke

Baseline resolution of 15 taxanes including paclitaxel is achieved on pentafluorophenyl HPLC columns. The methods developed are suitable for the determination of potency, content uniformity, and degradation profile of the paclitaxel bulk drug and injectable dosage form. Good resolution of taxanes from the excipient Cremophor EL (polyethoxylated castor oil) is achieved. The methods for the bulk drug and injectable form, were fully and partially validated respectively, according to USP guideline. The elution order of taxanes is related to molecular size, the number of acetylated hydroxyl groups, and the substitution of a xylosyl group at the 7-position. Thermodynamics of the separation were studied, and enthalpies of transfer, $\Delta H°$, determined. Conversion of a hydroxyl

group to an acetyl group has a large effect on the $\Delta H°$, as does the addition of a xylosyl derivative to the 7-hydroxy.

Micellar electrokinetic capillary chromatographic technique is applied to the separation of 15 taxanes in 11.5 minutes. An aqueous acetonitrile buffer with SDS surfactant allows resolution of the 15 taxanes from each other and from the principal matrix ingredient, Cremophor EL, in the injectable dosage form. The migration order is apparently that of decreasing aqueous phase solubility, which is related to the presence of a side chain at the carbon-13 position; to the addition of a xylosyl group at the 7-position; to the number of acetylated hydroxyl groups; and to the increasing affinity of the taxane side chain for the micellar phase. The retention factor, k', increases linearly with SDS concentration above the CMC. With increasing concentration of ACN, k' values for taxanes without a side chain decrease; for the most hydrophobic taxanes, k' increases up to 20 % (v/v) ACN and then decreases rapidly at higher concentrations. Similar behavior was observed with methanol but the break in k' occurred between 30% and 40% (v/v). Resolution was unacceptably poor if samples dissolved in methanol were injected; samples dissolved in buffer containing SDS were well-behaved, probably because of stacking of the micelles during injection. The $\Delta H°$ of transfer of taxanes from aqueous phase to micelle phase were determined.

Dedicated to

My beloved son Jonathan D. Shao

ACKNOWLEDGMENTS

I would like to express my deepest appreciation to my research advisor, Professor David C. Locke, for his encouragement, intellectual inspiration, constant support and never failing guidance throughout this research and my entire graduate study at the City University of New York. Working with him has been a pleasure and a rewarding educational experience. I thank him from the bottom of my heart.

My thanks also go to : my thesis committee members, Professor William F. Berkowitz and Professor David Gosser for their careful reading, valuable advice and encouragement of this research.

I am very grateful to Drs. Tom Warden and Brian Starbuck, of Hauser Chemical Research Inc., for their generous donation of the paclitaxel bulk drug, various taxanes and mixtures; Elaine Heilweil, of Whatman Incorporated, for the gift of the Whatman TAC-1 Columns and Guard Cartridge kit; Bristol-Myers Squibb Corporation for a gift of Taxol ® for injection concentrate and Taxol ®

bulk drug; the National Cancer Institute, Drug Synthesis & Chemistry Branch, for a gift of a Six- Taxane Standard kit # 9501635-X; BASF Corporation for a gift of Cremophor EL; Ellis Gitlin and Wilhard Reuter, of Perkin-Elmer Corporation for the loan of an Applied Biosystems 270A-HT Capillary Electrophoresis System, and the Hewlett-Packard Company for the gift of a Hewlett-Packard 1090 HPLC under the University Grants Program.

Many thanks to Robert Wurman and Claude Y. Masse at Stock Room of Chemistry Department of Queens College for providing chemicals and supplies in an efficient manner. Special thanks are due to Dr. Siril Wijesundara for assistance in SAS computer program.

I acknowledge my father for his continued encouragement, insight and immutable support during these years.

Last, but not least, thank God for leading me through the course of this endeavor.

In memory of my mother

TABLE OF CONTENTS

Part I. Determination of Paclitaxel and Related Taxanes in Bulk Drug and Injectable Dosage Forms by Reversed Phase Liquid Chromatography

Chapter One. Background		**Page**
1.1	Efficacy of Paclitaxel	3
1.2	Clinical Development of Paclitaxel and its Production	5
1.3	Mechanism of Action	8
1.4	Structure-Activity Relationship of Paclitaxel	9
1.5	Analytical Methods for Paclitaxel and its Related Taxanes	19
1.6	Basics of HPLC	23
Chapter Two. Experimental		
2.1	Chemicals	26
2.2	HPLC	27
2.3	Assay of Taxanes in Paclitaxel Bulk Drug	28
2.3.1	HPLC Method A	30
2.3.2	HPLC Method B	31
2.3.3	Analysis of Sample Weight/Weight %	32

2.3.4	Analysis of Purity Profile of Paclitaxel Bulk Drug	34
2.4	Assay of Taxanes in Paclitaxel Injectable Dosage Form	37
2.4.1	HPLC Method C	38
2.4.2	HPLC Method D	39
2.4.3	Potency Analysis of Paclitaxel Injectable Dosage Form	40
2.4.4	Analysis of Related Compounds in Paclitaxel Injectable Dosage Form	42
2.5	Determination of Unretained Volume V_0	44
2.6	Analysis of Metal Contents in Cremophor EL by Ultrasonic Nebulization Inductively Coupled Plasma-Atomic Emission Spectrometry (ICP-AES)	45
2.6.1	Instrumentation	45
2.6.2	Method	46

Chapter Three. Results and Discussion

3.1	HPLC Conditions	50
3.2	Thermodynamics of the Separation	68
3.3	Separation of Taxanes From Excipient in Injectable Form	76
3.4	Purity Profile of Paclitaxel Bulk Drug	83
3.5	Method Validation	85

3.5.1	Accuracy	87
3.5.2	Method Precision	91
3.5.3	Specificity	94
3.5.4	Chromatographic Precision and Reproducibility	112
3.5.5	Stability in Diluent	116
3.5.6	Limits of Detection and Quantitation	120
3.5.7	Linearity and Range	121
3.5.8	Ruggedness	124
3.5.9	Robustness	125
3.6	Metal Contents in Cremophor EL	128
3.7	Determination of Molar Absorptivity of Various Taxanes by HPLC	130
3.8	Conclusions	135

Appendix I

SAS Computer Program to Analyze Retention Time, Capacity Factor, Resolution and Selectivity by Analysis of Variance (ANOVA) 138

Part II. Separation of Paclitaxel and Related Taxanes by Micellar Electrokinetic Capillary Chromatography

Chapter One. Introduction		**Page**
1.1	The Significance of the Use of Capillary Electrophoresis Techniques for Resolving Various Taxanes	143
1.2	Introduction to Capillary Electrophoresis	144
1.3	Basic Theory of Capillary Electrophoresis	149
1.3.1	Electrical Double Layer and Zeta Potential	149
1.3.2	Electrophoretic Mobility	150
1.3.3	Electroosmosis	151
1.3.4	Micellar Electrokinetic Capillary Chromatography (MECC)	157
1.4	Background of Separation of Paclitaxel and Related Taxanes by Capillary Electrophoresis and the Objective of this Research	160

Chapter Two. Experimental		
2.1.	Instrument	163
2.2.	Chemicals and Materials	165
2.3.	Procedure and Solutions	167

Chapter Three. Results and Discussion

3.1.	MECC Separation of the 13-Taxane Mixture	170
3.1.1	Migration Order of Taxanes in MECC	171
3.1.2	Effect of SDS Concentration	175
3.1.3	Effect of Organic Additive	179
3.1.4	Effect of Other Buffer Constituents	209
3.1.5	Effect of the Capillary Dimension	212
3.1.6	Effect of Sample matrix	219
3.1.7	Effect of Temperature	225
3.1.8	Limit of Detection	231
3.2	MECC Separation of Paclitaxel From Excipient in Injectable Form	234
3.3	Conclusions	243

References

Part I	245-251
Part II	252-256

LIST OF FIGURES

Part I **Page**

Figure 1. Structures of Taxanes Studied 10-17

Figure 2. Structure - Activity Relationships of Taxanes 18

Figure 3. Chromatogram of 15-Taxane Standard Mixture on Curosil PFP Column 51-52

Figure 4. Chromatogram of 13-Taxane Standard Mixture on TAC-1 Column 53

Figure 5. Chromatograms Showing the Effect of Gradient Rate 59-60

Figure 6. Variation of ln k' with Percent ACN - Curosil PFP Column 66

Figure 7. Effect of ACN on Elution Order of Taxane - TAC-1 Column 67

Figure 8. van't Hoff Plot for Curosil PFP Column 71

Figure 9. van't Hoff Plot for Whatman TAC-1 Column 72

Figure 10. UV Spectra of Paclitaxel and Cremophor EL 79

Figure 11. Chromatograms of the 13-Taxane Standard Mixture, Paclitaxel Injectable Form and Cremophor EL on Curosil PFP Column 80-81

Figure 12. Chromatograms of Paclitaxel/Cremophor EL Mixture and Cremophor EL on TAC-1 Column 82

Figure 13. Effect of Degradation by NaOH 97

Figure 14. Effect of Degradation by HCl 98

Figure 15. Effect of Degradation by UV Light 99

Figure 16. Effect of Degradation by Visible Light 100

Figure 17. Effect of Degradation by H_2O_2 101

Figure 18. Effect of Degradation by Heat 102-104

Figure 19. Paclitaxel Peak Purity Under Forced Degradation by UV Light 106

Figure 20. Paclitaxel Peak Purity Under Forced Degradation by Visible Light 107

Figure 21. Paclitaxel Peak Purity Under Forced Degradation by HCl 108

Figure 22. Paclitaxel Peak Purity Under Forced Degradation by H_2O_2 109

Figure 23. Paclitaxel Peak Purity Under Forced Degradation by Heat 110-111

Figure 24. Paclitaxel Bulk Drug Stability in Diluent - Method A 117

Figure 25. Paclitaxel Bulk Drug Stability in Diluent - Method B 118

Figure 26. Paclitaxel Injectable Form Stability in Diluent - Method C 119

Figure 27. Linearity of Method A 122

Figure 28. Linearity of Method B 123

Part II. **Page**

Figure 1.1	Schematic Diagram of a Capillary Electrophoresis Apparatus	148
Figure 1.2	Schematic Diagram of Electroosmotic Flow	152
Figure 1.3	Comparison of the Flow Profile of (a) CE and (b) HPLC	154
Figure 1.4	Illustration of Mobility Vectors of Cations (+), Neutral Species (◆), and Anions (–) Under the Influence of Electroosmotic Flow	156
Figure 1.5	Schematic Diagram of the Separation Mechanism of Micellar Electrokinetic Capillary Chromatography	158
Figure 3.1.1	Electropherogram of 13 Taxanes mixture	172
Figure 3.1.2	Effect of SDS Concentrations on Separation of Taxanes	176-177
Figure 3.1.3	Effect of Acetonitrile on Separation of Taxanes	186-187
Figure 3.1.4	Effect of Methanol on Separation of Taxanes	188-189
Figure 3.1.5	Effect of Acetonitrile on the Apparent Mobility of Taxanes	193-194
Figure 3.1.6	Effect of Acetonitrile on the Effective Mobility of Taxanes	196-197
Figure 3.1.7	Effect of Acetonitrile on SDS Micelle Mobility	199
Figure 3.1.8	Electropherograms of Sudan III	203-204

Figure 3.1.9	Effect of Acetonitrile on Current	208
Figure 3.1.10	Effect of Buffer Concentration	210-211
Figure 3.1.11	Ohm's Law Plots for 50 μm i.d. Capillaries	215
Figure 3.1.12	Ohm's Law Plots for 75 μm i.d. Capillaries	216
Figure 3.1.13	Effect of Capillary Internal Diameter on Joule Heating	218
Figure 3.1.14	Effect of Sample Matrix	221-222
Figure 3.1.15	Plate Height vs. Field Strength for Baccatin III at 30 °C	223
Figure 3.1.16	Plate Height vs. Field Strength for Baccatin III at 60 °C	224
Figure 3.1.17	van't Hoff Plot for Eight Taxanes	228
Figure 3.2.1	Electropherograms of Injectable Paclitaxel (top) and Cremophor EL (bottom)	236-237
Figure 3.2.2	Effect of SDS Concentration on the Separation of Paclitaxel Injectable Form	239-240
Figure 3.2.3	Effect of SDS Concentration on the Excipient Cremophor EL	241-242

LIST OF TABLES

Part I **Page**

Table 1. HPLC Injection Sequence 35

Table 2. Selected Spectral Lines from an Argon ICP 47

Table 3. Effect of Starting Composition of Acetonitrile on Resolution 54

Table 4. Analysis of Variance Table - Effect of Starting Composition 56-57

Table 5. Analysis of Variance Table - Effect of Gradient Rate 61-62

Table 6. Enthalpy and Entropy Change for Taxanes 75

Table 7. Purity Profile of Paclitaxel Bulk Drug 84

Table 8. Accuracy of Method A 89

Table 9. Accuracy of Method B 90

Table 10. Method Precision 93

Table 11. Specificity of the Method by Forced Degradation 96

Table 12. Chromatographic Precision and Repeatability of Method A 113

Table 13. Chromatographic Precision and Repeatability of Method B 114

Table 14. Chromatographic Precision and Repeatability of Method C 115

Table 15. Robustness of Method A - Resolution 126

Table 16. Robustness of Method A - Peak Symmetry 127

Table 17. Metal Contents in Cremophor EL 129

Table 18. Molar Absorptivity of Taxanes 134

Part II

Table 3.1 Effect of Acetonitrile on Migration Time and k' 202

Table 3.2 Thermodynamic Quantities from the van't Hoff Plot 230

Part I

Determination of Paclitaxel and Related Taxanes in Bulk Drug and Injectable Dosage Forms by Reversed Phase Liquid Chromatography

Chapter One

Background

1.1 Efficacy of Paclitaxel

Paclitaxel, the generic name of Taxol (5ß, 20-epoxy-1,2 α, 4,7ß, 10ß, 13α - hexahydroxytax - 11 - en - 9 - one - 4, 10 - diacetate - 2 - benzoate - 13 ester with (2R, 3S) - N - benzoyl - 3 - phenylisoserine) is a potent naturally occurring anti-neoplastic agent that was first extracted from the stem bark of the Pacific yew tree, *Taxus brevifolia* [1]. This natural product has proven to be useful in the treatment of a variety of cancers including chemotherapy-resistant ovarian cancer, advanced breast cancer, small cell and non-small cell lung cancer, advanced squamous cell carcinoma of the head and neck, malignant melanoma, urothelial cancer, oesophageal cancer, non-Hodgkins lymphoma and multiple myeloma [2-12].

Paclitaxel's antitumor activity was discovered in the 1960s during a large-scale plant-screening program sponsored by the National Cancer Institute (NCI). In 1971, paclitaxel was reported to be moderately active against murine L1210, P388, and P1534 leukemias, Walker 256 carcinosarcoma, sarcoma 180, and Lewis lung carcinoma, and cytotoxic in the

KB cell culture system [1], but was not selected for clinical development by the National Cancer Institute until 1979, when scientists found that paclitaxel has a unique mechanism for preventing the growth of the cancer cells. In 1983, the NCI began conducting clinical trials of paxlitaxel's safety and its effectiveness against various types of cancer. In December 1992, the FDA approved the use of paclitaxel for the treatment of refractory ovarian cancer. In April 1994, the FDA approved the use of the paclitaxel for metastatic breast cancer that is not responding to combination chemotherapy.

1.2 Clinical Development of Paclitaxel and its Production

The cytotoxicity of *Taxus* plants has been known for a long time and was attributed to taxine, a complex mixture, which was first isolated from leaves in 1856. The interest in paclitaxel itself dates from 1962, when crude extracts of bark from *Taxus brevifolia* were tested in a collaborative plant screening program of the United States Department of Agriculture (USDA) and the National Cancer Institute (NCI). Taxol was later identified in 1971 [1] as the active cytotoxic constituent of the bark extracts. However, its clinical development was made at a pretty slow pace largely because of:

1) The restriction on bark collection because the Pacific yew is a limited resource located in old-growth forests that are the habitat of the endangered spotted owl.

2) The extraction of paclitaxel is complex and expensive. The low yield (0.01 %) of paclitaxel in the dried bark of *Taxus brevifolia* [13] , and the very slow growth (10-50 years/inch diameter of the stem bark) of the Pacific yew tree hampers the reliable supply for large scale clinical use. It is estimated that about

three yew trees are required to produce one gram of paclitaxel, which is sufficient to treat only one patient.

3) Problems in formulating the paclitaxel, which lacks aqueous solubility.

4) Severe hypersensitivity reactions attributed to the solubilizer, Cremophor EL, used in the formulation in phase I clinical trials [14].

Because of insufficient aqueous solubility, intensive efforts were devoted to the development of vehicles for parenteral administration of paclitaxel. The formulation of paclitaxel for injection developed by NCI, which is used currently in the clinic, consists of paclitaxel solubilized at a concentration of 6 mg/mL in a 1:1 (vol:vol) mixture of anhydrous ethanol and polyethoxylated castor oil (Cremophor EL) [15].

On account of its novel mechanism of action (discussed below) and potency in treating a variety of classes of cancers, paclitaxel was destined to be the most important new anticancer drug of the 1990s. Various alternative routes of taxol production have been actively explored. At present, several of the paclitaxel sources are:

1) Partial synthesis of paclitaxel and its analogs from baccatin III or 10-deacetylbaccatin III. This precursor is accessible from the renewable needles of *Taxus baccata* and other yews [16-17].

2) Culturing of plant cell tissues to produce taxol [18-20]. The biosynthetic pathway of taxanes needs to be fully understood in this approach, and the question remains whether the cost will be competitive with semisynthesis.

3) Fungal production, by the fungus *Taxomyces andreanae* [21].

4) Total synthesis of taxol has been completed by both the Nicolaou and Holton groups [22-24]. However, these syntheses appear too long to have commercial value [25-28].

5) Recently it was found that clippings (needles and small stems) of certain cultivars of ornamental *Taxus* contain a higher amount of taxol than does the bark and needles from the Pacific yew [29]. Since the ornamental plants are fast growing, plantations of cultivars of *Taxus* might serve as a sustainable, economic and reliable source for taxol.

1.3 Mechanism of Action

Much research has been conducted on the mechanism of action of paclitaxel. Horwitz and coworkers at the Albert Einstein College of Medicine, New York, first discovered that taxol stabilizes the fiber-like cell structures called microtubules, which play an important role in cell division and other important cell functions. Normally, at the onset of the cell division, a large number of microtubules are formed, as cell division comes to an end, these microtubules are broken down. However, paclitaxel stabilizes microtubules and prevents them from breaking down, thus cancer cells, which attempt to divide frequently, become so clogged with microtubules that they stop growing and dividing. Taxol is the only substance known to cease mitosis of cancer cells by this unique mechanism [30]. Now it is commonly believed that paclitaxel's anti-tumor activities are mainly associated with its ability to promote the assembly of microtubules from tubulin dimers and to stabilize microtubules, resulting in inhibition of tumor cell mitosis, ciliary and flagellar motility and intracellular transport [31-34].

1.4 Structure-Activity Relationships of Paclitaxel

Extensive chemical characterization of paclitaxel and related taxanes has been conducted [35-36]. The structures of the 15 available taxanes of this study are given in Figure 1. A broad summary of the structure-activity relationships to date is shown in the Figure 2, and can be stated as follows:

1) Side chain: The presence of the C-13 side chain N-benzoyl-β-phenylisoserine is an absolute requirement for activity[1,35]. Minor changes in the side chain will effect the activity.

2) Positions 7, 8, 9 and 10: Varying the structure in these positions across the top of the molecule do not affect the activity and even fairly large substituents are permissible [15].

3) Positions 2, 4 and 5: Removal of either the 2-benzoate or the 4-acetate causes dramatic loss of activity. These positions appear necessary for interaction with the binding site; the oxetane ring at 4, 5 is a crucial component of the structure of paclitaxel. Opening of the oxetane ring destroys cytotoxicity [35].

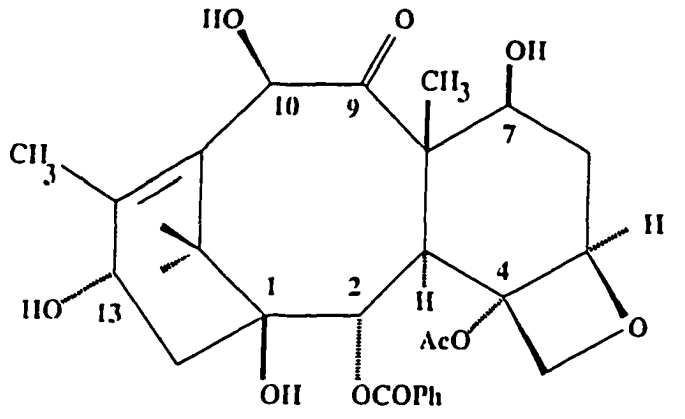

#1: 10-Deacetyl baccatin III

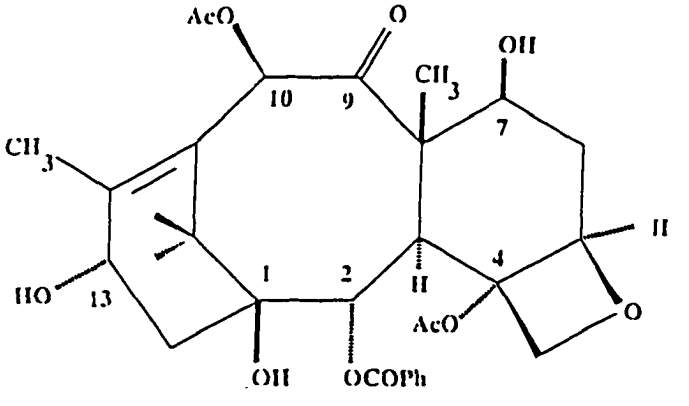

#2: Baccatin III

Figure 1. Structures of Taxanes Studied

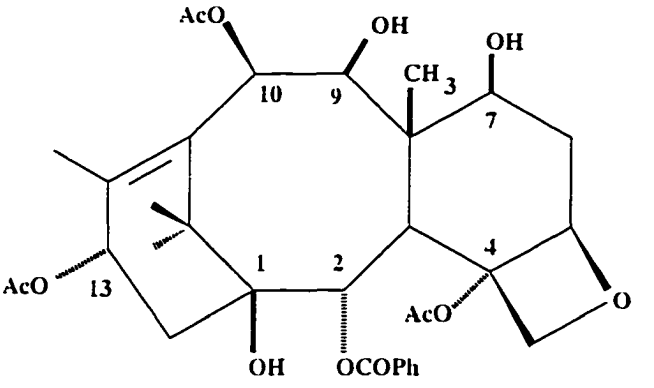

#3: 13-Acetyl-9-dihydrobaccatin III

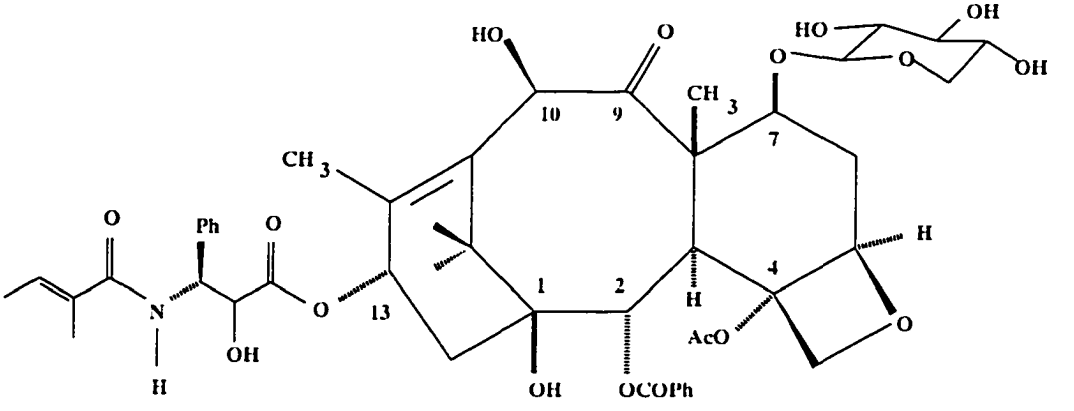

#4: 10-Deacetyl-7-xylosyl taxol B

Figure 1, continued

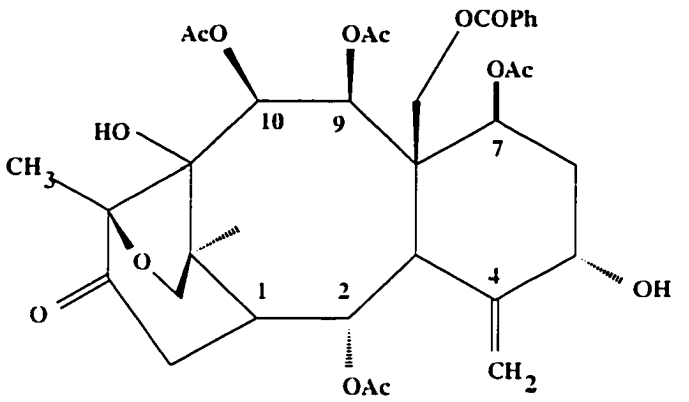

#5: Taxinine M

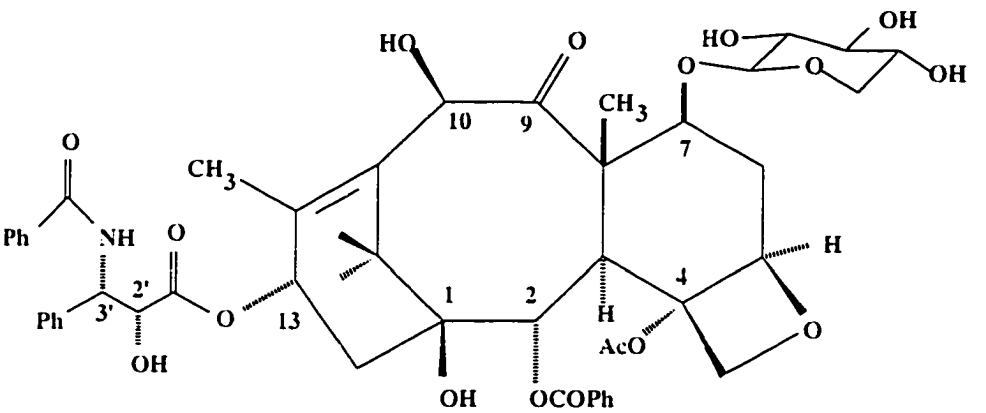

#6: 10-Deacetyl-7-xylosyl taxol

Figure 1,continued.

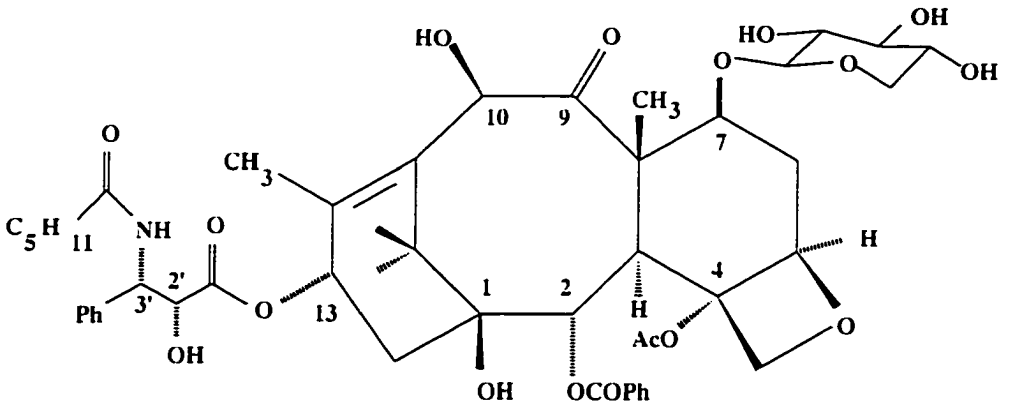

#7: 10-Deacetyl-7-xylosyl taxol C

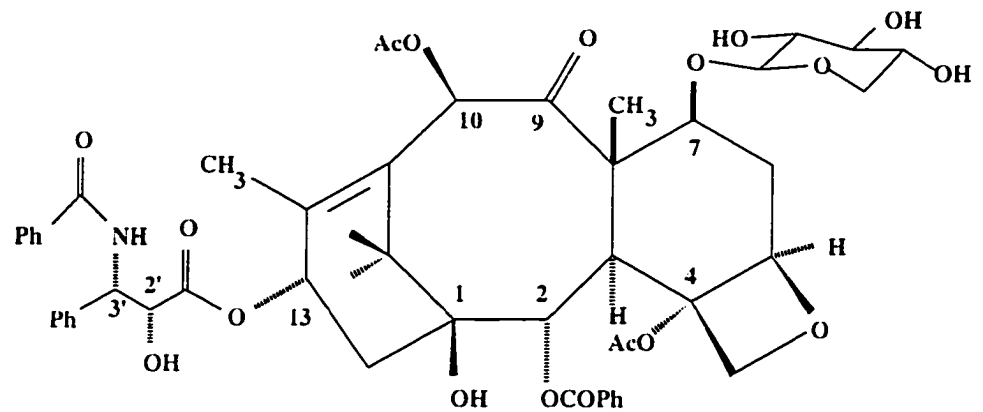

#8: 7-xylosyl taxol

Figure 1, continued.

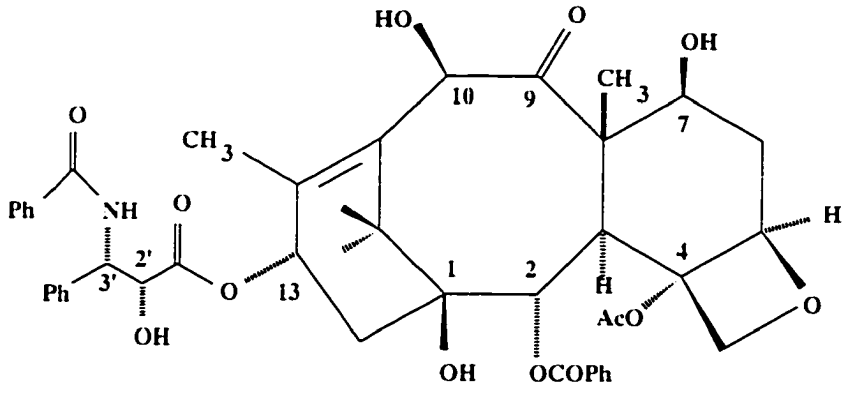

#9: 10-Deacetyl taxol

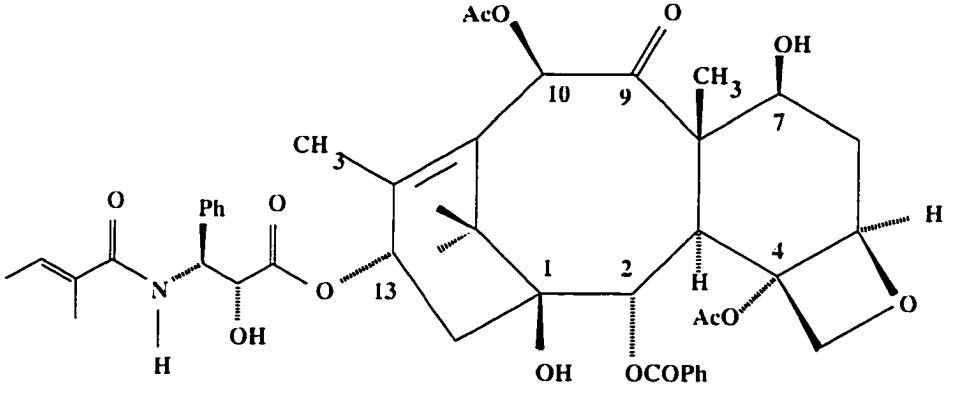

#10: Cephalomannine (Taxol B)

Figure 1, continued.

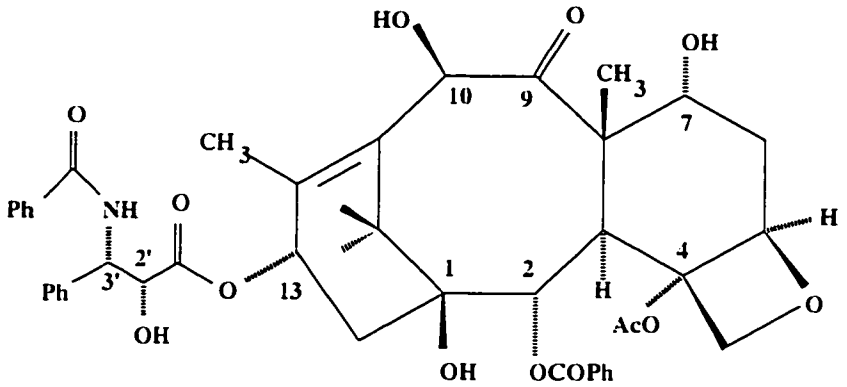

#11: 10-Deacetyl-7-epi-taxol

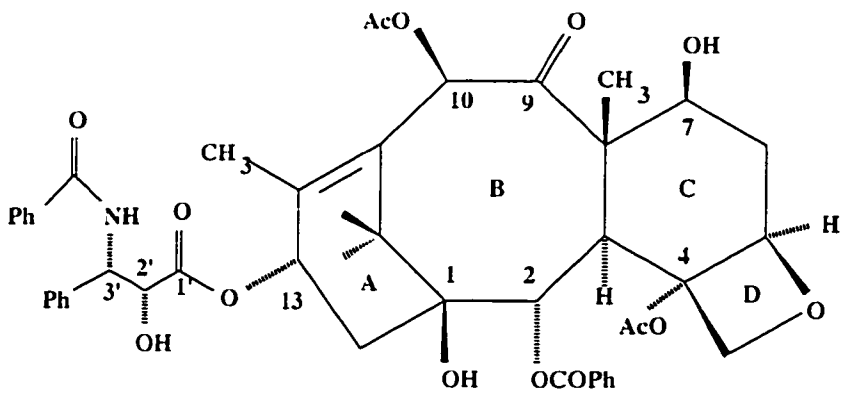

#12: Paclitaxel (Taxol A)

Figure 1, continued

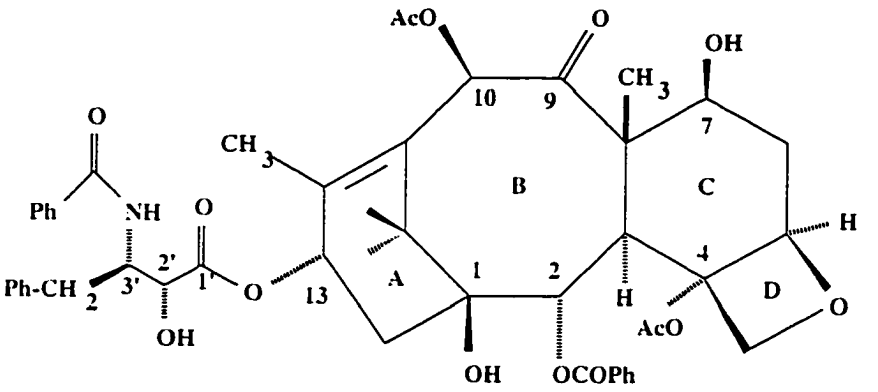

#13: Benzyl analog (N-Debenzoyl-N-phenylacetyl taxol)

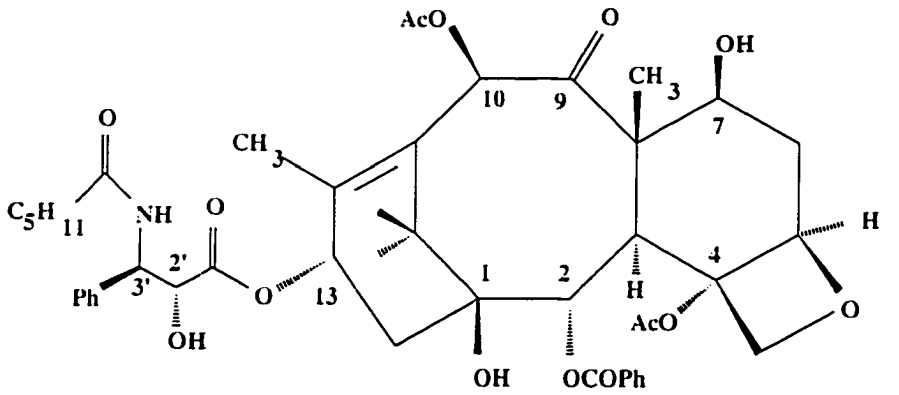

#14: Taxol C

Figure 1, continued.

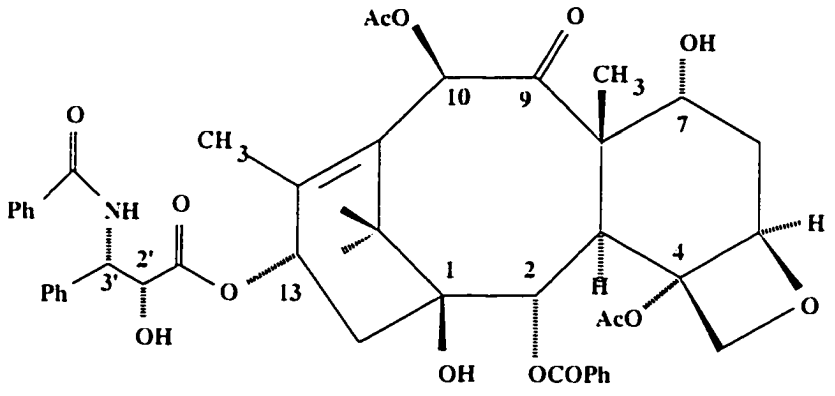

#15: 7-Epi-taxol

Figure 1, continued

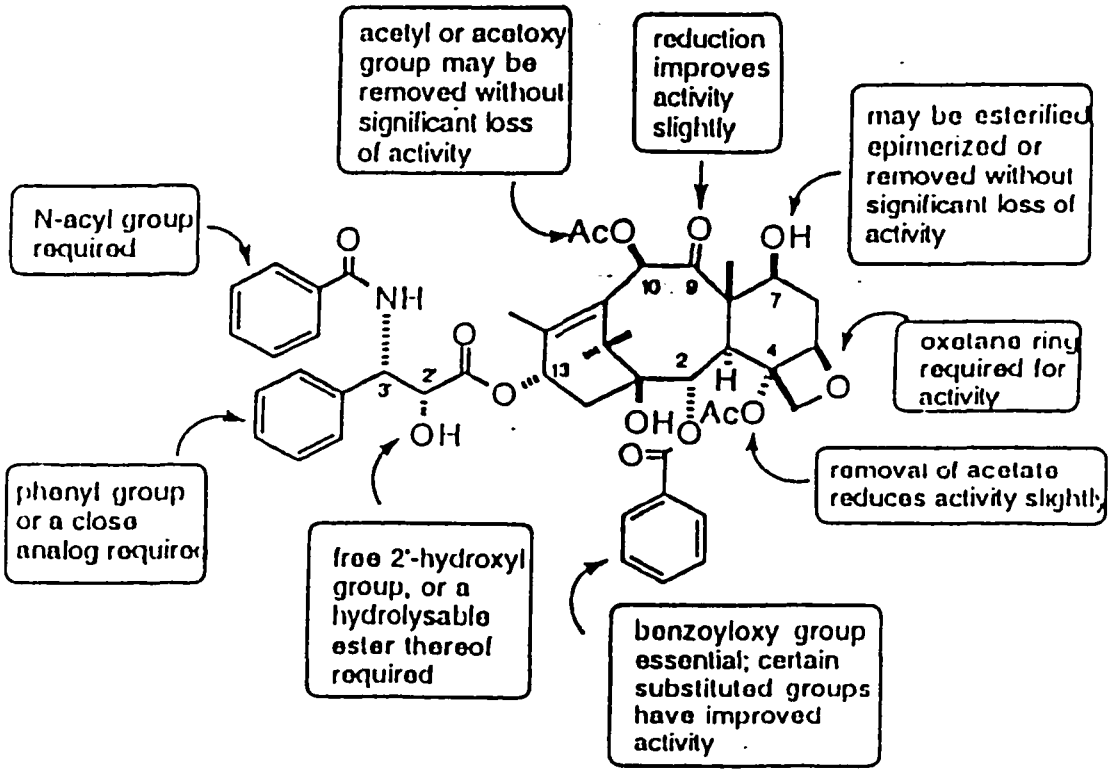

Figure 2. Structure-activity relationships of taxol

Reproduced with permission from ref. 35. Copyright 1994.

1.5 Overview of the Analytical Methods for Paclitaxel and its Related Taxanes

In the process of production of paclitaxel via various routes, it is important to develop an analytical procedure that can resolve those closely structurally-related taxanes. The method must be sensitive, selective, accurate, precise, rugged, and stability-indicating. Consequently the method must separate not only the individual taxanes but also all the taxanes from the excipient in the pharmaceutical formulations.

Analysis of paclitaxel and its related taxanes is a challenge task for the separation scientist due to the wide range of taxane impurities which appear at low levels. These taxanes have very small difference in molecular structure. Due to the intricacy of the chemistry of taxol, it was not possible to cleanly enhance sensitivity by either pre-column or post-column derivatization.

The analysis of taxol has been performed mostly by high performance liquid chromatography (HPLC), although other techniques have been reported, including immunological methods such as enzyme linked immunoassay

(ELISA), radioimmunoassay, and competitive inhibition enzyme immunoassay (CIEIA). These methods have the major drawback of the cross reaction of taxol and cephalomannine.

The problem of analysis of taxanes by HPLC is apparent from the published HPLC chromatograms [13, 38-41] which show long analysis times, poor resolution and broad peaks. Most researchers focus their interest on the separation of paclitaxel from cephalomannine, which possesses isobutylene versus phenyl at the end of C-13 side chain, and which also has cytotoxic activity. Baccatin III and 10-deacetyl baccatin III are also very interesting for the analyst since these compounds can serve as the precursor for the synthesis of paclitaxel. 7-Epi-taxol is a degradation product of paclitaxel which is cytotoxic, and is difficult to separate from paclitaxel [38]. 7-Epi-taxol differs from paclitaxel only in the stereochemistry of the hydroxyl group in the C-7 position. The deacetyl derivatives of paclitaxel, 7-epi-taxol, baccatin III, and cephalomannine are frequently the subject of analysis [38-41].

A number of studies of the HPLC separation of various taxanes have been conducted. Originally, cyano-, phenyl-, or octadecyl-bonded phases were

used. Witherup et al. [42] separated five taxanes in extracts of the bark using these columns in the reversed phase (RP) mode. Xu and Liu [43] used normal phase LC on silica gel to determine paclitaxel in *Taxus chinensis*. Ketchum and Gibson [44] used columns designed by Phenomenex containing a proprietary bonded phase (presumably pentafluoro phenyl, PFP) with an aqueous acetate/acetonitrile eluent to separate eight taxane standards in 20 min. These columns were shown to be superior to the conventional RP columns. The method was applied to crude extracts of *Taxus* bark. RPLC on a phenyl column and micellar electrokinetic capillary chromatography were used by Chan et al. [45,46] for extracts of *Taxus* bark and needles. Five taxanes in needle extracts cleaned by octadecyl-bonded solid phase extraction were resolved in 15 min using a Phenomenex PFP column [47]. Kopycki et al. [39] compared two PFP columns and a diphenyl column in developing a quantitative method for determining seven taxanes in plant extracts in 45 min. Methods for the determination of paclitaxel and metabolites in various biological media have also been published [48-50]. Four taxanes were quantitated in *Taxus baccata* foliage by Lauren et al. on an octyl-bonded RP column [51]. Recently, supercritical fluid extraction using nitrous oxide was applied to the analysis of *T. brevifolia* [52]. A new fluorinated alkyl phase

(Fluofix, Keystone Scientific) was used recently to separate four taxanes and it was suggested the method might to be applicable to the determination of paclitaxel in the pharmaceutical dosage form [53] although no results were presented. The only published [54] full-scale validated method for paclitaxel in the bulk drug form or in process samples used a PFP column with an aqueous acetonitrile gradient; seven taxanes were separated in 50 min. There are no reports in the literature concerned with the HPLC analysis of the excipient-containing injectable dosage form of the paclitaxel.

1.6 Basics of HPLC

Chromatographic separation results from specific interactions between sample molecules and the stationary and mobile phases. The most widely used stationary phases for high performance liquid chromatography are those with surface-reacted (chemically bonded) organic phases. Chromatography using bonded phases is easier, more versatile and has much better reproducibility than chromatography with untreated silica. In bonded phase, the highly polar surface of the silica is altered by the attached functional groups, which can be non-polar (e.g. C18, phenyl) or polar (-NH_2, -CN) or ionizable (sulphonic acid, quaternary ammonium). Polar bonded phases are used for normal phase separations in the same way as silica packings, while non-polar bonded phases are used for reversed phase separations. The bonded phases used in this research are penta fluoro phenyl type proprietary stationary phase which is also considered to be reversed phase. Samples of moderate to strong polarity are usually well separated on the polar bonded phase packings. Samples of nonpolar to moderately polar are well separated on reversed phase packings in conjunction with a polar mobile phase.

In HPLC, resolution or separation of a mixture of solutes is caused by the differential equilibrium distribution of different solutes between the mobile phase and stationary phase. The differential partitioning of solutes is determined by the composition of the stationary phase, the composition of the mobile phase, and the column temperature. The relative distribution of a solute between two phases is determined by the interactions of the solute species with each phase. The relative strengths of these interactions are determined by the intermolecular forces, i.e. by the polarity of the sample and that of the mobile and stationary phases. Intermolecular forces may result from a solute molecule having a dipole moment, whereby it can interact selectively with other dipoles, or if a molecule is a proton donor or acceptor it can interact with other such molecules by hydrogen bonding. Molecules can also interact via much weaker dispersion forces, that is, a given molecule being polarized by another molecule.

Chapter Two

Experimental

2.1 Chemicals

Acetonitrile (ACN) and methanol (MeOH) were Fisher HPLC grade, and glacial acetic acid was Baker Analyzed, both obtained from Fisher Scientific (Springfield, NJ). Ethyl alcohol, Absolute, was USP grade and was obtained from Aaper Alcohol and Chemical Co.(Shelbyville, KY). Water was glass distilled and passed through a Milli-Q system (Millipore Corp., Bedford, MA). The diluent for the bulk drug standards and samples was MeOH containing 0.1% acetic acid and that for the injectable samples was ACN/water/acetic acid (70/30/0.1, v/v). Standards and samples were generously donated: from Hauser Chemical Research (Boulder, CO) we received the Hauser 13 taxane standard mixture, the paclitaxel bulk drug, and 15 individual taxanes; from Bristol-Myers Squibb, Taxol® injectable concentrate and bulk drug Taxol®; from BASF, Cremophore EL, Pharmaceutical grade; and from the National Cancer Institute, a six-taxane standard kit (Lot #9501635-X). Reference solutions for Ultrasonic Nebulization Inductively Coupled Plasma - Atomic Emission Spectrometry (ICP-AES) were A.C.S. certified and obtained from Fisher Scientific.

2.2 HPLC

A Curosil PFP column, 25 cm x 4.6 mm id, 5 μ particle size, was obtained from Phenomenex (Torrance, CA). A Whatman TAC-1 (PFP) column, 25 cm x 4.6 mm id, 5 μ particle size, 159 Å pore size, was donated to us by Whatman, Inc. (Clifton, NJ). The HPLC was a Hewlett-Packard 1090 system with an autosampler and a diode array UV detector run under Hewlett-Packard Chemstation software. For both columns, the detector wavelength used was 230 nm, the column was operated at ambient temperature (except when the effect of temperature was studied), and the injection volume was 15 μL. For the Curosil column the flow rate was 1 mL/min; for the Whatman TAC-1 column the lower back pressure allowed a flow rate of 1.5 mL/min.

2.3 Assay of Taxanes in Paclitaxel Bulk Drug

Proprietary pentafluorophenyl (PFP) columns were selected for the separation of various taxanes. With the PFP HPLC columns used, the possibility of selectivity of the stationary phase results from the interactions of fluorines and phenyl group with the taxanes. In order to resolve various taxanes, isocratic methods were first tried on Curosil-PFP, Curosil G and TAC-1 columns. The results showed that prolonged run times had to be employed, especially for late eluting taxanes (taxanes #10 to #15). This constant mobile phase composition reduced selectivity and resolution. The excessive run time increased band broadening and decreased efficiency and sensitivity. The method was too inefficient to be used in the fast-paced pharmaceutical analysis environment.

A gradient method on Curosil G column was tried using 25 % to 40 % (v/v) ACN as initial composition and gradient rates were varied from 0.444 %/min to 1.125 %/min. The best separation was achieved at 25 % ACN initial composition and a gradient rate of 1 % ACN/min. However, taxanes #7 and # 8, #8 and #9 were not baseline-resolved (resolution < 1.5).

The optimized methods with baseline resolution for all 15 taxanes in a reasonable time frame and low backpressure are described in sections 2.3.1 and 2.3.2.

2.3.1 HPLC Method A

HPLC method A used the Phenomenex Curosil-PFP column, and a linear solvent gradient from 40/60 ACN/water (v/v) at 0.444 %/min until the paclitaxel peak eluted (approximately 24 min), followed by rapid return to the initial composition and equilibration prior to the next injection.

2.3.2 HPLC Method B

HPLC Method B used the Whatman TAC-1 column with an initial 12 min isocratic 38/62 ACN/water (v/v), followed by linear gradient at 4.0 %/min until the paclitaxel peak eluted (approximately 17 min), and then return to the initial composition and equilibration.

2.3.3 Analysis of Sample Weight/Weight (Wt/Wt) %

Preparation of Standard Solution:

Accurately weigh and transfer approximately 12 mg of paclitaxel reference standard of known purity into a 25 mL volumetric flask. Dissolve in and dilute to volume with MeOH containing 0.1 % acetic acid and sonicate for five minutes if necessary.

Preparation of Sample Solution:

Accurately weigh and transfer approximately 12 mg of paclitaxel bulk drug into a 25 mL volumetric flask. Dissolve in and dilute to volume with the same diluent and sonicate for five minutes if necessary.

Analysis of Sample (% wt/wt "as is"):

Make alternate replicate injections of the standard and sample solutions. Compare the peak areas of paclitaxel in the sample and standard solutions. Calculate the weight/weight percentage of the sample against a reference standard of known purity.

Calculation for % wt/wt "as is":

K_f = (Peak Area Standard × 100) / (Standard wt in mg × % Purity Std.)

% wt / wt "as is" = (Peak Area Sample × 100) / (K_f × Sample wt in mg)

2.3.4 Analysis of Purity Profile of Paclitaxel Bulk Drug

The procedures used for analyzing purity profile of paclitaxel bulk drug were as follows:

Accurately weigh approximately 30 mg of paclitaxel bulk drug into a 10 mL volumetric flask. Dissolve in and dilute to volume with 0.1 % acetic acid in methanol. This is the concentrated (approx. 3 mg/mL) sample solution. The diluted sample solution was then obtained by 1/5 dilution of the above concentrated solution. Two sample weights were taken in the analysis for either concentrated sample solution and diluted sample solution. Make alternate replicate injections of the concentrated and diluted sample solutions. A typical HPLC injection sequence for purity profile of paclitaxel drug is shown in Table 1.

Table 1. HPLC Injection Sequence for Paclitaxel Bulk Purity Profile

Inj. #	Sample Description
1	System Suitability Solution (15 Taxanes mixture)
2	Blank (0.1 % acetic acid in methanol)
3	Paclitaxel -1 diluted solution
4	Paclitaxel -1 diluted solution
5	Paclitaxel -1 concentrated solution
6	Paclitaxel -1 concentrated solution
7	System Suitability Solution (15 Taxanes mixture)
8	Blank (0.1 % acetic acid in methanol)
9	Paclitaxel -2 diluted solution
10	Paclitaxel -2 diluted solution
11	Paclitaxel -2 concentrated solution
12	Paclitaxel -2 concentrated solution
13	Blank (0.1 % acetic acid in methanol)

Total related compounds were calculated using the following formula. In the calculation, the individual and total peak area of related compounds were taken from the concentrated solution; the peak area of paclitaxel was taken from the diluted solution.

Calculation for Related Compounds:

Total Related Compounds Area % $= (\Sigma A_{conc} \times 100)/(\Sigma A_{conc} + 5 \times A_{dil})$

Area % of paclitaxel in the bulk drug

= 100 - (Total Related Compounds Area %)

Area % of individual related compound in the bulk drug

$= (A_{conc} \times 100) / (\Sigma A_{conc} + 5 \times A_{dil})$

Where:

A_{conc} = Peak area of each related compound in the concentrated sample solution.

ΣA_{conc} = Sum of peak area of all related compounds after blank correction, excluding the paclitaxel peak area from the concentrated sample solution.

A_{dil} = Peak area of paclitaxel in the diluted sample solution.

2.4 Assay of Taxanes in Paclitaxel Injectable Dosage Form

The current formulation of paclitaxel for injection developed by the National Cancer Institute contains 50 % polyethoxylated castor oil (Cremophor EL) and 50 % anhydrous ethanol as excipients. Cremophor EL is not a single molecular entity, but is a complicated mixture of hydrophilic and hydrophobic components [55]. In developing HPLC methods to assay taxanes in the paclitaxel dosage form, it should be considered that not only individual taxanes must be resolved, but also all the taxanes must be separated from the excipients. The methods developed in this thesis research for analysis of taxanes in paclitaxel injectable forms are described in section 2.4.1 and 2.4.2. In both methods, the Cremophor EL starts to elute after the last-eluting taxane, 7-epi-taxol, so any potential interference from Cremophor is eliminated. The 5 min holding time with 80/20 ACN/water (v/v) in Method C and 15 min holding with 70/30 ACN/water (v/v) are used to wash the excipient out of the column.

2.4.1 HPLC Method C

HPLC Method C used the Curosil-PFP column with a linear gradient from 40/60 ACN/water (v/v) at the start time to 60/40 ACN/water (v/v) in 45 min (0.444 %/min) followed by a linear gradient to 80/20 ACN/water (v/v) in 5 min with a 5 min hold time, followed by return to the starting composition and equilibration.

2.4.2 HPLC Method D

HPLC Method D used the Whatman TAC-1 column with an initial 12 min isocratic 38/62 ACN/water (v/v), then linear gradient to 70/30 ACN/water (v/v) in 8 min (4.0%/min) with 15 min hold, and finally a return to the starting composition and equilibration prior to the next injection.

2.4.3 Potency Analysis of Paclitaxel Injectable Form

Preparation of Standard Solution:

Same as 2.3.3.

Preparation of Sample Solution:

Using a to-contain pipette, transfer 2 mL of paclitaxel for injection from the sample vial into a 25 mL volumetric flask. Rinse the pipette with about 15 mL of sample diluent directly into the volumetric flask. Dissolve and dilute the sample to volume with the sample diluent (70/30/0.1 by volume of ACN/water/acetic acid).

Analysis of Sample (Potency):

Make replicate injections of the standard and sample solutions. Compare the peak areas of paclitaxel in the sample and standardsolutions. Calculate the potency of the sample against a reference standard of known purity.

Calculation for Potency:

Paclitaxel standard solution (mg/mL) = PA /PAS × WS/25 × 25/2 × PU

where: PA = peak area of paclitaxel in the sample solution

PAS = peak area of paclitaxel in sample

WS = weight of the standard in mg

PU = % purity "as is" of the standard /100

2.4.4 Analysis of Related Taxanes in Paclitaxel Injectable Dosage Form

Preparation of Paclitaxel for Injection Placebo:

Mix 21.08 grams of Cremophor EL and 19.88 mL of absolute Ethyl Alcohol USP thoroughly using a magnetic stirrer, to give 40 mL placebo at concentration of 527 mg/mL Cremophor EL and 49.7 % (v/v) Ethyl alcohol.

Preparation of Placebo Blank Solution:

Using a to-contain pipette, transfer 2 mL of paclitaxel for injection placebo from the vial into a 25 mL volumetric flask. Rinse the pipette with about 15 mL of sample diluent directly into the volumetric flask. Dissolve and dilute the placebo to volume with the sample diluent.

Preparation of Sample Solution:

Same as 2.4.3.

Analysis of Sample (Related Compounds):

Make replicate injections of the placebo blank and sample solutions. Calculate individual and total related compounds by area %.

Calculation for Related Compounds:

Area % of Individual Related Cmpds.= (PA ×100) / TPA

Total Area % of Related Cmpds. = ($\sum$ PA × 100) / TPA

Where:

PA = Peak area of individual related compound in the sample solution.

$\sum$PA = Sum of peak areas of individual related compound peaks in the sample solution.

TPA = Sum of peak areas of all peaks including paclitaxel in the sample solution (subtract any placebo interference).

2.5 Determination of Unretained Volume V_0

The void volume, V_0 is defined as the total volume of the eluent in the column. The void volume is a fixed physical parameter which represents both the interpartical and intraparticle (pore) volume of a given column.

Because of its high water solubility, uracil is commonly used as an unretained compound in reversed phase liquid chromatography with aqueous eluents. It is often detected at its maximum UV absorption of 259 nm. Methanol and the water can also be served to unretained compounds in reversed phase liquid chromatography with aqueous mobile phase. It is usually detected at 210 nm. On the Curosil-PFP column, using 38% (v/v), 40 % and 42 % aqueous ACN as the initial composition, the % ACN was varied from 0.422 %/min to 0.488 %/min. Uracil, Methanol, and water were chromatographed in duplicate at each condition. Uracil gave the best peak shape and was employed to determine V_0 in all related experiments. The measurements of V_0 from 30° C to 70° C on both Curosil PFP and TAC-1 columns suggested that V_0 was independent of the temperature under the elution conditions described in the experiment.

2.6 Analysis of Metal Contents in Cremophor EL by Ultrasonic Nebulization Inductively Coupled Plasma-Atomic Emission Spectrometry (ICP-AES)

Inductively Coupled Plasma-Atomic Emission Spectrometry (ICP-AES) is one of the more reliable analytical techniques for elemental analysis compared with flame and electrothermal atomic absorption spectrometric techniques. It has fewer interelement interferences because of the higher temperatures of the plasma source, wider concentration range of detection (several decades), possibility of sequential or simultaneous multielement analysis and greater reproducibility.

2.6.1 Instrumentation

A SpectroFlame Modula ICP-AES system with two monochromators was used. One monochromator is used to cover the UV/VIS range from 160 to 440 nm and the other from 240 to 800 nm.

2.6.2 Method

The wavelengths for analysis of potassium, sodium, calcium, magnesium, cadmium, nickel, zinc, iron, manganese, selenium, molybdenum, arsenic and copper are listed in Table 2. These wavelength were chosen because they gave the highest sensitivity and fewer interferences.

Table 2. Selected Spectral Lines from an Argon ICP

Element	Wavelength (nm)
K	766.491
Na	588.995
Ca	315.887
Mg	279.079
Cd	228.812
Ni	341.476
Zn	213.856
Fe	259.940
Mn	259.373
Se	196.026
Mo	379.825
As	193.696
Cu	284.352

Chapter Three

Results and Discussion

Four HPLC separation methods were developed and optimized using the 15 available standards. Methods A and B are suitable for bulk drug potency determination. Methods C and D are useful for the determination of the degradation profile of both the paclitaxel bulk and injectable forms; potency and content uniformity of the injectable form; and the chromatographic purity profile of the bulk drug.

3.1 HPLC Conditions

In Figure 3 is shown the separation of fifteen taxanes and derivatives in 33 min on the Curosil PFP column using method A. In Figure 4 is shown the separation of thirteen taxanes and derivatives in 20 min on the TAC-1 column using method B. The resolution achieved under the conditions in Figures 3 and 4 for a few of the compounds is a rather sensitive function of the starting eluent composition and the programming rate, and it is for these components that the eluent conditions must be optimized. The optimum HPLC operating conditions were chosen by adjusting the starting composition of acetonitrile, the gradient rate or/and the flow rate which produce the best resolution and efficiency in a shortest run time and reasonable back pressure. A SAS statistical program was used in the method optimization, and is included in Appendix I.

Table 3 shows the effect of starting composition of acetonitrile on resolution; it can be seen that resolutions larger than 1.9 for all the band pairs were achieved on the TAC-1 column using a starting composition of 38 % acetonitrile.

Figure 3. Separation of 15-taxane standard mixture. Conditions: Curosil PFP column, 25 cm × 4.6 mm i.d., 5 μm, with linear solvent gradient from 40/60 ACN/water (v/v) at 0.444 %/min, 1.0 mL/min.

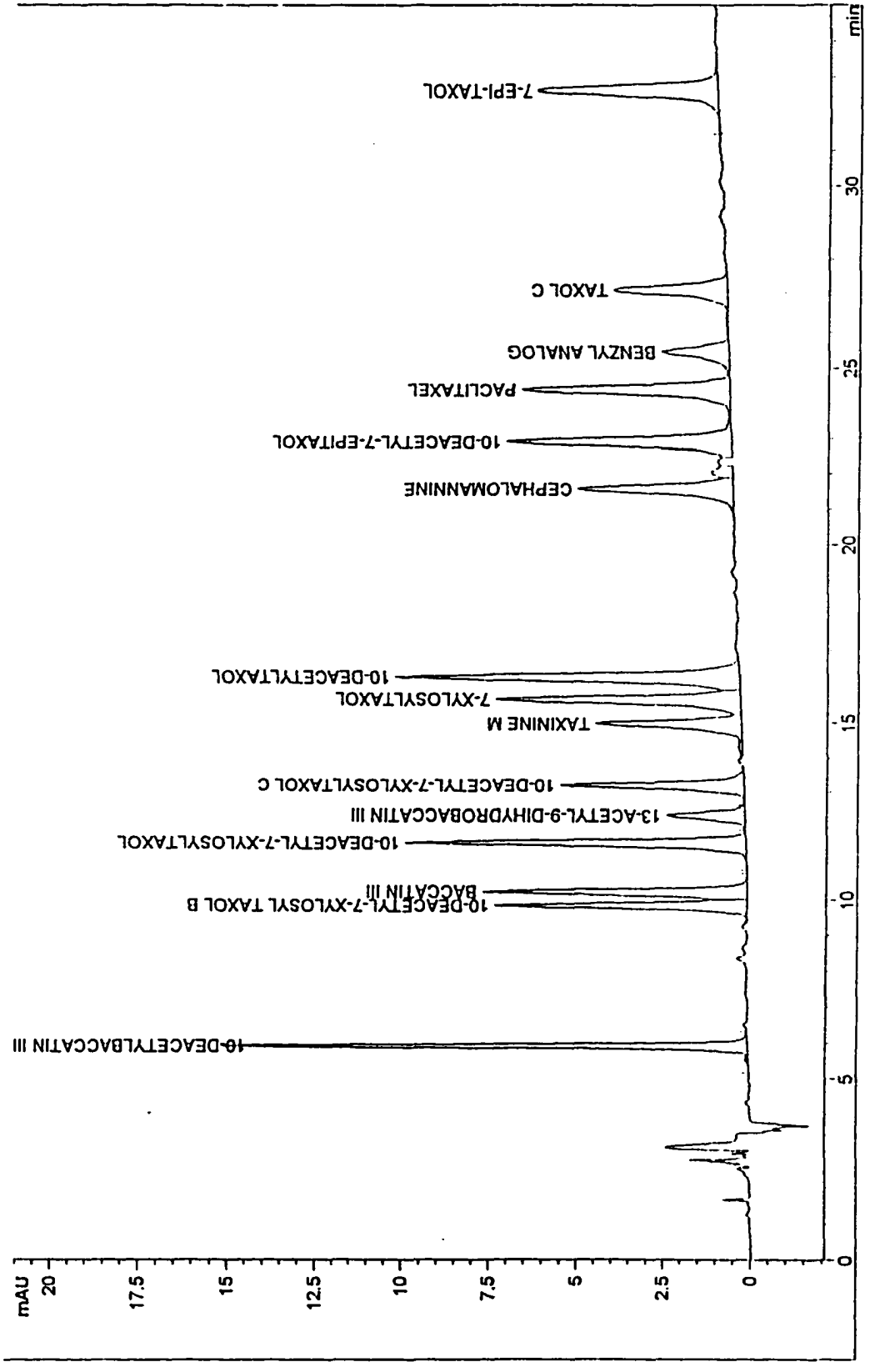

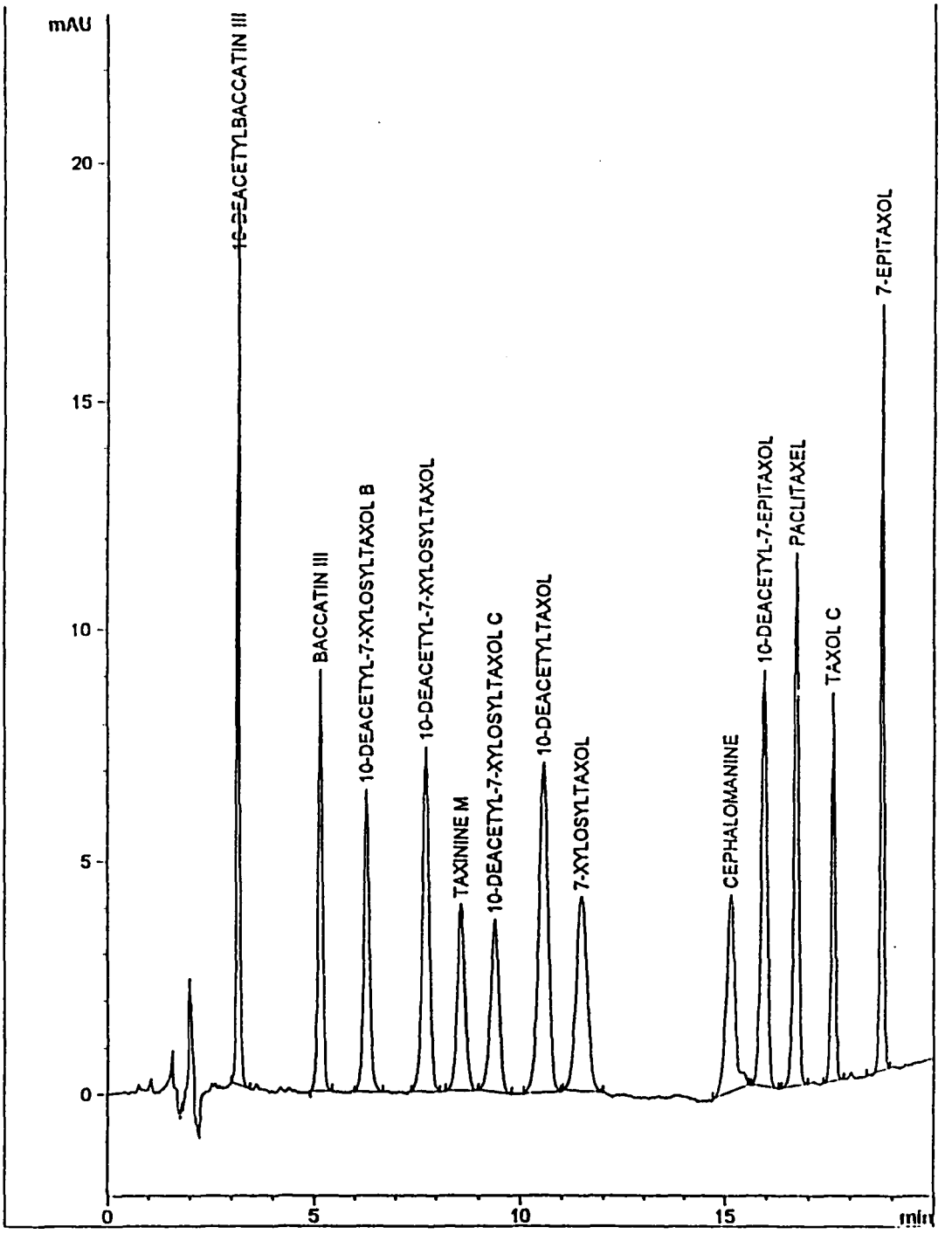

Figure 4. Separation of 13-taxane standard mixture. Conditions : Whatman TAC-1 column, 25 cm x 4.6 mm i.d., 5 µm, with initial 12 min isocratic 38/62 ACN/water (v/v) followed by linear solvent gradient at 4.0 %/min, 1.5 mL/min.

Table 3. Effect of Starting Composition of Acetonitrile on Resolutions of Taxanes for Whatman TAC-1 Column

Starting Acetonitrile %	36	38	40
		Resolution	
Taxane # 2 - # 1	14.09	12.33	11.29
Taxane # 4 - # 2	7.88	4.66	2.09
Taxane # 6 - # 4	4.3	4.99	3.87
Taxane # 5 - # 6	0	2.91	3.99
Taxane # 7 - # 5	3.93	2.23	0
Taxane # 9 - # 7	1.88	3.01	3.86
Taxane # 8 - # 9	3.15	1.92	0.84
Taxane # 10 - # 8	6.04	9.82	8.13
Taxane # 11 - # 10	2.03	2.61	2.5
Taxane # 12 - # 11	2.77	3.33	3.8
Taxane # 14 - # 12	3.99	4.77	4.37
Taxane # 15 - # 14	6.07	7.65	7.15

For the Curosil PFP column, using 38 %, 40 %, 42 % acetonitrile as the initial composition, the % acetonitrile/min was varied from 0.422 %/min to 0.488 %/min. Retention time, t_r ; capacity factor, k'; resolution , R_s; and selectivity, α, of 13 taxanes were analyzed utilizing analysis of variance (ANOVA). The results as shown in Table 4, indicate that changing the starting composition of acetonitrile has a significant impact on retention time (P_r= 0.0001), capacity factor (P_r= 0.0001), resolution (P_r= 0.0012) and selectivity (P_r= 0.0115). (P_r is the probability of the null hypothesis being correct. The null hypothesis is defined as there being no statistically significant difference between the resultant parameters being tested under different conditions.) Varying the gradient rates has a significant impact on t_r (P= 0.0011) and k' (P_r= 0.0016). However, gradient rate does not appear to significantly influence the R_s (P_r= 0.9311) and α (P_r= 0.2648), but this is caused by there being too small an interval between data sets (an interval of gradient rate of 0.022 %/min). If the gradient rate interval was increased (discussed below), it can influence the R_s and α extensively.

Table 4. Analysis of Variance Table - Effect of Starting Composition

Analysis of Variance Table for Retention Time

Source	DF	Sum of Squares	Mean Square	F Value	Pr>F
Start	2	446.047	223.02	312.06	0.0001
Rate	2	10.469	5.235	7.32	0.0011
Peak	12	6210.81	517.56	724.20	0.0001
Error	100	71.465	0.7146		
Corrected Total	116	6738.79			

R-Square	C.V.	Root MSE	Mean
0.989	4.883	0.845	17.311

Analysis of Variance Table for Capacity factor

Source	DF	Sum of Squares	Mean Square	F Value	Pr>F
Start	2	48.179	24.089	315.29	0.0001
Rate	2	1.050	0.525	6.87	0.0016
Peak	12	767.294	63.941	836.89	0.0001
Error	100	7.640	0.0764		
Corrected Total	116	824.16			

R- Square	C.V.	Root MSE	Mean
0.991	5.436	0.276	5.085

Where: Start = Starting composition, Rate = Gradient Rate, Peak = Taxanes

Table 4. continued.

Analysis Variance Table for Resolution Factor

Source	DF	Sum of Squares	Mean Square	F Value	Pr>F
Start	2	14.774	7.387	7.26	0.0012
Rate	2	0.143	0.0726	0.07	0.9311
Peak	11	2253.016	204.819	201.23	0.0001
Error	92	93.64	1.02		
Corrected Total	107	2361.58			

R-Square	C.V.	Root MSE	Mean
0.960	7.135	1.009	5.888

Analysis of Variance Table for Selectivity

Source	DF	Sum of Squares	Mean Square	F Value	Pr>F
Start	2	0.176	0.0878	4.56	0.0115
Rate	2	0.0515	0.0257	1.34	0.2648
Peak	1	25.894	2.354	122.23	0.0001
Error	199	3.832	0.0192		
Corrected Total	215	29.95			

R-Square	C.V.	Root MSE	Mean
0.872	11.359	0.138	1.222

Where: Start = Starting composition, Rate = Gradient Rate, Peak = Taxanes

In Figure 5 is given an example of the effect of the gradient rate on the separation of the 13-taxane standard. Using 42% (v/v) aqueous ACN as the initial composition, the % acetonitrile/min was varied from 0.4 %/min to 1.29 %/min at a minimum interval 0.1 %/min. Increasing the gradient rate reduces the retention time of all the components, but the rate of retention time decreases for peak #4 (peak # in the top chromatogram, not taxane #) (10-deacetyl-7-xylosyl taxol) is greater than that of peak #3 (baccatin III) such that at 1.29% ACN/min, the two peaks overlap. Similarly, peak #7 (7-xylosyl taxol) elutes after peak #6 (taxinine M) at 0.4 %/min but moves through peak #6 with increasing gradient rate and at 1.29 %/min elutes before that peak. Peak #8 (10-deacetyl taxol) changes at about the same rate as peak #7 and at 1.29 %/min is only partly resolved from peak #6.

Figure 5. Effect of linear solvent gradient on the separation of the 13-taxane standard mixture. Conditions: Curosil PFP column; starting composition in all cases, 42/58 ACN/water (v/v), 1.0 mL/min.

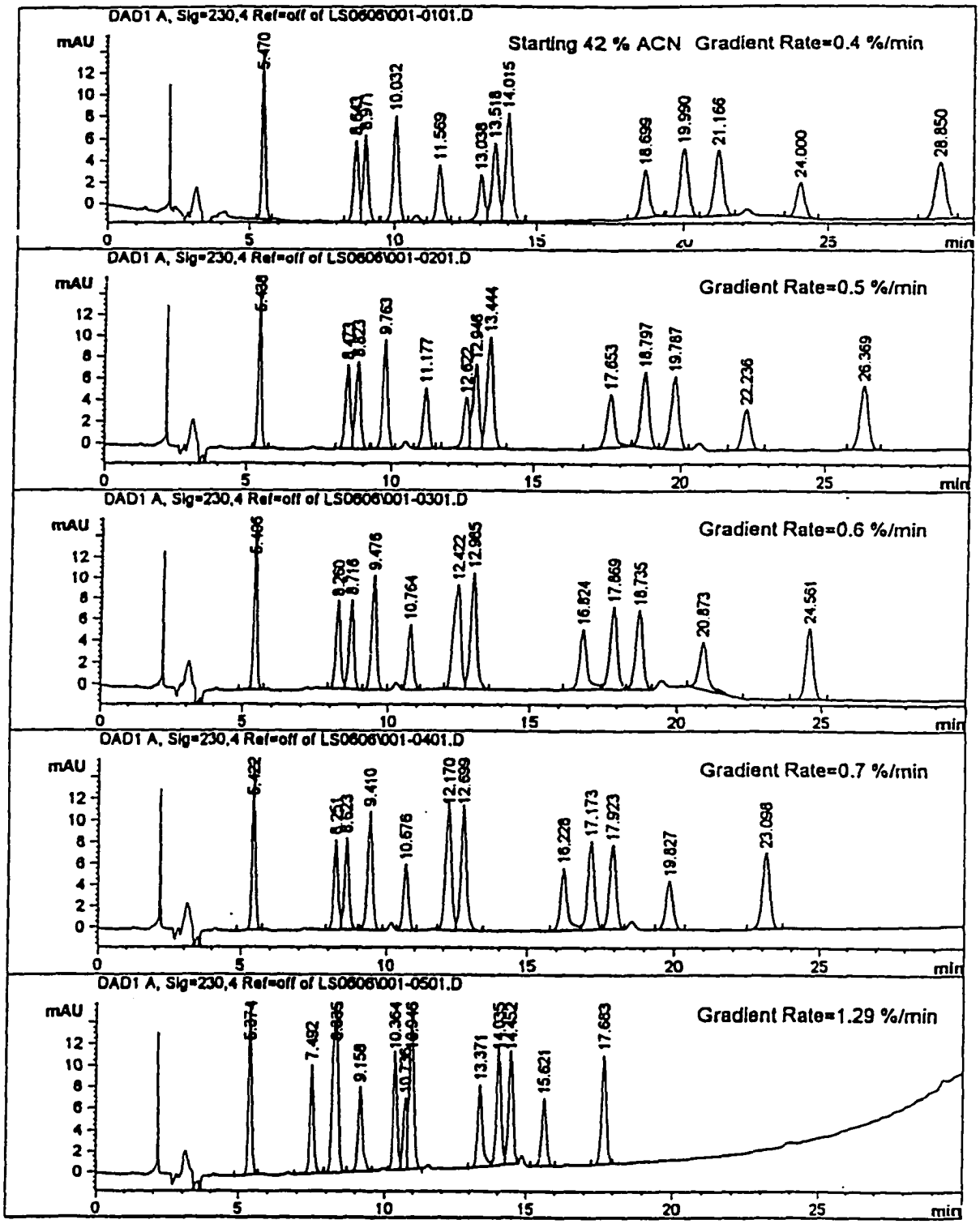

Table 5. Analysis of Variance Table - Effect of Gradient Rate

Analysis of Variance Table for Capacity Factor

Source	DF	Sum of Squares	Mean Square	F Value	Pr>F
Rate	4	14.901	3.725	19.23	0.0001
Peak	12	225.007	18.751	96.77	0.0001
Error	48	9.300	0.194		
Corrected Total	64	249.209			

R-Square	C.V.	Root MSE	Mean
0.963	11.477	0.440	3.835

Analysis of Variance for Retention time

Source	DF	Sum of Squares	Mean Square	F Value	Pr>F
Rate	4	118.01	29.50	19.23	0.0001
Peak	12	1781.75	148.48	96.76	0.0001
Error	48	73.6532	1.5344		
Corrected Total	64	1973.42			

R-Square	C.V.	Root MSE	Mean
0.962677	9.104	1.2387	13.6058

Table 5. Continued

Analysis of Variance Table for Resolution Factor

Source	DF	Sum of Squares	Mean Square	F Value	Pr>F
Rate	4	7.077	1.769	4.45	0.0042
Peak	11	729.525	66.321	166.63	0.0001
Error	44	17.513	0.398		
Corrected Total	59	754.116			

R-Square	C.V.	Root MSE	Mean
0.977	14.327	0.631	4.403

Analysis of Variance for Selectivity

Source	DF	Sum of Squares	Mean Square	F Value	Pr>F
Rate	4	0.01684	0.004210	5.45	0.0012
Peak	11	1.0729	0.097538	126.23	0.0001
Error	44	0.0340	0.0007273		
Corrected Total	59	1.1237			

R-Square	C.V.	Root MSE	Mean
0.969745	2.4416	0.02779	1.1385

An analysis of variance calculation using SAS for the conditions in Figure 5 (shown in Table 5) indicated that changing the gradient rate of acetonitrile at intervals > 0.1 %/min had considerable influence on the retention time (P_r= 0.0001), retention factor (P_r= 0.0001), resolution (P_r= 0.0042) and selectivity (P_r= 0.0012).

The elution order in Figure 3 seems related to molecular size, the number of acetylated hydroxyl groups, and the substitution of the xylosyl group at the 7-position. The hydroxyls and the sugar group increase the solubility of the compounds in the aqueous eluent. The fluorines on the PFP should interact most strongly with the carbonyl oxygens, the principal electron-rich groups in the taxanes. Thus 10-deacetyl baccatin III, with the smallest size and four free hydroxyl groups, elutes first; one of these hydroxyls is acetylated in baccatin III, which elutes just after 10-deacetyl-7-xylosyl taxol B, despite the latter's long 13-ester-amide chain at the C-13 position. The 10-deacetyl-7-xylosyl taxol B elutes before the corresponding taxol A derivative, which elutes before the corresponding taxol C; the groups at the end of the chain are isobutylene, phenyl, and n-pentyl, respectively, arguably the order of increasing hydrophobicity. Similarly, cephalomannine

(a.k.a taxol B) elutes before paclitaxel (a.k.a. taxol A) before taxol C; the benzyl analog with a benzyl rather than a phenyl group in the chain, elutes after paclitaxel. The 7-xylosyl taxol and the 10-deacetyl taxol elute well before paclitaxel itself, as does 10-deacetyl-7-epitaxol before 7-epitaxol. 7-epitaxol elutes last; based on a stereoview of the molecule, the 7-epi-OH may be able to hydrogen bond to the 9-carbonyl oxygen, further increasing its hydrophobicity.

As shown in Figure 4, the elution order of taxanes #10-15 on the TAC-1 PFP column is the same as that on the Curosil PFP column. However, there are differences in retention for the earlier-eluting compounds. In particular, the xylosyl derivatives elute earlier on the Curosil PFP than on the TAC-1 column. Thus, on Curosil column, 10-deacetyl-7-xylosyl taxol B elutes before baccatin III ; 10-deacetyl-7-xylosyl taxol C elutes before taxinine M; and 7-xylosyl taxol elutes earlier than 10-deacetyl taxol. These elution orders are reversed on the TAC-1 column, using method B. With this method, the eluent is isocratic 38/62 ACN/H_2O until the 7-xylosyl taxol elutes. Even with this initial isocratic condition, the separation speed on the TAC-1 column is almost twice that on the other column; 7-epi-taxol elutes in 19 min under

these conditions. The flow rate on the TAC-1 column was 1.5 mL/min, and in addition this column is less retentive (V=25.5ml vs. 31ml), as is clear from Figures 11 and 12 (discussed below). The effect of the method B gradient on peak width is quite clear in Figure 4; up to about 12 min the peaks broaden as usual for an isocratic run; once the gradient starts, the more strongly retained sample components are eluted as much sharper, narrower zones resulting peak widths shrink and apparent plate numbers increase.

The starting composition and gradient rate have a statistically significant effect on k' and resolution as suggested by analysis of variance (ANOVA). These changes also reflect the variation of isocratic ln k' values with percent ACN for the first nine taxanes on the Curosil column, as shown in Figure 6, and five taxanes on the TAC-1 column, as shown in Figure 7. The six later-eluting taxanes have parallel slopes on both columns.

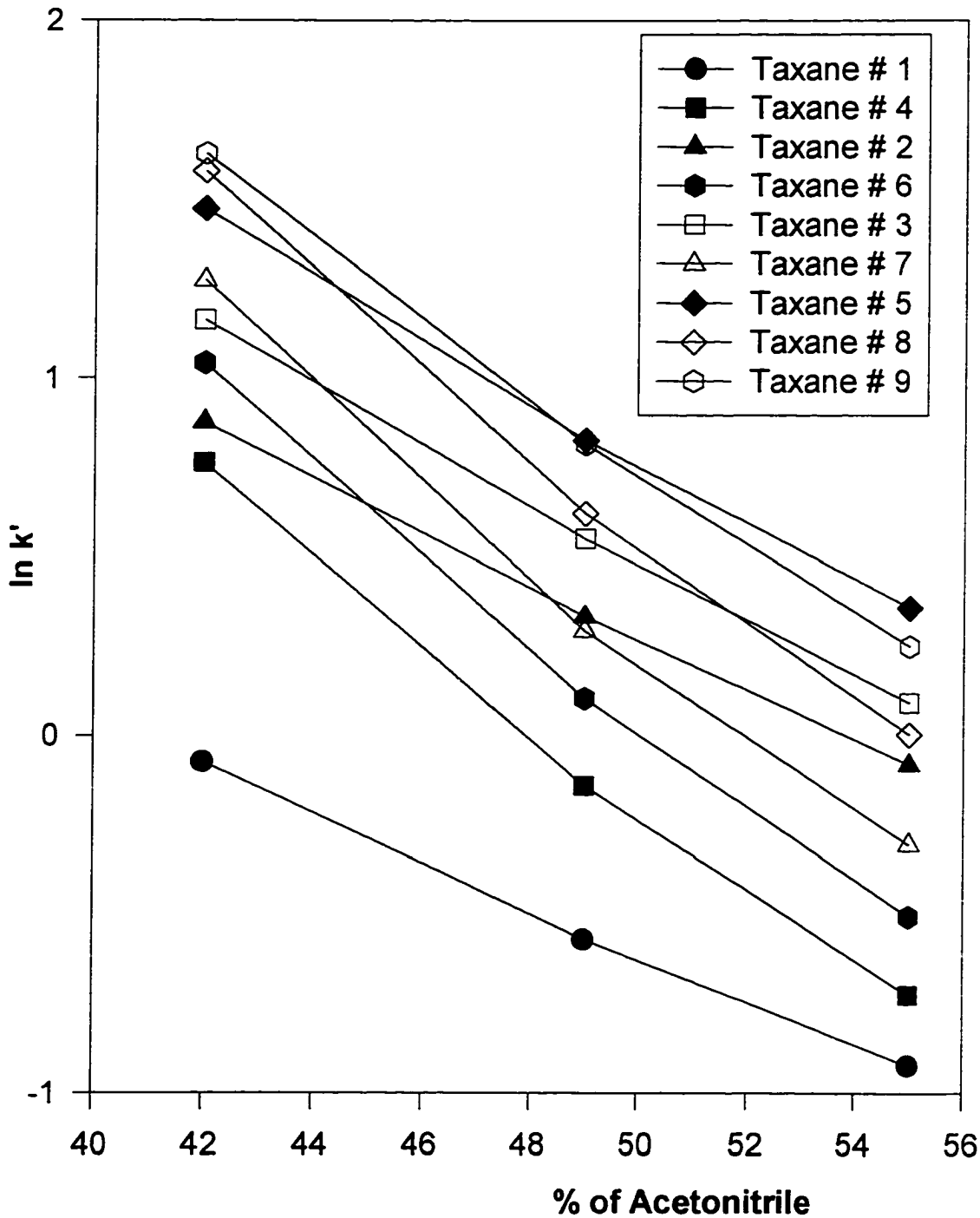

Figure 6. Variation of ln k' with % ACN on Elution Order of Taxanes. Conditions: Curosil PFP column, isocratic elution, 1.0 mL/min. Taxane number refers to Figure 1.

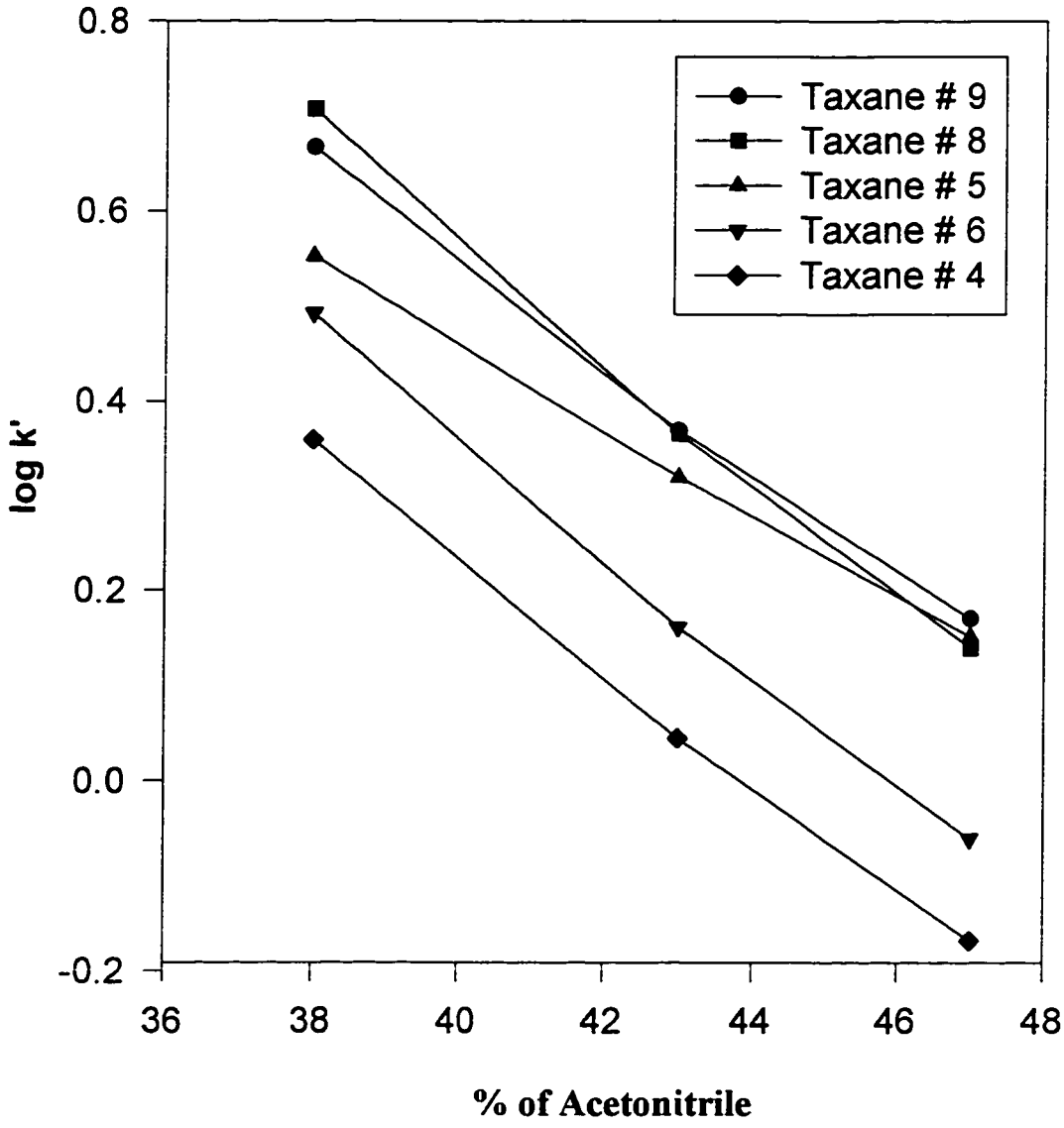

Figure 7. Effect of ACN on Elution Order of Taxanes. Conditions: Whatman TAC-1 column, isocratic elution, 1.0 mL/min. Taxane number refers to Figure 1.

3.2 Thermodynamics of the Separation

To attempt to study further the mechanism of retention of the taxanes on the PFP columns, k' values of the compounds in the Hauser 10-component standard were measured under isocratic HPLC conditions at 10°C increments from 30°C to 70°C. Instrumental temperature control was within $\pm$ 0.5 °C . For the Curosil column, the eluent was 45/55 (v/v) ACN/water at 1 mL/min, and for the TAC-1 column 40/60 (v/v) ACN/water at 1.5 mL/min.

Solute retention is usually expressed in terms of the retention factor, k', which is defined as (the total moles of solute in the stationary phase) / (the total moles of solute in the mobile phase) at equilibrium. The retention factor k' is proportional to the distribution coefficient K and can be written

$$k' = \Phi K \qquad (3.1)$$

The Φ is the phase ratio, the ratio of the volume of the stationary phase in the column to that of the eluent, $\Phi = V_s/V_m$. Because the chromatographic process is an effectively equilibrium distribution of molecules between the

stationary phase and the mobile phase, the Gibbs free energy is related to distribution coefficient in equation (3.2), and equation (3.3) is the familiar relationship between the standard enthalpies ($\Delta H°$) and entropies ($\Delta S°$) and standard free energy ($\Delta G°$) of transfer from mobile to stationary phase.

$$\Delta G° = - RT \ln K \qquad (3.2)$$

$$\Delta G° = \Delta H° - T\Delta S° \qquad (3.3)$$

On combination of equations (3.1-3.3), the retention factor can be expressed as shown in equation (3.4).

$$\ln k' = - \Delta H°/RT + \Delta S°/ R + \ln V_s / V_m \qquad (3.4)$$

$\Delta H°$ can be obtained from the slope of the plot of ln k' versus 1/T, the van't Hoff plot. $\Delta S°$ can be obtained from the intercept , $\Delta S°/ R + \ln V_s/V_m$.

The van't Hoff plots for the Curosil-PFP and TAC-1 columns were linear for all compounds, with R^2 values of 0.996 or better as shown in Figures 8 and 9, respectively. The problem in evaluating the entropy of transfer from the intercept of the plot of ln k' vs 1/T is Φ, which is essentially inaccessible. Precisely what is meant by the volume of the bonded PFP phase is not clear, let alone how to measure it, and in addition, the stationary phase volume should include the volume of any layer of adsorbed eluent component, however that may be measured. Further confounding the interpretation of Φ is the lack of agreement as to what is the best method to measure V_m. Notwithstanding, Yamamoto et al. [55] purported to have measured V_s, and obtained Φ values from 0.3 to 0.8 for various octadecyl-bonded phases; Sander and Field [56] did a calculation based on surface coverage and came up with phase ratios of 0.2 for a cyano column and 0.4 for an octadecyl-bonded column. Notwithstanding, we do not believe meaningful $\Delta S°$ values are realizable using these methods.

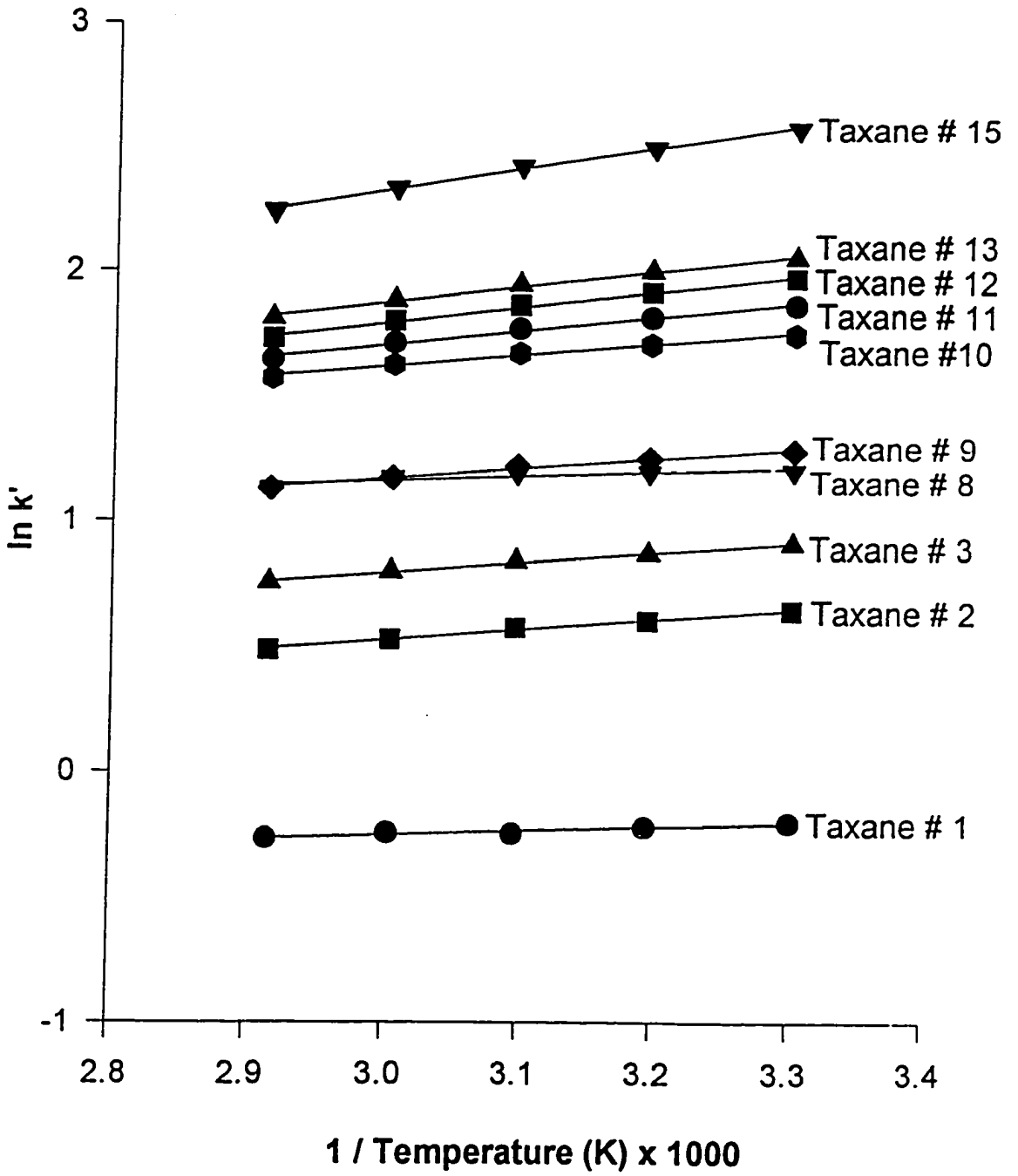

Figure 8. van't Hoff Plot for Curosil PFP column.

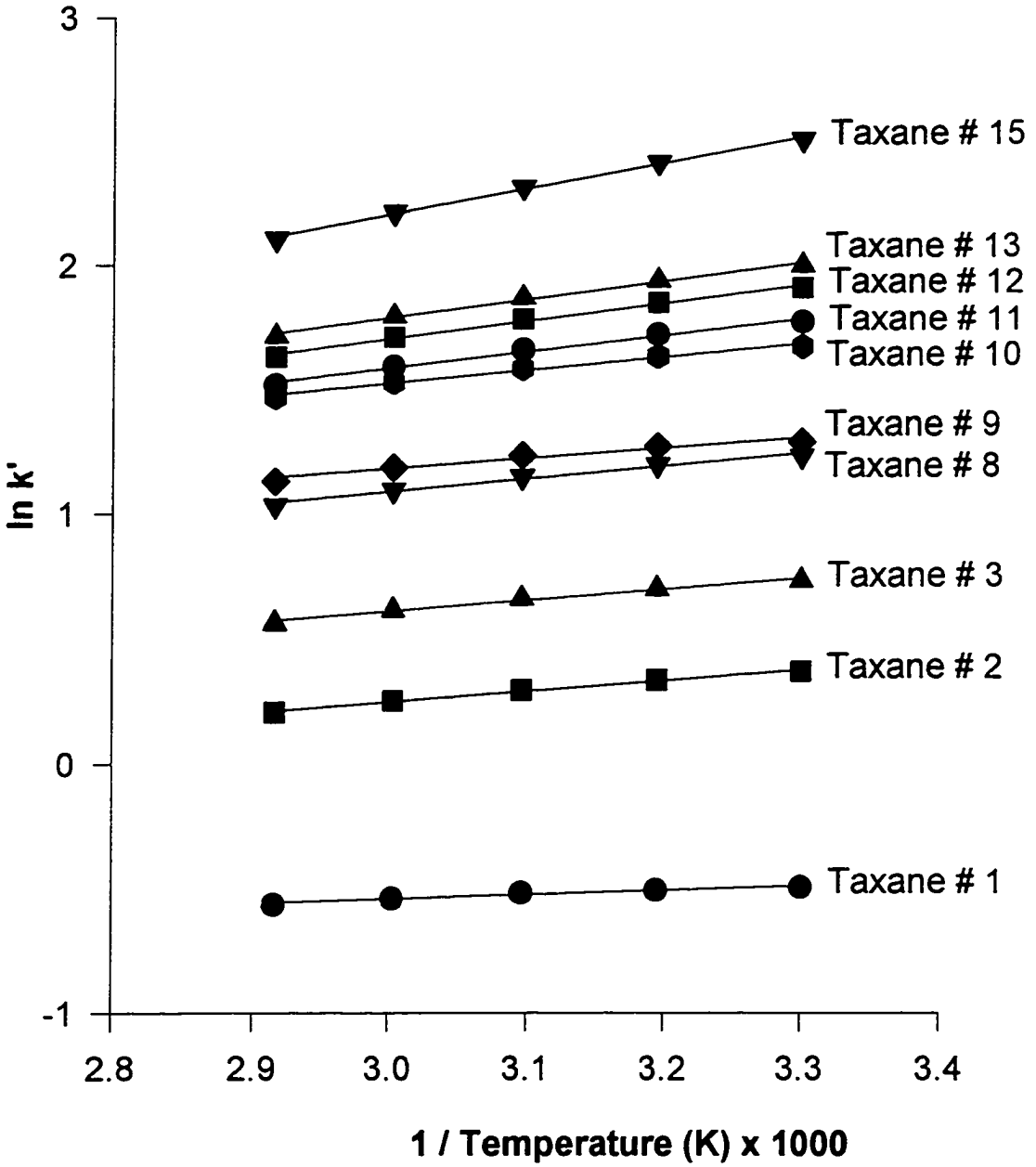

Figure 9. van't Hoff Plot for TAC-1 column

The intercepts ($\Delta S°/R + \ln \Phi$) and the $\Delta H°$ values obtained from the equation above are given in Table 6. The $\Delta H°$ are repeatable to within approximately 0.5 %. For 10-deacetyl taxol (taxane #9) and later-eluting compounds, there seems a general trend of increasing $\Delta H°$ with retention. This corresponds to stronger adsorption, because of the side chain and increasing hydrophobicity. 7-Xylosyl taxol (taxane #8), the only xylosyl derivative in this solute set, has a smaller slope than 10-deacetyl taxol on the Curosil-PFP column but a slightly larger slope on the TAC-1 column, and thus a disproportionately smaller $\Delta H°$ on Curosil-PFP and larger $\Delta H°$ on TAC-1. This higher extent of interaction of the xylosyl derivative with the TAC-1 PFP stationary phase accounts for the difference in elution order of the xylosyl compounds on the two columns. The basic reason for the larger $\Delta H°$, however, is not clear. 10-Deacetyl baccatin III has the lowest $\Delta H°$ on both columns; it lacks a side chain and has the most hydroxyl groups. An acetyl group seems to have a significant effect on the $\Delta H°$, possibly because of its better dipole-dipole interaction with the PFP phase than that of the deacetylated hydroxyl. Thus, on the Curosil-PFP column, baccatin III, with one acetylated hydroxyl, gains 2 KJ/mol over the corresponding deacetyl baccatin III; paclitaxel, 1.6 KJ/mol over 10-deacetyl taxol; and 7-epitaxol, 2.8

KJ/mol over 10-deacetyl-7-epitaxol. For the later-eluting taxanes (#10-15), the enthalpies on the Curosil-PFP column are generally larger than those on the TAC-1 column, reflecting weaker solute adsorptive interactions with the latter. This could result from different degrees of PFP surface coverage or end capping, although the manufacturer of the Curosil column would not divulge this information for comparison with the data Whatman made available to us. The entropy-related quantities, while not directly interpretable, are generally similar on both columns with the exception of taxane #8.

Table 6. Enthalpy and Entropy Change for 10 Taxanes

	Curosil Column		TAC-1 Column	
Analyte	**Δ H° (J/mol)**	**Δ S°/R + ln Φ**	**Δ H°(J/mol)**	**Δ S°/R + ln Φ**
Taxane #1	**-1360**	**-0.75**	**-1453**	**-1.07**
Taxane # 2	**-3422**	**-0.70**	**-3552**	**-1.03**
Taxane # 3	**-3297**	**-0.39**	**-3636**	**-0.70**
Taxane # 8	**-1581**	**-0.59**	**-4254**	**-0.45**
Taxane # 9	**-3410**	**-0.05**	**-3416**	**-0.05**
Taxane # 10	**-3715**	**0.29**	**-3089**	**0.44**
Taxane # 11	**-4544**	**0.08**	**-4038**	**0.17**
Taxane # 12	**-5046**	**-0.02**	**-4695**	**0.04**
Taxane # 13	**-5136**	**0.02**	**-4794**	**0.10**
Taxane # 15	**-7322**	**-0.32**	**-7336**	**-0.41**

3.3 Separation of Taxanes from Excipient in the Injectable Form

Taxol is a complex diterpenoid natural product consisting of a bulky, fused ring system and an extended side chain at C13 that is required for activity. Although the molecule has relatively hydrophilic domains (in the vicinity of C7-C10 and C1'-C2'), hydrophobic domains of the taxane backbone and side chain [57] contribute to the overall poor aqueous solubility of the compound. The extremely low aqueous solubility of the drug causes big problems in paclitaxel therapy. The paclitaxel injectable dosage form is composed of paclitaxel in a mixture of large amount of Cremophor EL and ethanol.

Cremophor EL is a complex non-ionic surfactant and emulsifier [58] used with absolute ethanol as a parenteral vehicle for many hydrophobic pharmaceuticals, including paclitaxel [59]. Cremophor EL forms micelles in aqueous solution which solubilize the paclitaxel. The material is produced by reacting castor oil with an excess of ethylene oxide and is composed mainly of esters of ricinoleic acid with glycerol and polyglycol ethers, plus glycerol/polyglycol ethers and polyglycols [58]. A variety of drugs are administered with excipient Cremophor EL. However, the dose of Cremophor EL that accompanies a dose of taxol is the highest for any marketed drug [60].

It is curious that the UV absorption spectrum of the Cremophor EL is identical to that of paclitaxel (λ_{max} = 230 nm as shown in Figure 10), which could allow excipient components to interfere with any co-eluting taxane peaks in HPLC with UV detection. Cremophor EL is soluble in a diverse range of solvents, including water, ethanol, and chloroform, which causes problems for sample cleanup using solid phase extraction or solvent extraction prior to HPLC.

Consequently the HPLC method must separate not only the individual taxanes but also all the taxanes from the excipient. In the methods developed in this thesis research, the Cremophor EL starts to elute after the last-eluting taxane, 7-epitaxol, thus eliminating any interference. Figure 11 shows chromatograms on the Curosil-PFP column of the 13- taxane standard, the paclitaxel injectable form, and the Cremophor EL itself. Figure 12 shows chromatograms on the TAC-1 column of the paclitaxel injectable form and the Cremophor EL itself. Good resolution of the excipient from the taxanes is achieved on Curosil-PFP as well as TAC-1. Comparison of Figures 11 and 12 shows the separations of the components of the Cremophor EL are quite different on the two columns. It is possible that the base silicas have different

silica pore sizes, producing different molecular sieving effects. However, we did not study this further.

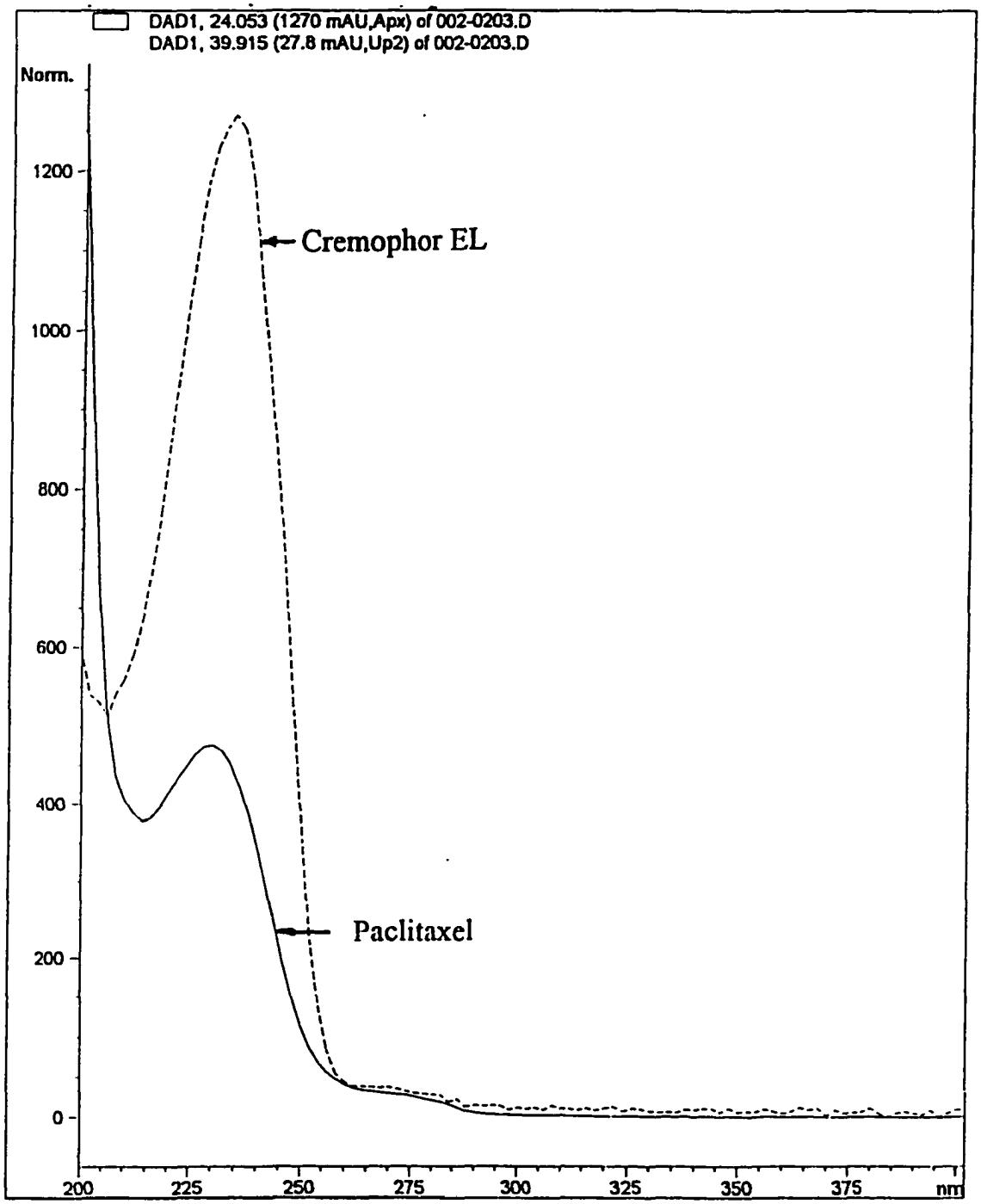

Figure 10. UV Spectrum of Paclitaxel and Cremophor EL

Figure 11. Comparison of the chromatograms of the 13-taxane standard mixture (top), Paclitaxel Injectable Form (middle), and Cremophor EL (bottom). Conditions: Curosil PFP column, method C, 1.0 mL/min.

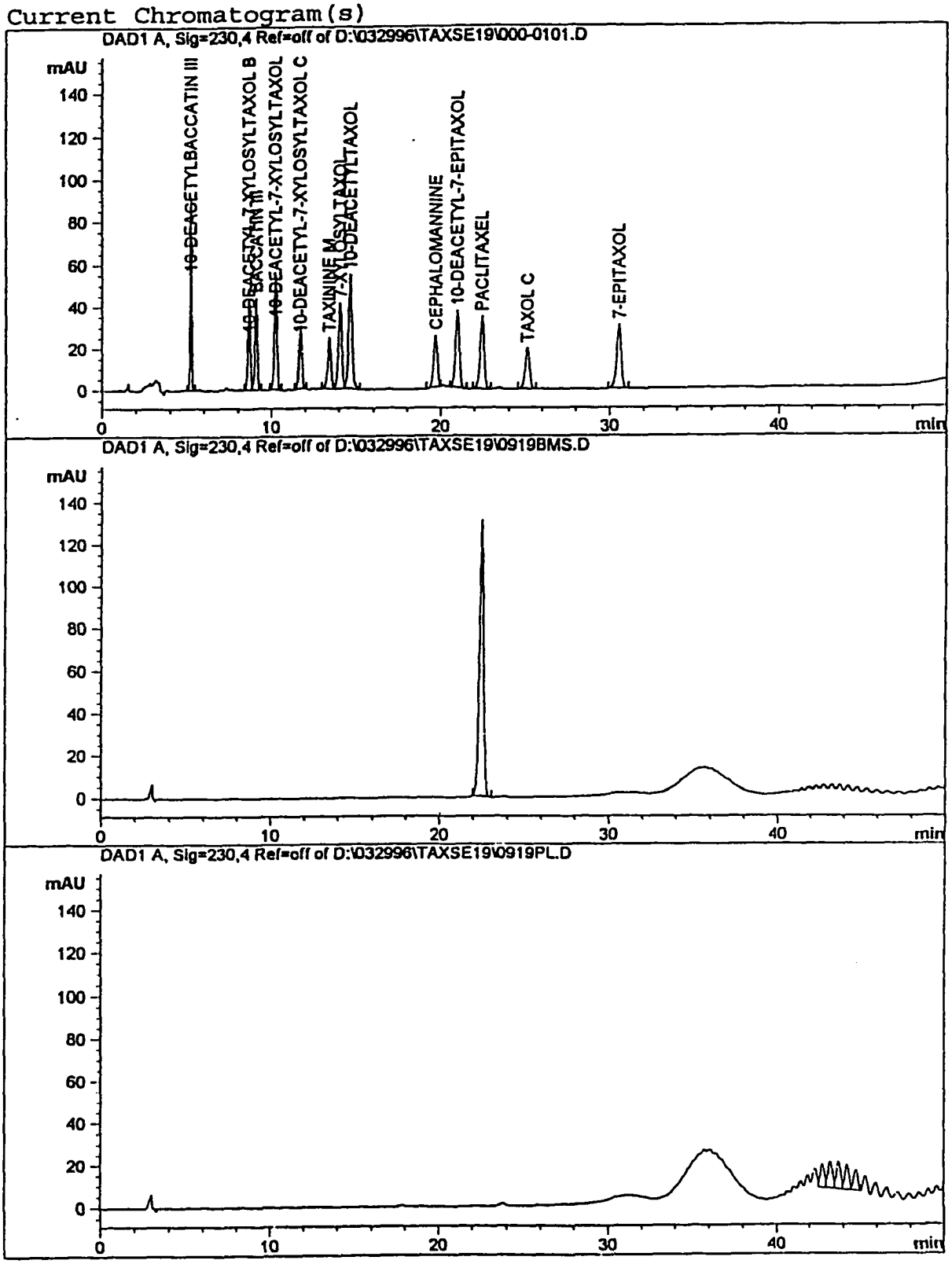

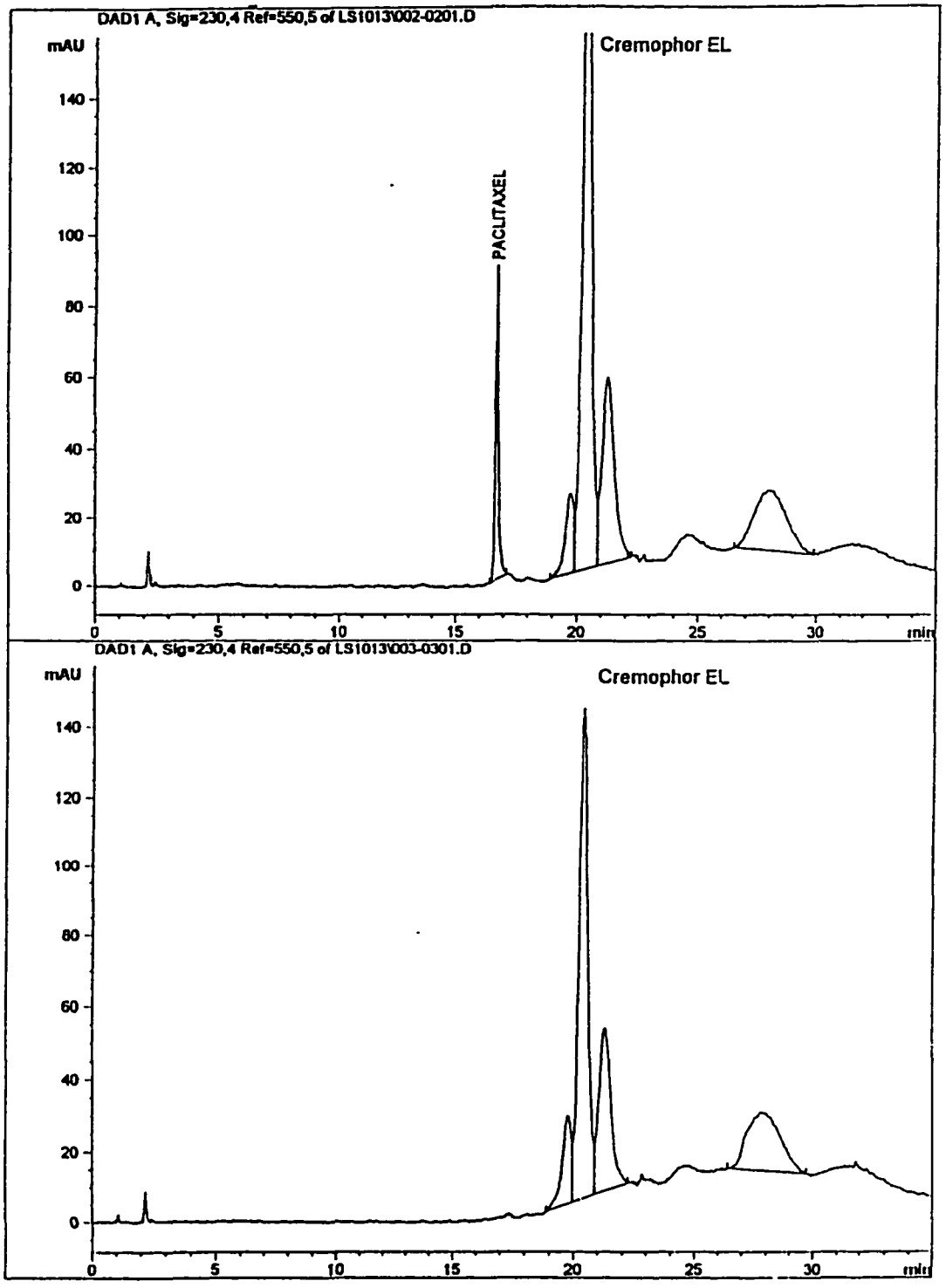

Figure 12. Comparison of the chromatograms of paclitaxel/Cremophor EL mixture (top) and Cremophor EL (bottom). Conditions: Whatman TAC-1 PFP column, method D, 1.5 mL/min.

3.4 Purity Profile of Paclitaxel Bulk Drug

The purities of paclitaxel bulk drug from Hauser Chemical Research Inc. (Hauser) and Bristol-Myers Squibb Corp. (BMS) were determined on a Curosil PFP column using HPLC method C and the procedures discussed in section 2.3.4. Results are summarized in Table 7.

Table 7

Summary of Hauser Paclitaxel Bulk Purity Profile

(Average of Sample1 and Sample 2)

	# Peaks	Area %
Related Compounds < 0.05 %	15	0.278
Related Compounds 0.05 to 0.099 %	0	
Related Compounds > 0.1 %	2	0.55
Total Related Compounds Area %		0.828

Purity of Paclitaxel = 99.17 %

Summary of BMS Paclitaxel Bulk Purity Profile

(Average of Sample 1 and Sample 2)

	# Peaks	Area %
Related Compounds < 0.05 %	17	0.303
Related Compounds 0.05 to 0.099 %	4	0.307
Related Compounds > 0.1 %	4	0.813
Total Related Compounds Area %		1.423

Purity of Paclitaxel = 98.58 %

3.5 Method Validation

Validation of analytical methodologies is widely recognized as an important aspect of the development/utilization of analytical procedures and is expansively required in trade, in regulatory control and in cases of dispute wherein the results must be unambiguous and interpretable in only one way. Validation of the analytical procedures is subject to strict FDA legal standards in pharmaceutical applications. Validation of an analytical method is carried out to demonstrate that it is scientifically sound and that the performance characteristics of the method meet the requirements for the proposed analytical applications. Detailed, specific and comprehensive guidelines for the performance of analytical validations are not universally available. In this manuscript, the standard USP validation procedures [61] were followed to assess the accuracy, precision, specificity, limit of detection, limit of quantitation, linearity and range, ruggedness, robustness, chromatographic precision and repeatability, and stability in diluent for the paclitaxel bulk drug. For the injectable dosage form, only partial validation of methods C and D could be carried out because the Taxol-grade Cremophor EL was unavailable from the manufacturer, and the commercially available grade of

Cremophor EL contains sufficient water to cause possible degradation of the paclitaxel.

3.5.1 Accuracy

Accuracy is a measure of the exactness of an analytical method. The accuracy of an analytical method can be described as the closeness of a measured or computed value obtained by that method to its true value or accepted reference value. Accuracy is usually expressed as the percent of analyte recovered by the assay of known, added amounts of analyte. According to USP 23, Validation of Compendial Methods, [61] "The accuracy of an analytical method may be determined by applying that method to samples or mixtures or mixtures of excipients to which known amounts of analyte have been added both above and below the normal levels expected in the sample."

Two sets of samples of the paclitaxel in ACN/water/acetic acid (70/30/0.1, v/v) diluent were prepared in triplicate at approximately 50, 75, 100, 125, and 150% of the working standard concentration (0.5 mg/mL). One set was assayed using method A and the second using method B. Table 8 and 9 are the results of accuracy obtained using methods A and B. The average recovery using method A was 100.1% with an % RSD of 0.203 % (n = 15).

For Method B the average recovery was 99.9% with an % RSD of 0.326 % (n = 15).

Table 8.
Accuracy of Paclitaxel Bulk Drug
Method A - Curosil PFP Column

Approximate % of Working Standard Concentration	Sample #	mg/mL of Paclitaxel Added	mg/mL of Paclitaxel Recovered	% Paclitaxel Recovered
50	1	0.2478	0.2490	100.5
50	2	0.2500	0.2505	100.2
50	3	0.2496	0.2503	100.3
75	1	0.3750	0.3748	99.95
75	2	0.3901	0.3905	100.1
75	3	0.3831	0.3836	100.1
100	1	0.5002	0.5003	100.0
100	2	0.5005	0.5012	100.1
100	3	0.5011	0.5023	100.2
125	1	0.6240	0.6220	99.68
125	2	0.6259	0.6252	99.89
125	3	0.6251	0.6259	100.1
150	1	0.7661	0.7667	100.0
150	2	0.7668	0.7658	99.82
150	3	0.7543	0.7564	100.3
			Average	100.1
			% RSD	0.203

* Working Standard concentration is 0.5 mg/mL

Table 9
Accuracy of Paclitaxel Bulk Drug
Method B - TAC-1 Column

Approximate % of Working Standard Concentration	Sample #	mg/mL of Paclitaxel Added	mg/mL of Paclitaxel Recovered	% Paclitaxel Recovered
50	1	0.2492	0.2489	99.88
50	2	0.2561	0.2564	100.1
50	3	0.2496	0.2508	100.5
75	1	0.3802	0.3770	99.2
75	2	0.3909	0.3905	99.92
75	3	0.3811	0.3826	100.4
100	1	0.5210	0.5198	99.8
100	2	0.5024	0.5023	100.0
100	3	0.5017	0.5023	100.1
125	1	0.6310	0.6220	99.90
125	2	0.6267	0.6236	99.51
125	3	0.6224	0.6230	100.0
150	1	0.7542	0.7527	99.80
150	2	0.7668	0.7646	99.71
150	3	0.7523	0.7541	100.2
			Average	99.9
			% RSD	0.326

* Working Standard concentration is 0.5 mg/mL

3.5.2 Method Precision

The precision of a method is the measure of the closeness of agreement between a series of measurements obtained from multiple sampling of the same homogeneous sample. The precision of an analytical method is usually expressed as the percent relative standard deviation (% RSD) for a statistically significant number of samples.

The USP does not give a specific protocol, so the method precision was determined using the procedure of Debesis et al.[62]. A sample of paclitaxel received from Hauser Chemical Research was tested to be 99.17 % pure (see section 3.4), which served as the standard. Another sample from Bristol-Myers Squibb Corp. was considered to be the sample. For each, three solutions were accurately prepared to contain approximately 0.5 mg/mL paclitaxel, and each solution was analyzed in triplicate using method A. The response factor for each standard peak was calculated as the peak area divided by the concentration of paclitaxel, i.e. the weighed standard × the percent purity. The standard RSD, $RSD_{STD,}$ was the RSD of the average response factor. Similarly, the peak area of each of the samples was divided by the

concentration of weighed sample, and the sample RSD, RSD_{SPL}, was the RSD of the average weight percent of paclitaxel in the sample set.

The method precision was calculated to be 1.1 % as shown on Table 10.

Table 10. Method Precision On Curosil PFP Column

Standard Set

Standard #	Conc.(mg/mL)	Injection #	Area response	Reponse Factor
1	0.4872	1	8918.62	18459.08
	0.4872	2	8901.81	18424.29
	0.4872	3	8997.12	18621.55
2	0.4868	1	8966.6	18573.64
	0.4868	2	8919.88	18476.86
	0.4868	3	8996.13	18634.80
3	0.482	1	8770.16	18347.64
	0.482	2	8753.91	18313.64
	0.482	3	8747.82	18300.90
			Average	18461.38
			RSD %	0.69

Sample Set

Sample #	Conc.(mg/mL)	Injection #	Area response	% wt/wt as is
1	0.4992	1	9109.92	98.85
	0.4992	2	8990.66	97.56
	0.4992	3	9143.89	99.22
2	0.4992	1	9000.04	97.66
	0.4992	2	8897.91	96.55
	0.4992	3	8906.38	96.64
3	0.5252	1	9483.44	97.81
	0.5252	2	9438.31	97.34
	0.5252	3	9448.77	97.45
			Average	97.67
			RSD %	0.91

$$\text{Method Precision} = \sqrt{(RSD_{STD})^2 + (RSD_{SPLE})^2} = \sqrt{0.69^2 + 0.91^2} = 1.14\,\%$$

3.5.3 Specificity

The specificity of a method refers to its ability to measure the analyte of interest accurately and specifically in the presence of other components such as impurities, degradation products, excipients, and other active ingredients which may be expected to be present in the sample matrix. Specificity is a measure of the degree of interference (or absence thereof) in the analysis of complex sample mixtures. The specificity of an analytical method is determined by comparing test results from the analysis of samples containing added impurities, degradation products, related chemical compounds, or placebo ingredients when compared to test results from samples without added substances.

The methods A, B, C and D were found to be specific for paclitaxel in the presence of its process-related impurities and degradation products and excipients, as shown in Figures 3, 4, and 11-18.

Methods A and B were further tested for their stability-indicating ability under conditions of acid, base, oxidant, UV and visible light, and heat.

Accurately weighed portions of paclitaxel bulk powder were subjected to forced degradation procedures followed by HPLC analysis. For treatment with base, 10 mg of paclitaxel was dissolved in 1 mL of MeOH plus 1 mL of 0.1 M aqueous NaOH and stored at room temperature for 1 hour. Acid stability was tested by dissolving 10 mg of paclitaxel in 5 mL of MeOH plus 2 mL of 1 M aqueous HCl and storing at room temperature in the dark for three days. Oxidative degradation was studied by dissolving 10 mg of paclitaxel in 3 mL of MeOH plus 1 mL of 30% aqueous H_2O_2 and storing three days in the dark at room temperature. UV light was tested by subjecting 10 mg of paclitaxel powder to short-wavelength (λ = 254 nm) UV light for three days at room temperature. Similarly, 10 mg of paclitaxel was subjected to visible light (fluorescent bulb, 1000 foot-candles) for three days. Finally, the effect of heat was assessed by placing 10 mg portions of paclitaxel in ovens at 100°C, 120°C, and 150° C for three days. Recoveries of paclitaxel and the total area % of related compounds are given in Table 11. Chromatograms showing the effect of degradation by base, acid, UV light, visible light, oxidation and heat are given in Figures 13-18 respectively.

Table 11. Specificity of the Method- Forced Degradation

Degradation Condition	Time	Observations	% Recovery paclitaxel	% Related Cmpds (Area %)
NaOH	1 hour	Major degradation peaks observed at RRT 0.24, 0.29, 0.38, 0.55 and 0.59. No change in solution appearance.	0	100
HCl	72 hours	Major degradation peaks observed at RRT 0.11, 0.13, 0.18, 0.19, 0.24, 0.29 and 0.31. No change in solution appearance.	51.6	33.2
H_2O_2	72 hours	Major degradation peaks observed at RRT 0.63, 0.66, 0.76, 0.81 and 0.87. No change in solution appearance.	98.2	0.33
UV light (Short wavelength)	72 hours	Major degradation peaks observed at RRT 0.56, 0.64, 0.71, 0.75 and 0.93. No change in bulk appearance.	69.5	21.4
Visible light (1000 foot candlelight)	72 hours	Major degradation peaks observed at RRT 0.64, 0.71 and 0.93. No change in bulk appearance.	97.3	3.0
Heat (100°C)	72 hours	Major degradation peak observed at RRT 1.34. No change in bulk appearance.	97.4	4.1
Heat (120°C)	72 hours	Major degradation peak observed at RRT 1.34. No change in bulk appearance.	86.4	14.3
Heat (150°C)	72 hours	Major degradation peak observed at RRT 1.34. No change in bulk appearance.	52.5	48.9

RRT = relative retention time to paclitaxel,
Cmpds = compounds.

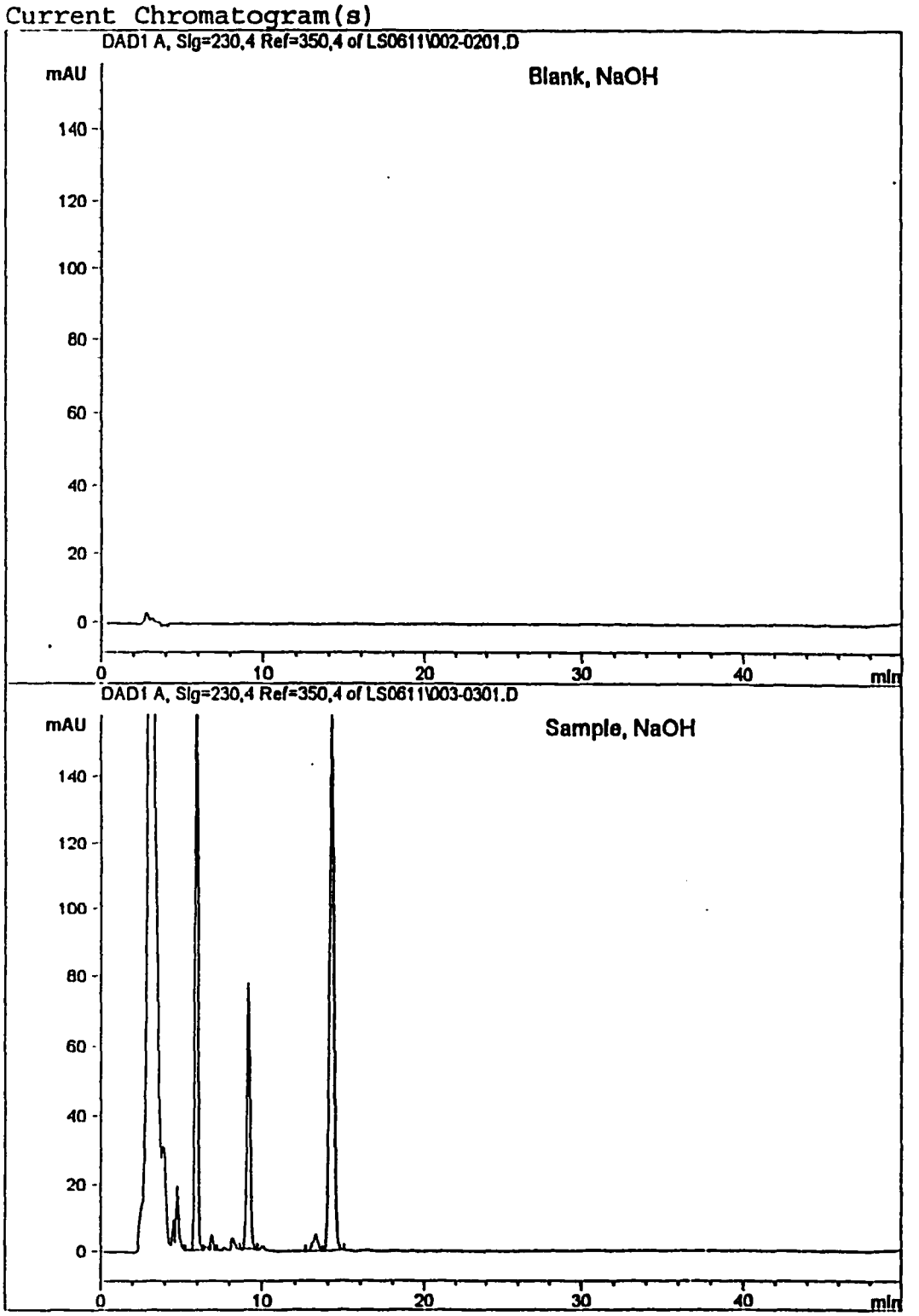

Figure 13. Chromatograms showing the effect of degradation by base. NaOH blank (top) and Paclitaxel degraded by NaOH (bottom).

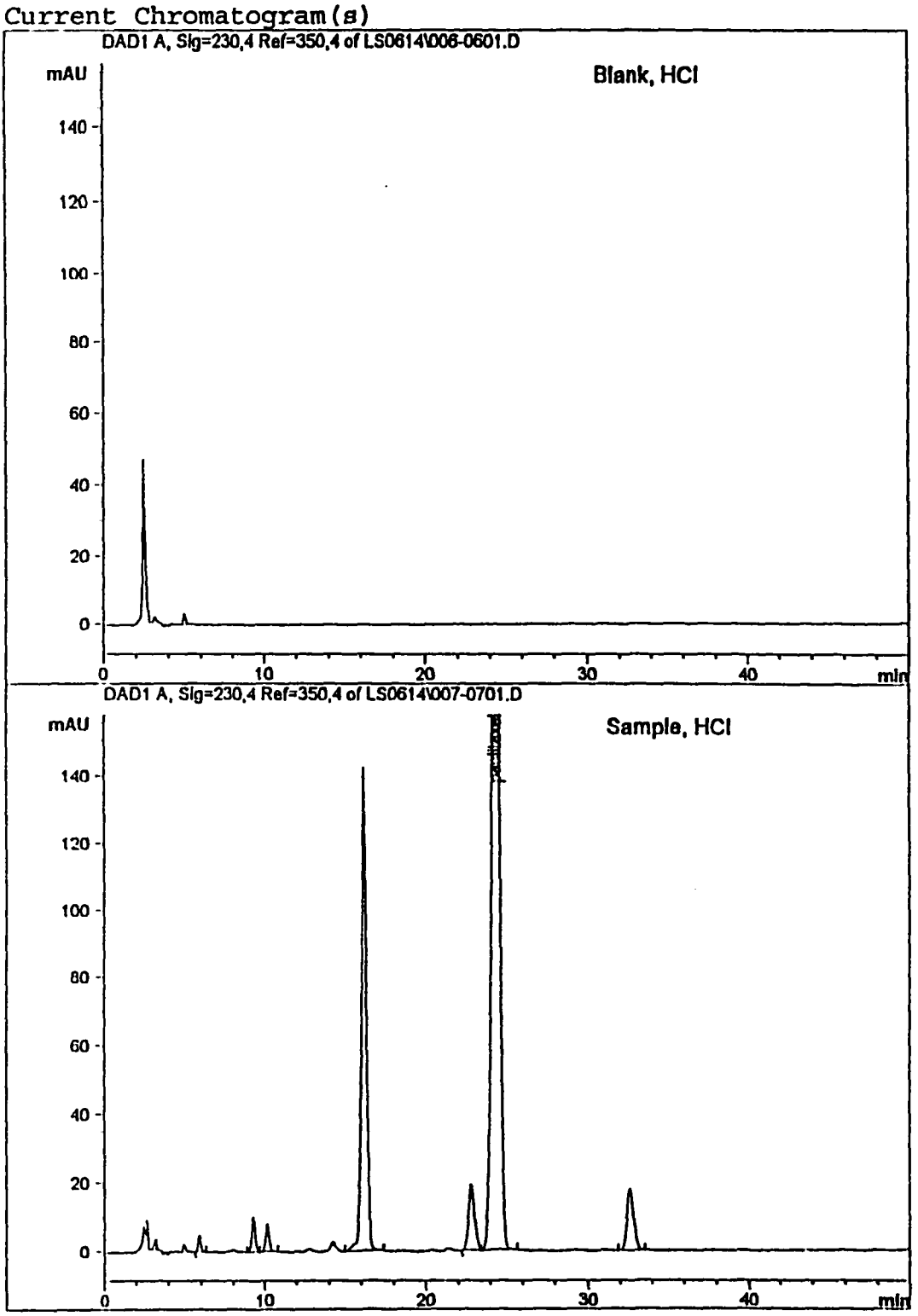

Figure 14. Chromatograms showing the effect of degradation by acid. HCL blank (top) and Paclitaxel degraded by HCL (bottom).

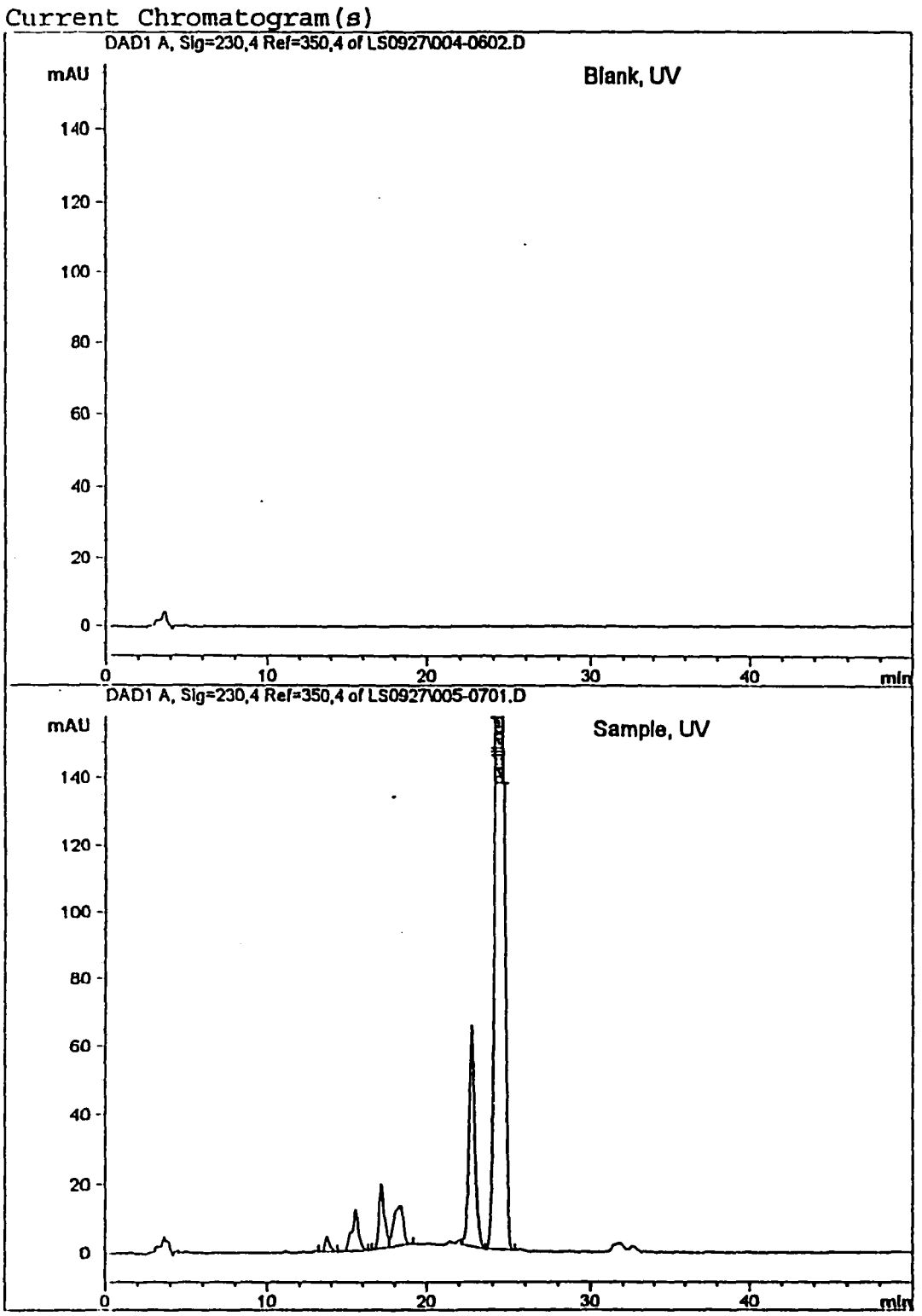

Figure 15. Chromatograms showing the effect of degradation by UV light. UV light blank (top) and Paclitaxel degraded by UV light (bottom).

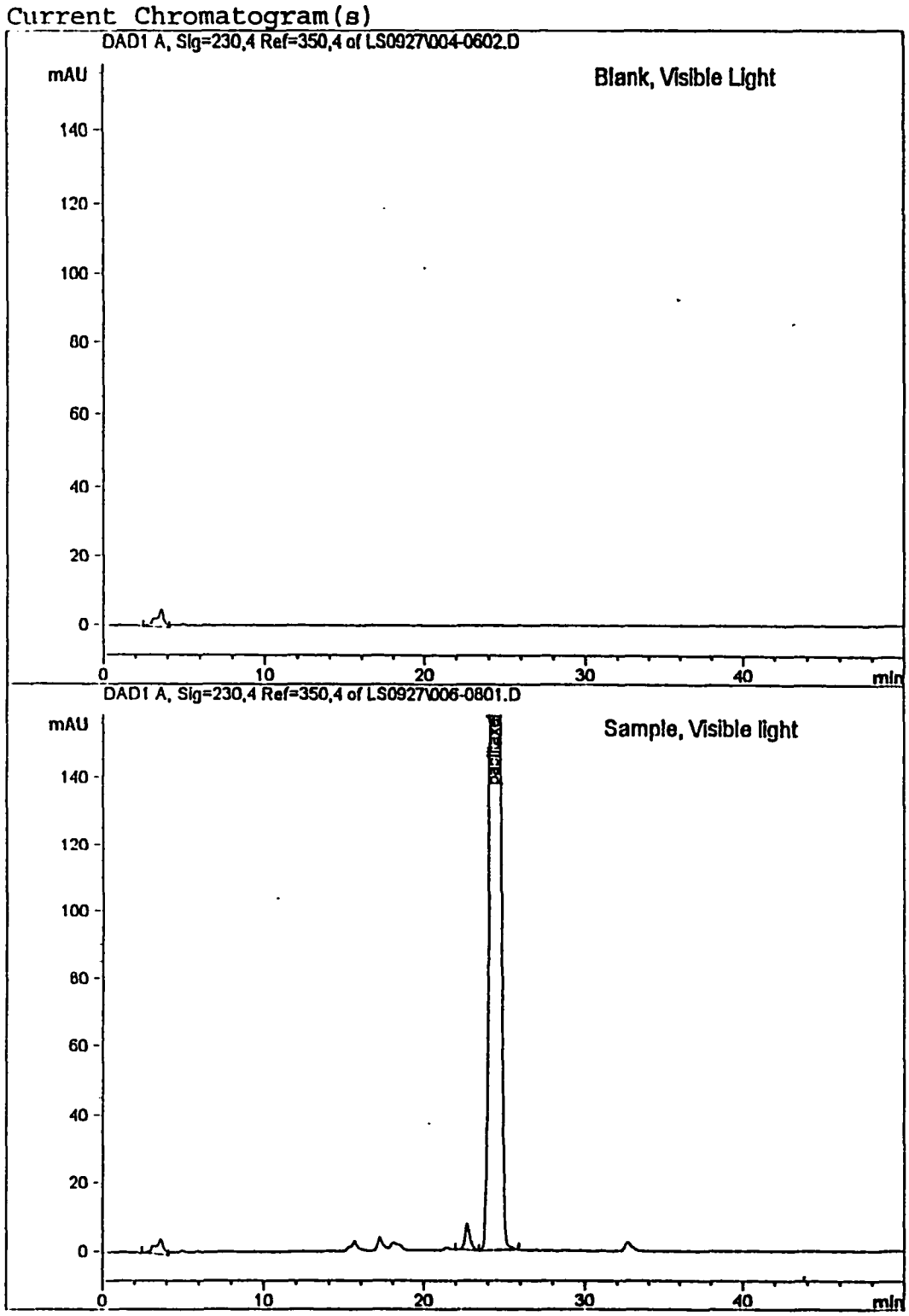

Figure 16. Chromatograms showing the effect of degradation by visible light. Visible light blank (top) and Paclitaxel degraded by visible light (bottom).

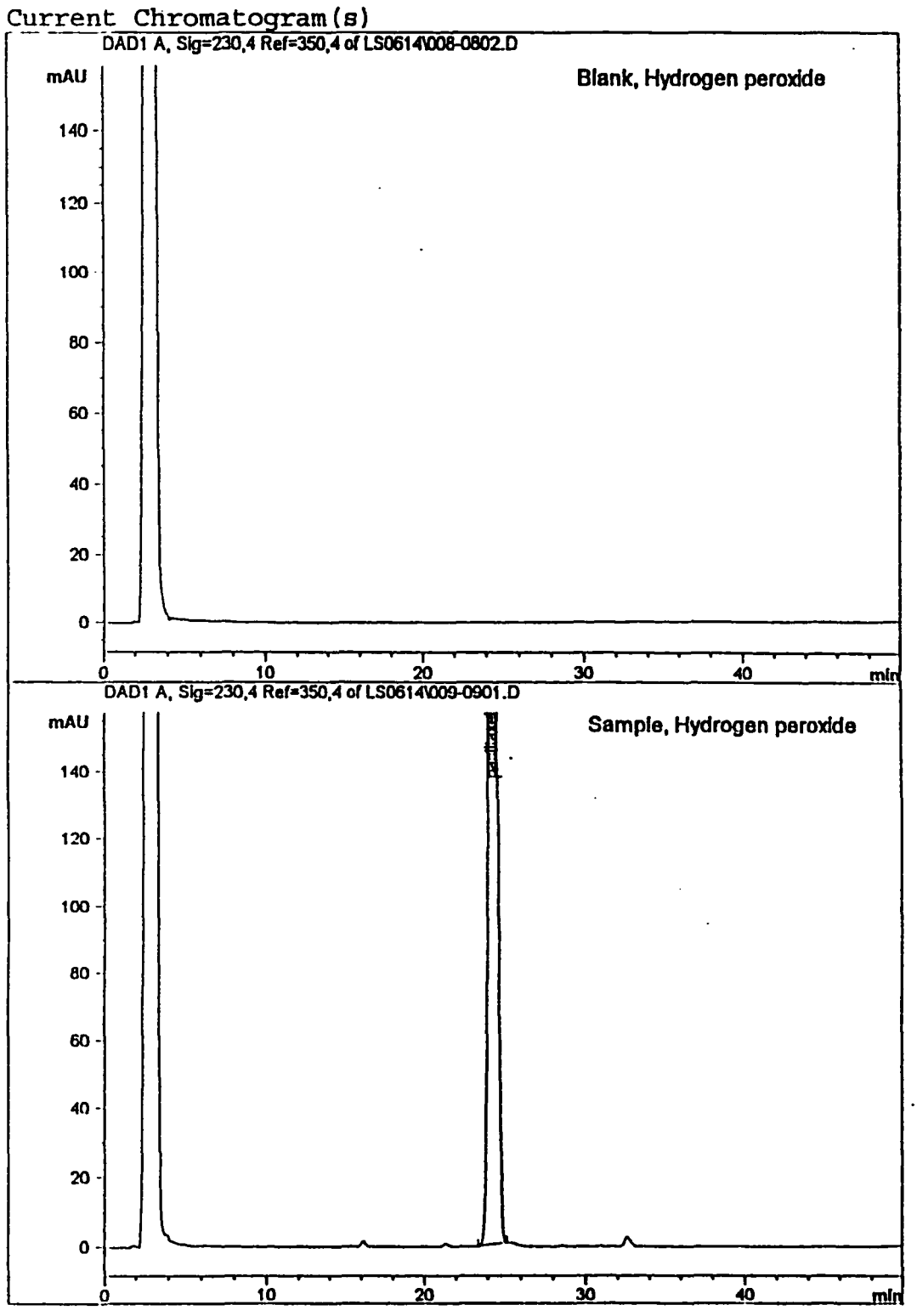

Figure 17. Chromatograms showing the effect of degradation by H_2O_2. H_2O_2 blank (top) and Paclitaxel degraded by H_2O_2 (bottom).

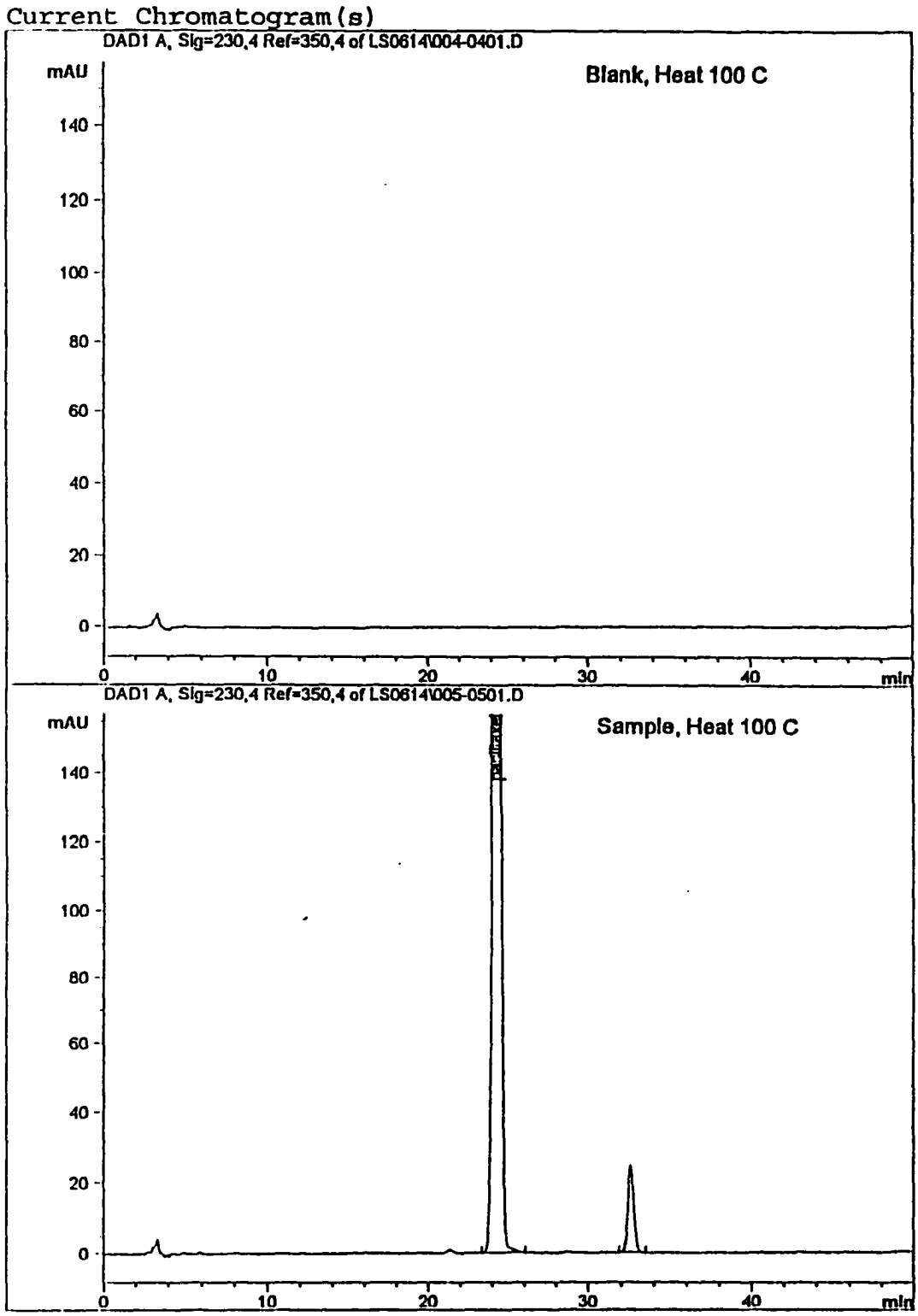

Figure 18. Chromatograms showing the effect of degradation by heat. Heat blank (top) and Paclitaxel degraded by heat (bottom).

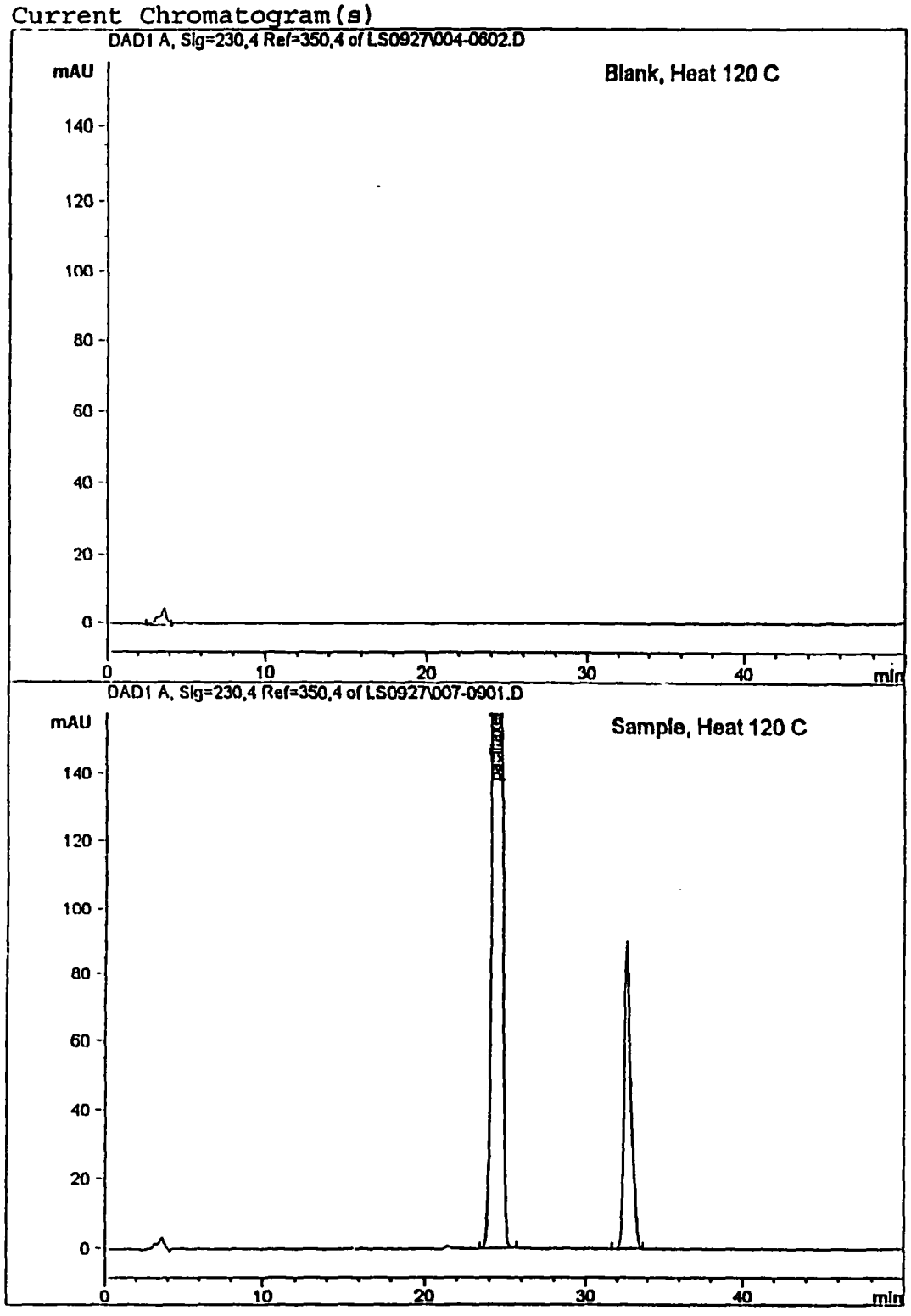

Figure 18. Continued.

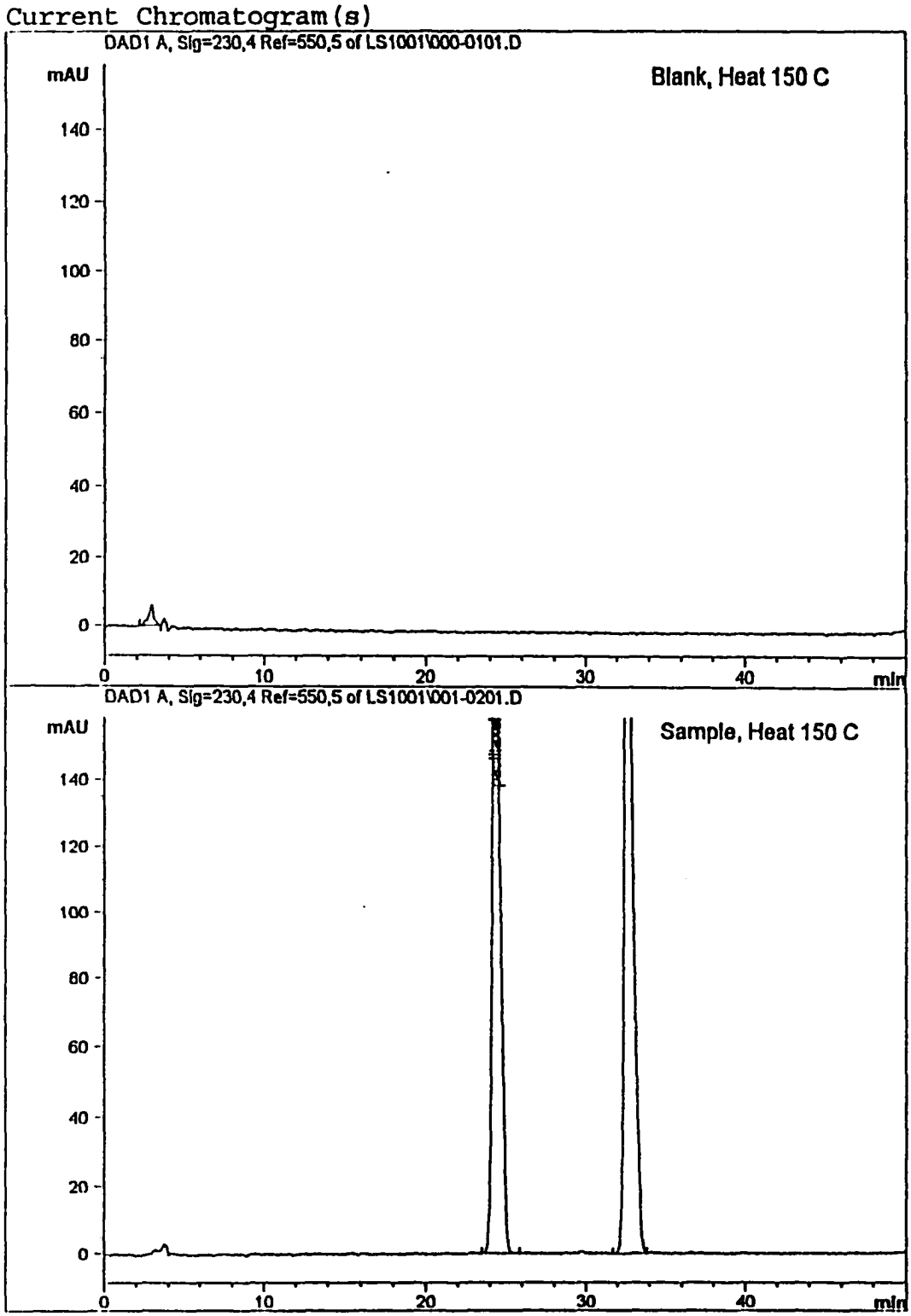

Figure 18. Continued.

Peak Integrity Using HP Diode Array Detector

For each condition, (except base, which totally degraded the paclitaxel), the integrity of the paclitaxel peak was determined using the photodiode array detector and the Hewlett-Packard ^{3D}Chemstation software. Absorption spectra from 200 nm to 400 nm of the peak were acquired, normalized, and overlaid. It is clear by visual comparison and by the purity factor calculated by the software that the paclitaxel peak contains only a single component as shown on Figure 19-23 respectively for forced degradations under UV light, visible light, acid, oxidation and heat.

Purity results peak 6 at 24.296 min.

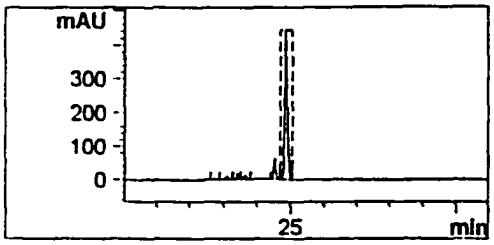

Data : 005-0701.D
Signal : DAD1 A
Peak : 6 at 24.296 min
Date : 9/27/96 11:25:25 PM

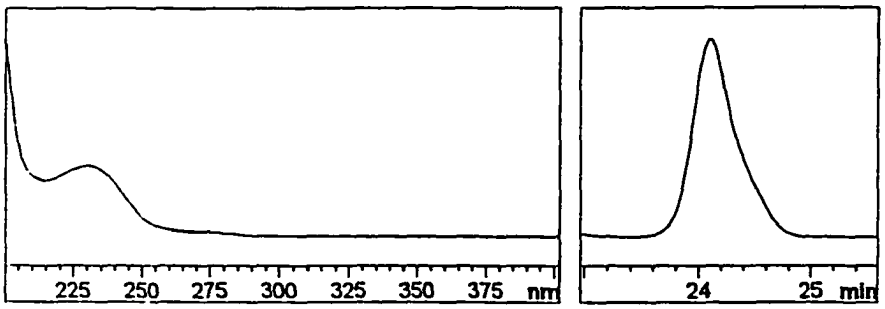

-> The purity factor is within the calculated threshold limit. <-

Purity factor : 999.99 (100% of spectra)
Threshold : 990 (Set by user)
Reference : Nearest Peak baseline spectra (stored)
(0.231167 / 54.884833)
Spectra : 3 (Selection automatic, All)
Warning : Spectral absorbances > 1000 mAU

Peak spectra
1 DAD1,24.149 (757 mAU,Up2) Ref= 0.231 & 54.885
2 DAD1,24.298 (1243 mAU,Apx) Ref= 0.231 & 54.885
3 DAD1,24.430 (934 mAU,Dn1) Ref= 0.231 & 54.885

Peak signals
1 DAD1 A, Sig=230,4 Ref=350,4 of LS0927\005-0701.D (0 mAU)

*** End of Report ***

Figure 19. Paclitaxel peak purity under forced degradation by UV light.

Purity results peak 2 at 24.296 min.

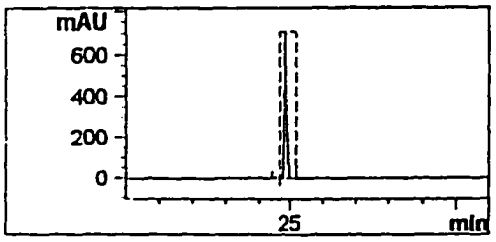

Data : 006-0801.D
Signal : DAD1 A
Peak : 2 at 24.296 min
Date : 9/28/96 1:46:48 AM

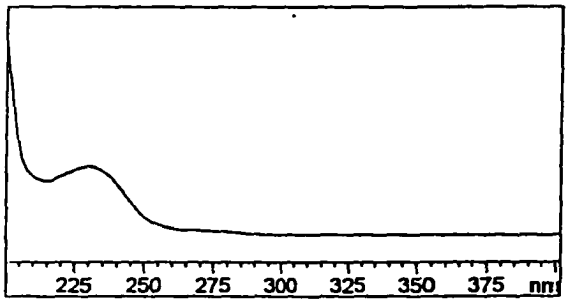

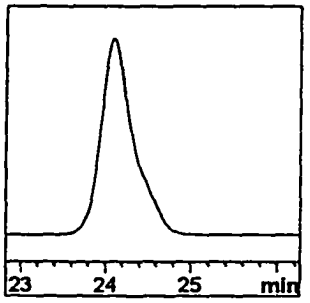

-> The purity factor is within the calculated threshold limit. <-

Purity factor : 999.866 (100% of spectra)
Threshold : 990 (Set by user)
Reference : Nearest Peak baseline spectra (stored)
(0.175667 / 54.8945)
Spectra : 5 (Selection automatic, All)
Warning : Spectral absorbances > 1000 mAU

Peak spectra
1 DAD1,24.153 (1220 mAU,Up2) Ref= 0.176 & 54.895
2 DAD1,24.302 (1917 mAU,Apx) Ref= 0.176 & 54.895
3 DAD1,24.430 (1444 mAU,Dn1) Ref= 0.176 & 54.895
4 DAD1,24.689 (540 mAU,Dn2) Ref= 0.176 & 54.895
5 DAD1,24.778 (360 mAU,Dn1) Ref= 0.176 & 54.895

Peak signals
1 DAD1 A, Sig=230,4 Ref=350,4 of LS0927\006-0801.D (0 mAU)

*** End of Report ***

Figure 20. Paclitaxel peak purity under forced degradation by visible light.

Purity results peak 6 at 24.264 min.

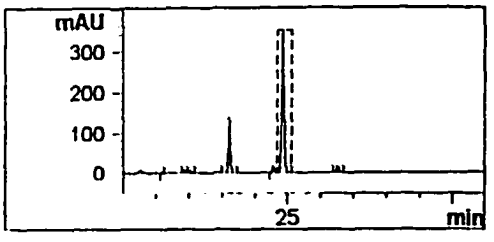

Data : 007-0701.D
Signal : DAD1 A
Peak : 6 at 24.264 min
Date : 6/15/96 5:03:55 AM

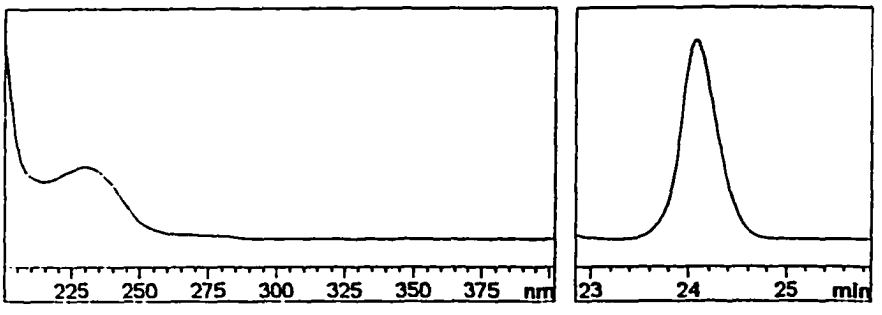

-> The purity factor is within the calculated threshold limit. <-

Purity factor : 999.885 (100% of spectra)
Threshold : 990 (Set by user)
Reference : Peak Apex (integrated) (24.266333)
Spectra : 2 (Selection automatic, 3)

Peak spectra
1 DAD1,24.117 (381 mAU,Up2) Ref=24.266
2 DAD1,24.397 (233 mAU,Dn1) Ref=24.266

Peak signals
1 DAD1 A, Sig=230,4 Ref=350,4 of LS0614\007-0701.D (0 mAU)

*** End of Report ***

Figure 21. Paclitaxel peak purity under forced degradation by HCL.

Purity results peak 1 at 24.280 min.

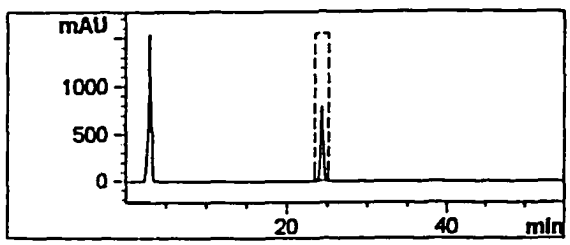

Data : 009-0901.D
Signal : DAD1 A
Peak : 1 at 24.280 min
Date : 6/15/96 9:46:51 AM

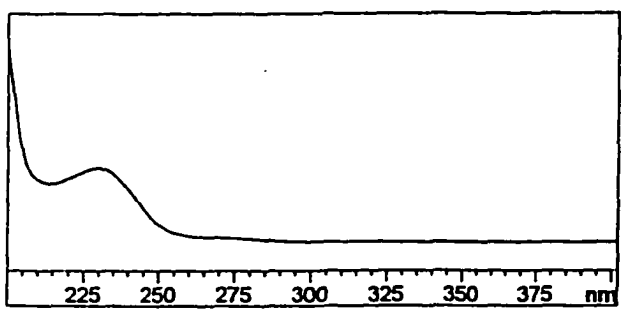

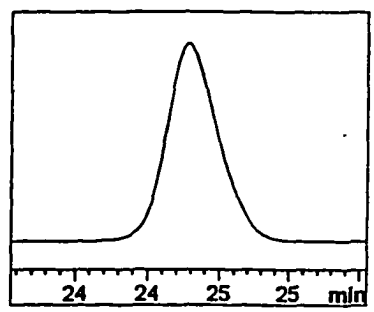

-> The purity factor is within the calculated threshold limit. <-

Purity factor : 999.806 (100% of spectra)
Threshold : 990 (Set by user)
Reference : Nearest Peak baseline spectra (stored)
(0.426167 / 54.887167)
Spectra : 3 (Selection automatic, All)
Warning : Spectral absorbances > 1000 mAU

Peak spectra
1 DAD1,24.128 (1217 mAU,Up2) Ref= 0.426 & 54.887
2 DAD1,24.281 (1990 mAU,Apx) Ref= 0.426 & 54.887
3 DAD1,24.433 (1438 mAU,Dn1) Ref= 0.426 & 54.887

Peak signals
1 DAD1 A, Sig=230,4 Ref=350,4 of LS0614\009-0901.D (0 mAU)

*** End of Report ***

Figure 22. Paclitaxel peak purity under forced degradation by H_2O_2.

Purity results peak 1 at 24.265 min.

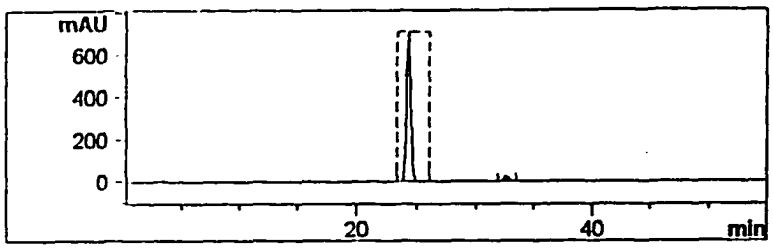

Data : 005-0501.D
Signal : DAD1 A
Peak : 1 at 24.265 min
Date : 6/15/96 12:21:02 AM

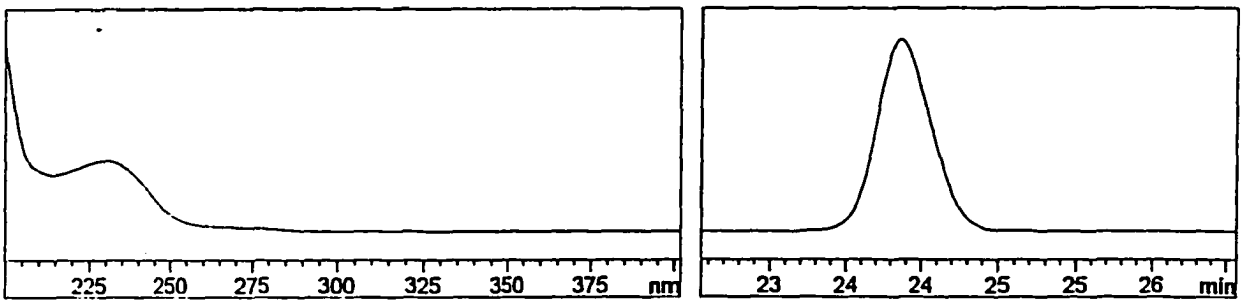

-> The purity factor is within the calculated threshold limit. <-

Purity factor : 999.952 (100% of spectra)
Threshold : 990 (Set by user)
Reference : Nearest Peak baseline spectra (stored) (0.172667 / 54.909333)
Spectra : 3 (Selection automatic, All)
Warning : Spectral absorbances > 1000 mAU

Peak spectra
1 DAD1,24.125 (1238 mAU,Up2) Ref= 0.173 & 54.909
2 DAD1,24.254 (1860 mAU,Apx) Ref= 0.173 & 54.909
3 DAD1,24.445 (1170 mAU,Dn1) Ref= 0.173 & 54.909

Peak signals
1 DAD1 A, Sig=230,4 Ref=350,4 of LS0614\005-0501.D (0 mAU)

*** End of Report ***

Figure 23. Paclitaxel peak purity under forced degradation by heat (100 °C).

Purity results peak 1 at 24.326 min.

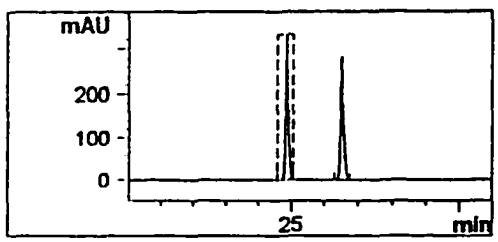

Data : 001-0201.D
Signal : DAD1 A
Peak : 1 at 24.326 min
Date : 10/1/96 6:35:05 PM

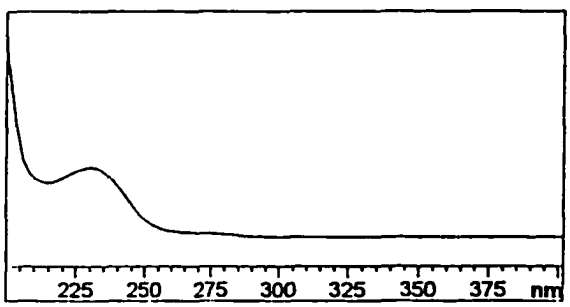

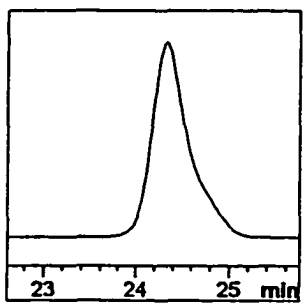

-> The purity factor is within the calculated threshold limit. <-

Purity factor : 999.977 (100% of spectra)
Threshold : 990 (Set by user)
Reference : Peak start and end spectra (integrated) (23.7115 / 25.314167)
Spectra : 3 (Selection automatic, 3)

Peak spectra
1 DAD1,24.059 (179 mAU, -) Ref=23.712 & 25.314
2 DAD1,24.318 (935 mAU,Apx) Ref=23.712 & 25.314
3 DAD1,24.751 (224 mAU, -) Ref=23.712 & 25.314

Peak signals
1 DAD1 A, Sig=230,4 Ref=550,5 of LS1001\001-0201.D (0 mAU)

*** End of Report ***

Figure 23. Continued.
Paclitaxel peak purity under forced degradation by heat (150 °C).

3.5.4 Chromatographic Precision and Repeatability

Paclitaxel peak areas for 33 replicate injections of the bulk drug and the injectable form dissolved in diluent and stored at room temperature were measured over a period of 40 hours. For the bulk drug using Methods A and B, the % RSDs were 1.79% and 0.57% for peak area and 0.087% and 0.077% for retention time, respectively. Results are shown in Tables 12 and 13. For the injectable form using Method C, the % RSD was 1.39% for peak area and 0.102% for retention time. The result is shown in Table 14.

Table 12
Paclitaxel Bulk Drug Chromatographic Precision and Repeatability
Method A - Curosil PFP Column

Run #	Date	Time		Ret.Time [min]	Amount [ng/ul]	Area [mAU*s]	Height [mAU]	Width [min]	Symmetry
1	5/28/96	6:26:47	PM	24.220	530.000	1019.098	50.358	0.309	0.985
2	5/28/96	7:42:30	PM	24.218	576.003	1099.054	54.261	0.317	0.973
3	5/28/96	8:58:09	PM	24.209	565.852	1088.034	53.698	0.316	1.001
4	5/28/96	10:13:49	PM	24.227	531.663	1022.296	50.268	0.316	0.975
5	5/28/96	11:29:32	PM	24.244	534.101	1026.983	50.707	0.317	0.992
6	5/29/96	12:45:12	AM	24.239	534.854	1028.431	51.065	0.301	1.001
7	5/29/96	2:00:52	AM	24.243	544.182	1046.368	51.263	0.315	0.982
8	5/29/96	3:16:33	AM	24.239	534.552	1027.850	51.008	0.312	0.997
9	5/29/96	4:32:14	AM	24.247	538.908	1036.226	51.270	0.306	0.985
10	5/29/96	5:47:55	AM	24.235	539.855	1038.047	51.181	0.308	0.986
11	5/29/96	7:03:36	AM	24.246	534.251	1027.272	50.198	0.319	0.992
12	5/29/96	8:19:18	AM	24.223	535.678	1030.016	50.674	0.312	1.010
13	5/29/96	9:35:01	AM	24.211	535.684	1030.028	50.526	0.312	0.994
14	5/29/96	10:50:43	AM	24.202	536.862	1032.293	50.237	0.318	0.999
15	5/29/96	12:06:24	PM	24.174	539.773	1037.890	52.107	0.311	1.004
16	5/29/96	1:22:05	PM	24.187	535.730	1030.116	51.884	0.310	1.033
17	5/29/96	2:37:48	PM	24.207	541.702	1041.599	52.542	0.304	1.016
18	5/29/96	3:53:30	PM	24.192	542.358	1042.860	52.184	0.308	1.004
19	5/29/96	5:09:12	PM	24.197	533.334	1025.508	51.578	0.308	1.021
20	5/29/96	6:24:55	PM	24.198	538.781	1035.982	52.574	0.305	0.989
21	5/29/96	7:40:37	PM	24.196	533.220	1025.290	51.391	0.310	1.005
22	5/29/96	8:56:21	PM	24.193	539.794	1037.930	52.033	0.308	0.988
23	5/29/96	10:12:02	PM	24.192	536.442	1031.485	51.894	0.308	0.997
24	5/29/96	11:27:45	PM	24.211	544.174	1046.352	52.788	0.307	1.014
25	5/30/96	12:43:27	AM	24.211	537.413	1033.353	52.456	0.303	1.031
26	5/30/96	1:59:11	AM	24.229	587.374	1089.007	56.866	0.306	1.032
27	5/30/96	3:14:54	AM	24.227	550.177	1057.895	53.017	0.309	1.038
28	5/30/96	4:30:34	AM	24.238	539.630	1037.615	54.943	0.289	1.000
29	5/30/96	5:46:14	AM	24.225	538.097	1034.666	52.249	0.309	1.035
30	5/30/96	7:01:54	AM	24.233	545.992	1049.848	53.430	0.305	1.030
31	5/30/96	8:17:35	AM	24.220	546.358	1050.551	53.213	0.303	1.037
32	5/30/96	9:33:16	AM	24.183	539.909	1038.151	52.488	0.305	1.042
33	5/30/96	10:48:56	AM	24.180	542.357	1042.858	54.375	0.296	1.003
			Mean:	24.215	541.972	1040.635	52.143	0.309	1.006
			S.D.:	0.021	12.228	23.512	1.515	0.006	0.020
			RSD	0.087	0.087	1.794	2.256	2.906	2.061
			T99*S.D.:	0.008	4.336	8.337	0.537	0.002	0.007

Table 13
Paclitaxel Bulk Drug Chromatographic Precision and Repeatability
Method B - Whatman TAC-1 Column

Run #	Date	Time		Ret.Time [min]	Amount [ng/ul]	Area [mAU*s]	Height [mAU]	Width [min]	Symmetry
1	6/12/96	12:08:40	PM	16.853	572.652	6765.801	673.030	0.155	1.024
2	6/12/96	12:54:16	PM	16.863	571.158	6748.160	682.337	0.153	1.061
3	6/12/96	1:39:52	PM	16.865	579.000	6840.807	716.464	0.148	1.054
4	6/12/96	2:36:25	PM	16.878	575.531	6799.821	701.113	0.149	1.089
5	6/12/96	3:51:59	PM	16.882	578.825	6838.745	709.811	0.149	1.101
6	6/12/96	5:07:35	PM	16.890	572.842	6768.056	691.179	0.151	1.112
7	6/12/96	6:23:11	PM	16.896	580.211	6855.113	705.371	0.150	1.096
8	6/12/96	7:38:47	PM	16.895	580.922	6863.521	712.690	0.148	1.116
9	6/12/96	8:54:23	PM	16.898	572.764	6767.135	695.113	0.150	1.121
10	6/12/96	10:09:59	PM	16.904	574.145	6783.440	703.301	0.149	1.111
11	6/12/96	11:25:34	PM	16.902	574.001	6781.746	694.638	0.151	1.113
12	6/13/96	12:41:11	AM	16.901	574.026	6782.044	696.730	0.150	1.109
13	6/13/96	1:56:47	AM	16.892	572.636	6765.620	691.822	0.151	1.106
14	6/13/96	3:12:22	AM	16.900	571.398	6750.988	666.315	0.157	1.090
15	6/13/96	4:27:59	AM	16.905	572.836	6767.977	679.609	0.154	1.102
16	6/13/96	5:43:36	AM	16.899	578.922	6839.886	680.058	0.156	1.069
17	6/13/96	6:59:11	AM	16.895	578.898	6839.603	689.110	0.153	1.114
18	6/13/96	8:14:48	AM	16.885	572.345	6762.181	671.205	0.156	1.083
19	6/13/96	9:30:25	AM	16.904	579.058	6841.492	682.628	0.155	1.120
20	6/13/96	10:46:01	AM	16.896	573.042	6770.416	641.973	0.164	1.075
21	6/13/96	12:01:38	PM	16.891	571.638	6753.829	634.072	0.166	1.056
22	6/13/96	1:17:14	PM	16.893	579.972	6852.293	657.344	0.162	1.063
23	6/13/96	2:32:50	PM	16.886	577.847	6827.181	659.360	0.161	1.077
24	6/13/96	3:48:27	PM	16.886	577.787	6826.473	654.719	0.162	1.070
25	6/13/96	5:04:03	PM	16.864	570.336	6738.442	628.239	0.167	1.080
26	6/13/96	6:19:39	PM	16.869	575.698	6801.790	634.307	0.167	1.070
27	6/13/96	7:35:16	PM	16.885	571.803	6755.772	619.473	0.170	1.059
28	6/13/96	8:50:53	PM	16.887	571.854	6756.380	634.654	0.166	1.079
29	6/13/96	10:06:29	PM	16.892	571.550	6752.781	618.001	0.171	1.073
30	6/13/96	11:22:05	PM	16.889	572.661	6765.911	603.622	0.176	1.049
31	6/14/96	12:37:42	AM	16.889	571.549	6752.776	596.565	0.178	1.012
32	6/14/96	1:53:18	AM	16.892	572.109	6759.389	599.563	0.177	1.007
33	6/14/96	3:08:55	AM	16.895	572.201	6760.476	592.685	0.179	0.991
			Mean:	16.889	574.613	6788.971	664.155	0.159	1.077
			S.D.:	0.013	3.268	38.608	37.242	0.010	0.034
			RSD	0.077	0.077	0.569	0.569	5.607	6.093
			T99*S.D	0.005	1.159	13.690	13.205	0.003	0.012

Table 14
Chromatographic Precision and Repeatability of Paclitaxel Injectable
Method C - Curosil PFP Column

Run #	Date	Time		Ret.Time [min]	Area [mAU*s]	Height [mAU]	Width [min]	Symmetry
1	5/31/96	2:56:49	PM	24.113	8834.062	468.469	0.283	1.050
2	5/31/96	4:12:34	PM	24.094	8976.540	480.862	0.280	1.061
3	5/31/96	5:28:16	PM	24.080	8864.706	474.788	0.280	1.080
4	5/31/96	6:44:05	PM	24.054	8806.119	477.423	0.277	1.053
5	5/31/96	7:59:47	PM	24.065	8914.229	476.456	0.283	1.046
6	5/31/96	9:15:29	PM	24.065	8982.185	475.769	0.280	1.050
7	5/31/96	10:31:11	PM	24.059	8777.744	463.016	0.280	1.037
8	5/31/96	11:46:53	PM	24.073	8804.715	462.408	0.288	1.031
9	6/1/96	1:02:36	AM	24.093	8853.419	486.282	0.264	1.093
10	6/1/96	2:18:19	AM	24.092	8847.460	459.196	0.288	1.059
11	6/1/96	3:34:01	AM	24.067	8945.893	467.648	0.288	1.039
12	6/1/96	4:49:44	AM	24.087	8873.106	465.964	0.280	1.061
13	6/1/96	6:05:27	AM	24.078	8846.006	463.206	0.280	1.041
14	6/1/96	7:21:10	AM	24.073	8875.984	464.517	0.288	1.048
15	6/1/96	8:36:52	AM	24.064	8934.040	468.571	0.280	1.038
16	6/1/96	9:52:36	AM	24.048	9234.588	482.969	0.288	1.047
17	6/1/96	11:08:19	AM	24.045	9262.767	488.446	0.288	1.063
18	6/1/96	12:24:02	PM	24.053	9287.654	481.952	0.288	1.029
19	6/1/96	1:39:46	PM	24.073	8834.462	457.955	0.280	1.043
20	6/1/96	2:55:30	PM	24.069	8845.612	457.970	0.288	1.034
21	6/1/96	4:11:14	PM	24.063	8857.526	474.756	0.272	1.014
22	6/1/96	5:26:57	PM	24.072	8835.116	456.490	0.288	1.024
23	6/1/96	6:42:41	PM	24.063	8864.434	457.823	0.288	1.045
24	6/1/96	7:58:25	PM	24.072	8833.923	474.347	0.280	1.100
25	6/1/96	9:14:09	PM	24.043	8889.190	460.935	0.280	1.057
26	6/1/96	10:29:53	PM	24.048	8861.293	469.854	0.283	1.050
27	6/1/96	11:45:37	PM	24.048	8906.563	469.983	0.280	1.060
28	6/2/96	1:01:18	AM	24.028	8847.313	459.849	0.288	1.035
29	6/2/96	2:16:58	AM	24.023	8842.714	459.314	0.288	1.031
30	6/2/96	3:32:40	AM	24.022	8829.964	460.901	0.288	1.033
31	6/2/96	4:48:21	AM	24.003	8895.604	465.198	0.288	1.038
32	6/2/96	6:04:03	AM	24.014	8882.307	460.764	0.280	1.044
33	6/2/96	7:19:45	AM	24.013	8868.219	480.721	0.272	0.995
		Mean:		24.059	8903.499	468.933	0.283	1.046
		S.D.:		0.025	123.736	9.259	0.006	0.020
		RSD		0.102	1.390	1.390	1.974	2.063
		T99*S.D.:		0.009	43.875	3.283	0.002	0.007

3.5.5 Stability In Diluent

Solutions of the bulk and injectable forms were prepared in diluent and aliquots injected into the HPLC over a 40 hour storage period at room temperature. Only for the injectable form did an extraneous peak appear. The peak, which appeared at 30 hours of storage, had a retention time relative to paclitaxel of 0.1, and probably originated from the emulsifier Cremophor EL. Results are summarized in Figures 24-26.

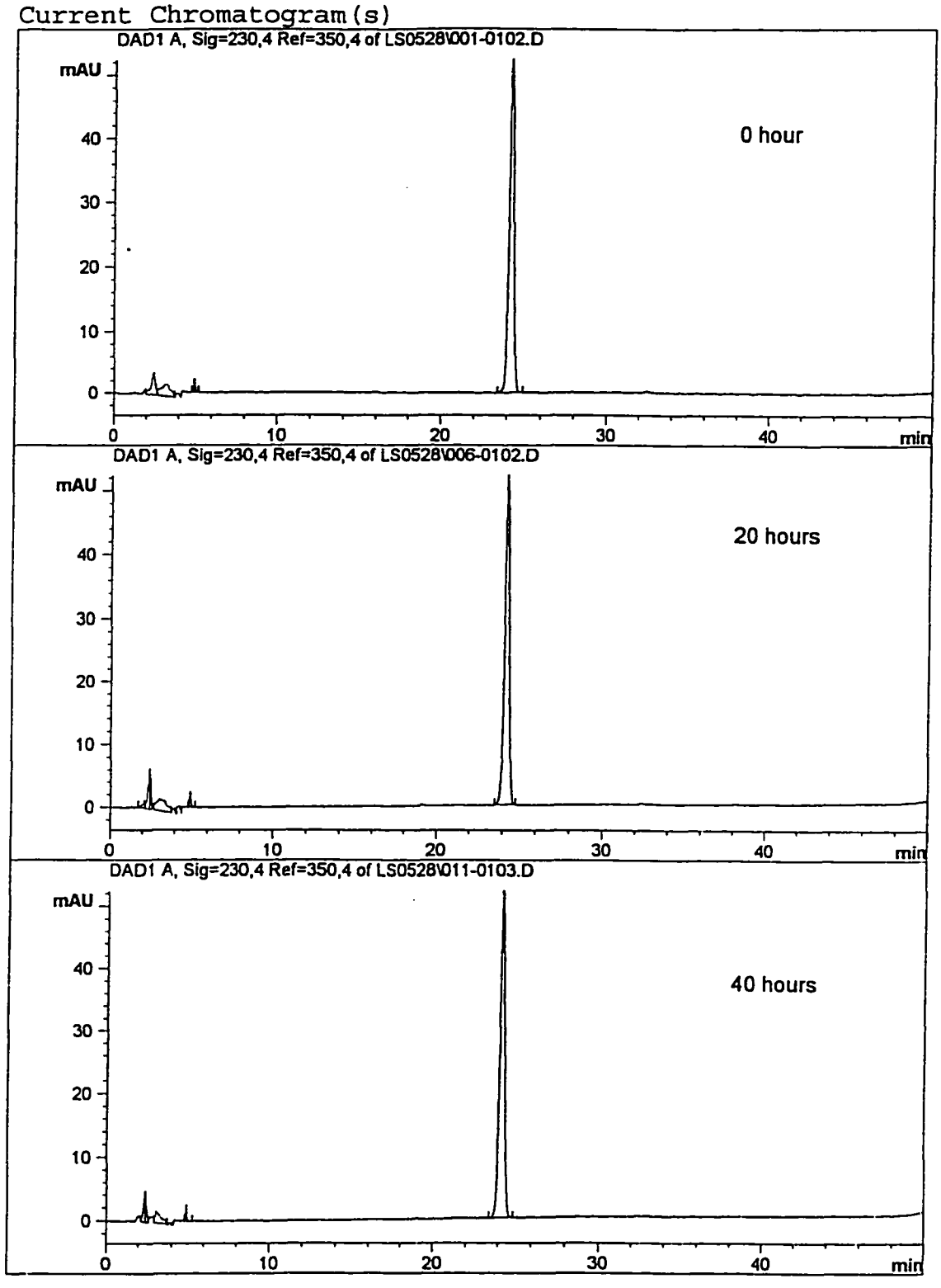

Figure 24. Paclitaxel bulk drug stability in diluent - Method A.

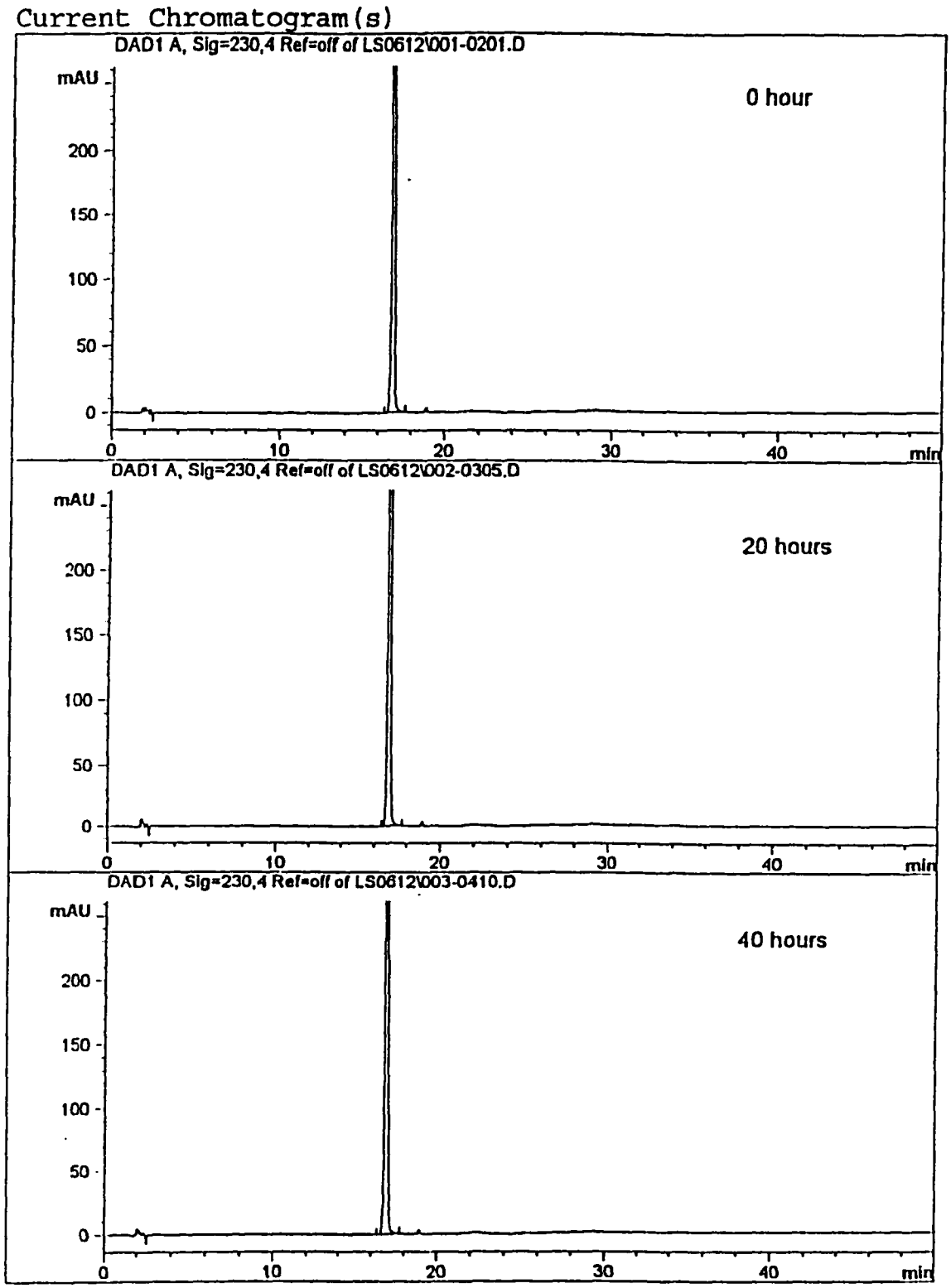

Figure 25. Paclitaxel bulk drug stability in diluent - Method B.

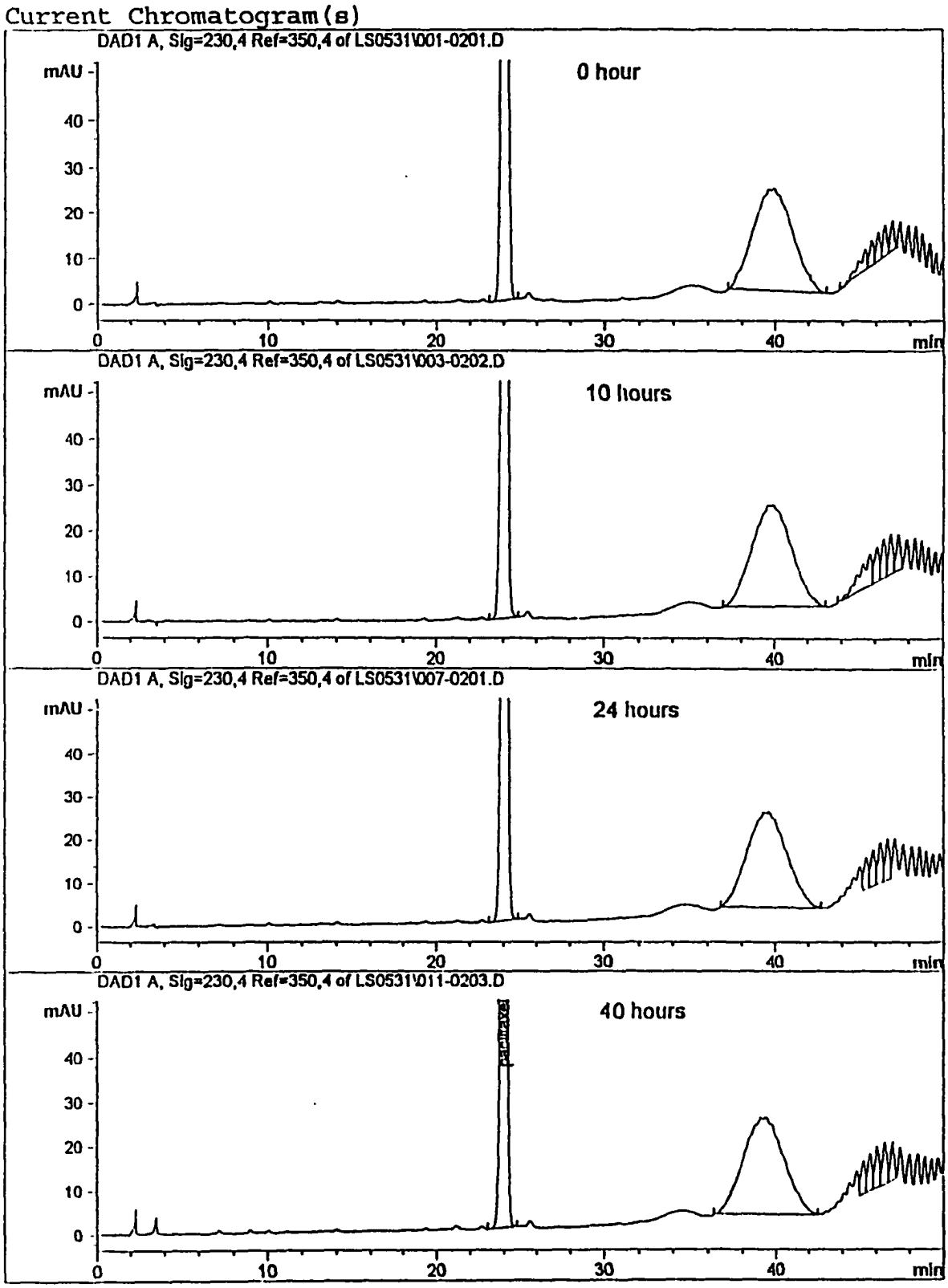

Figure 26. Paclitaxel injectable dosage form stability in diluent - Method C.

3.5.6 Limits Of Detection And Quantitation

The limit of detection (LOD) for paclitaxel, defined as the concentration injected producing a peak height 3 times the peak-to-peak noise, was 0.37 μg/mL, corresponding to 5.6 ng injected, for Method A, and was 0.31 μg/mL (4.6 ng) for Method B. The limit of quantitation is defined as three times the LOD and is thus 1.11 μg/mL (17 ng injected) and 0.93 μg/mL (14 ng), respectively, for Methods A and B.

3.5.7 Linearity And Range

The peak areas of paclitaxel over the range from 1.0 μg/mL to 1.5 mg/mL (0.2% to 300% of the working standard concentration of 500 μg/mL) were measured in triplicate. The R^2 values of the linear regression line were 0.9997 (n=9) for Method A and 0.9999 (n=9) for Method B. See Figures 27 and 28.

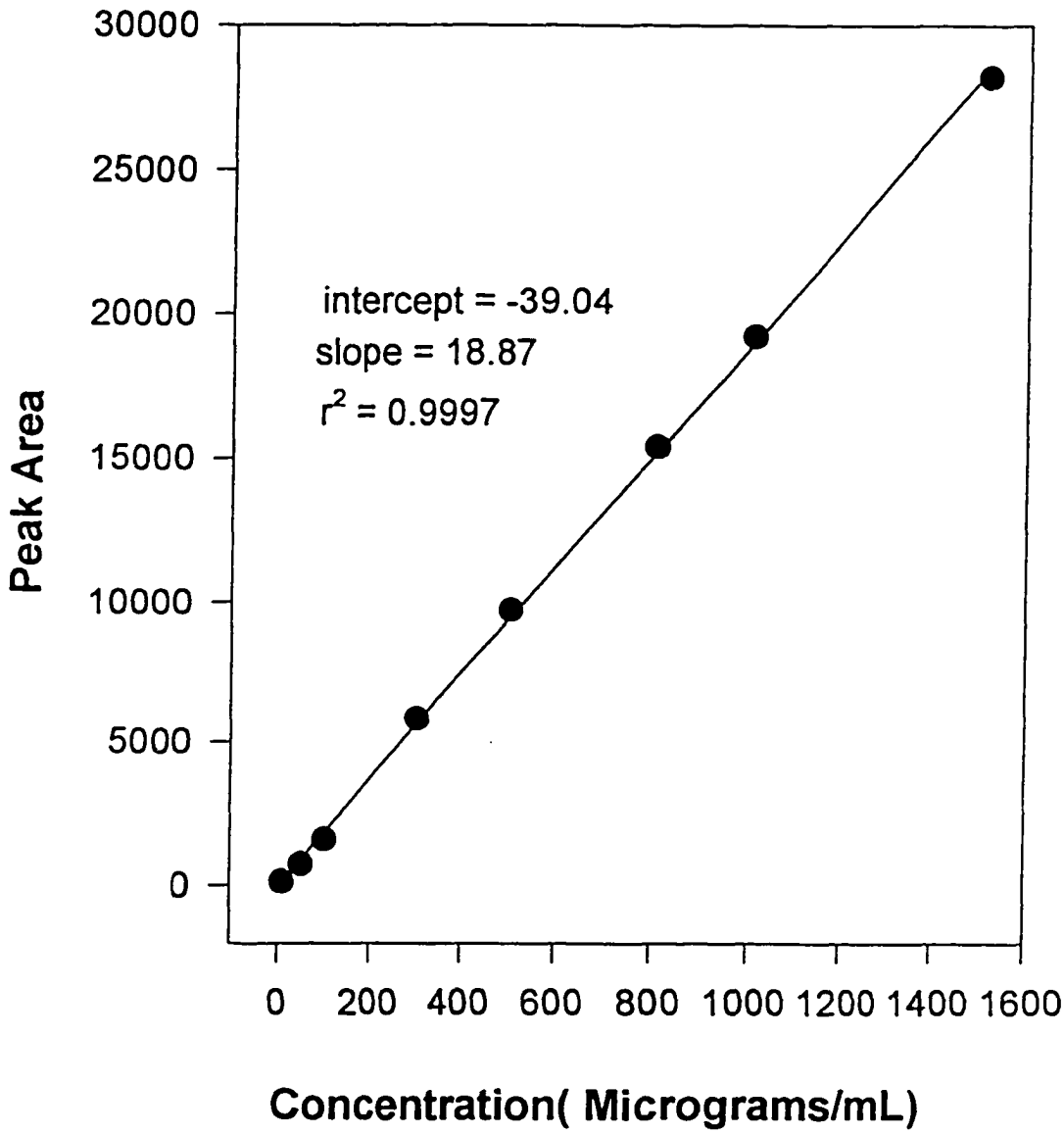

Figure 27. Linearity of Paclitaxel bulk drug - method A.

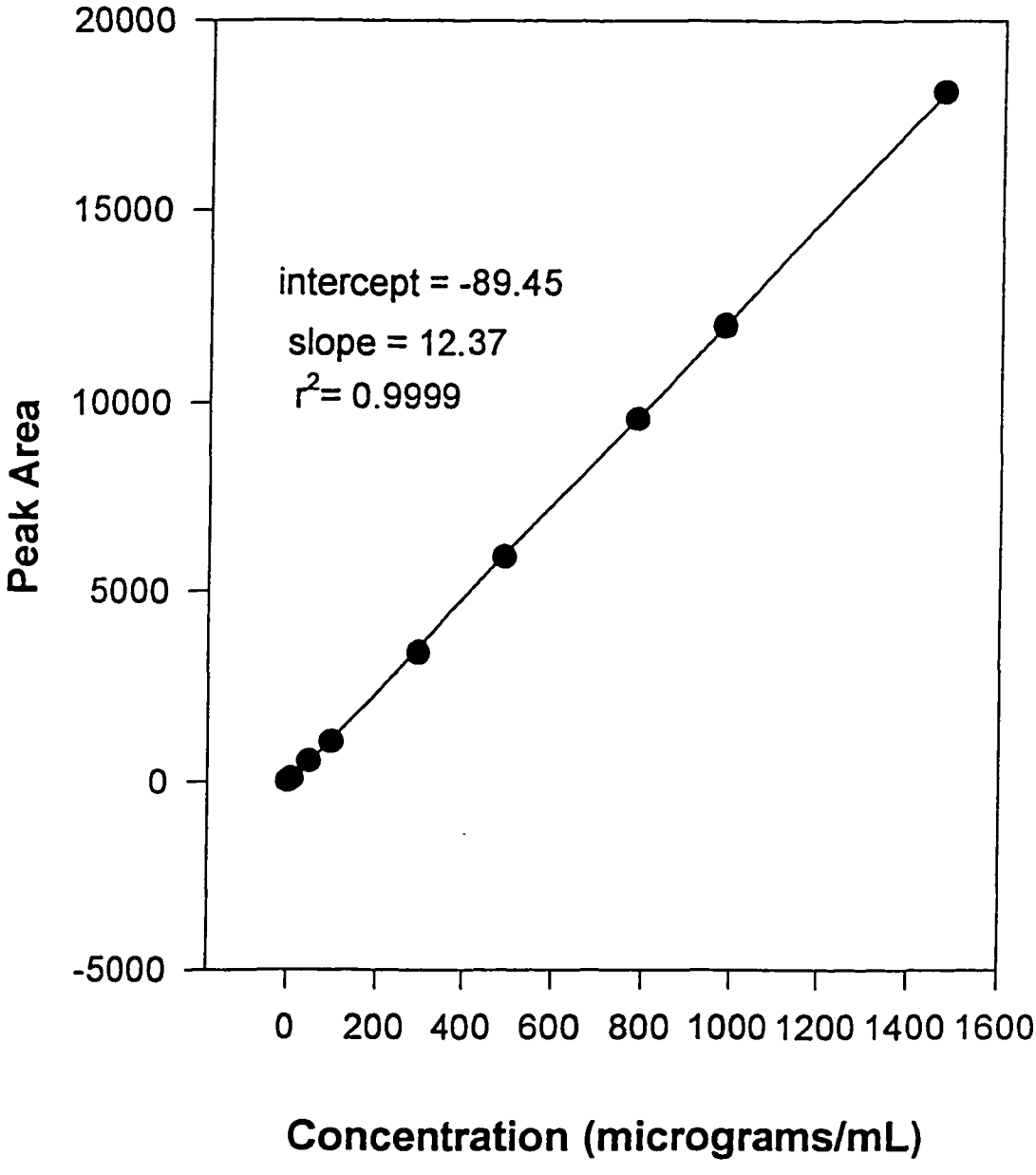

Figure 28. Linearity of Paclitaxel bulk drug - method B.

3.5.8 Ruggedness

The ruggedness of an analytical method is the degree of reproducibility of test results obtained by the analysis of the same samples under a variety of normal test conditions such as different laboratories, different analysts, different instruments, different lot of reagents, different lot of columns and different elapsed assay times. Due to the nature of this research (only one analyst) and laboratory conditions (only one HPLC instrument available), the method ruggedness was determined in two ways. First, storage of the paclitaxel working standard at 3°C for one week and assayed repetitively for paclitaxel gave a % RSD of 1.09%, indicating the compound is stable for at least one week at 3°C. Second, two different Whatman TAC-1 columns were tested on different days with different mobile phases. The system suitability test solution and the paclitaxel standard solution were chromatographed, and all peaks were baseline-separated on both columns.

3.5.9 Robustness

The robustness of an analytical procedure is a measure of its capacity to remain unaffected by small but deliberate variations in method parameters and provides an indication of its reliability during normal usage. The robustness of the method was determined by changing the gradient rate from 0.422 to 0.444 to 0.488%/min with a fixed 40% ACN starting composition. It produced no statistically significant change in resolution or peak symmetry, as shown in Tables 15 and 16.

Table 15. Robustness of Method A

Resolution

Starting Acetonitrile %	**40**	**40**	**40**
Gradient Rate ACN %/min	**0.422**	**0.444**	**0.488**
Taxane # 1 - # 4	17.44	17.69	16.38
Taxane # 4 - # 2	1.23	1.68	1.56
Taxane # 2 - # 6	5.34	5.34	4.79
Taxane # 6 - # 3	2.24	2.10	2.41
Taxane # 3 - # 7	3.16	3.12	2.97
Taxane # 7 - # 5	4.23	4.40	4.66
Taxane # 5 - # 8	2.37	2.30	2.06
Taxane # 8 - # 9	1.51	1.70	1.60
Taxane # 9 - # 10	12.36	12.51	12.45
Taxane # 10 - # 11	3.19	3.24	3.25
Taxane # 11 - # 12	3.01	2.97	2.88
Taxane # 12 - # 13	2.47	2.22	2.37
Taxane # 13 - # 14	4.01	3.75	3.65
Taxane # 14 - # 15	10.3	10.52	10.69

Table 16. Robustness of Method A

Peak Symmetry

Starting Acetonitrile %	**40**	**40**	**40**
Gradient Rate ACN (%/min)	**0.422**	**0.444**	**0.488**
Taxane # 1	0.97	0.98	0.95
Taxane # 4	1.08	0.98	1.03
Taxane # 2	0.94	1.04	1.00
Taxane # 6	1.06	1.04	1.03
Taxane # 3	1.00	0.97	1.08
Taxane # 7	1.04	0.99	0.99
Taxane # 5	1.09	1.06	1.09
Taxane # 8	1.05	1.04	1.03
Taxane # 9	1.04	0.99	0.99
Taxane # 10	1.08	1.03	1.08
Taxane # 11	1.05	1.01	1.01
Taxane # 12	1.08	1.08	1.05
Taxane # 13	1.00	1.02	1.02
Taxane # 14	1.04	1.07	1.06
Taxane # 15	1.06	1.04	1.04

3.6 Metal Contents in Cremophor EL

Cremophor EL from BASF, lot 34-1224 and lot 77-1278 were analyzed for the metal contents by ICP - AES. The method was described in section 2.5.2. and results are shown in Table 17.

Table 17. Metal Content in Cremophor EL

Element	Cremophor EL(lot 34-1224)	Cremophor EL(lot 77-1278)
K	201 ppm	170 ppm
Na	17.83 ppm	15.1 ppm
Ca	0	0
Mg	0	0
Cd	0.197 ppm	0.05 ppm
Ni	1.1 ppm	0.6 ppm
Zn	5.27 ppm	3.5 ppm
Fe	0	0
Mn	0	0
Se	0	0
Mo	0	0
As	0	0
Cu	0	0

3.7 Determination of Molar Absorptivity of Various Taxanes by HPLC

According to the Beer-Lambert law, the amount of light passing through a solution absorbed or transmitted is an exponential function of both the concentration of the absorber (provided that the solvent is transparent to the radiation in that region) and the length of the path of the radiation through the sample. The Beer-Lambert law can be expressed in the following equation:

$$\log I_0 / I = \varepsilon cb = A \qquad (3.5)$$

where I_0 = intensity of incident radiant energy, I = intensity of transmitted radiant energy, c = molar concentration of the solute, b = internal length of cell (cm), A = absorbance and ε is the molar absorptivity of the substance whose light absorption is under investigation. ε is a constant and is characteristic of a given absorbing molecule or ion in a particular solvent at a particular wavelength. ε is numerically equal to the absorbance of a solution of unit molar concentration (c = 1) in a cell of unit length (b = 1).

Using HPLC with an absorption detector, the molar absorptivity of a compound can be measured experimentally by dividing the peak height by the concentration. Although the concentration of the solute in the solution injected into the column is a known quantity, this concentration is decreased as the band eluting from the chromatographic column spreads and is diluted. The concentration at peak maximum is defined as $C_{max.}$ Assuming the peak has a Gaussian profile, the relationship between the C_{max} and the mass of injected solute m is [63]:

$$C_{max} = m(\sqrt{N})/ V_R (\sqrt{2\pi}) \qquad (3.6)$$

where:

$m = C_0 \times V_{0,}$

C_0 = initial concentration of solute in the sample,

V_0 = injected sample volume,

N (number of theoretical plates) = $5.54 (t_R/w_{1/2})$,

where:

t_R = the retention time,

$w_{1/2}$ = the peak width at half height,

V_R = the retention volume in mL.

HPLC method A was used to determine the molar absorptivity. Thirteen taxanes in MeOH at an initial concentration of 50 μg/mL each in the Hauser standard was used in the experiment. The actual concentration of paclitaxel in the taxane mixture was found to be 54 μg/mL, because of the evaporation of solvent MeOH. This value was employed as the initial concentration C_0 for all other taxanes in the mixture.

In Table 18 are listed the molar absorptivities at 230 nm of the thirteen taxanes determined by HPLC. It can be seen that taxanes #1, #2 and #5, which do not have a side chain, have the smallest ε values. Taxane #6 has considerably higher ε than taxane #7. The only difference between taxane #6 and #7 is phenyl versus n-pentyl at the end of the side chain. The stronger conjugation between the adjacent carbonyl group to phenyl than n-pentyl lowers the energy of the n - π^* transition, thus the higher ε value for taxane #6. Similarly, taxane # 6 gains ε about 8554 L/mole·cm over taxane #4, taxane #12 also gains 8687 L/mole over taxane #10, because of the phenyl versus the isobutylene at the end of the side chain. Taxanes #12 and #15 have almost the same values of ε, which indicates that epimerization of the hydroxyl group does not effect the electronic transition. Taxane #10 has a

larger ε than taxane #14; the only difference is the former consists of isobutylene at the end of the side chain while the latter consists of n-pentyl. There is no conjugation between the adjacent carbonyl group and n-pentyl group, thus a higher energy level of electronic transition and the lower ε.

Table 18. Molar Absorptivity of Taxanes

Taxane #	t (min)	N	Cmax(μg/mL)	Height(mAU)	MW	μmoles	ε (L/mole·cm)
1	5.789	4765	3.8532	70.87	544	0.007083	16676
4	9.301	8137	3.1340	45.76	921	0.003403	22413
2	9.968	8399	2.9710	42.23	609	0.004878	14427
6	10.952	9728	2.9101	57.34	943	0.003086	30967
7	12.446	11157	2.7424	31.81	937	0.002927	18114
5	14.507	11385	2.3767	25.21	686	0.003465	12127
8	14.932	10278	2.1940	44.58	985	0.002227	33358
9	15.665	12042	2.2637	56.19	811	0.002791	33552
10	20.857	16344	1.9807	27.24	831	0.002384	19047
11	22.219	17094	1.9015	38.54	811	0.002345	27396
12	23.686	18429	1.8521	36.13	853	0.002171	27734
14	26.347	21663	1.8052	20.67	847	0.002131	16164
15	31.927	26229	1.6392	31.84	853	0.001922	27615

3.8 Conclusions

Four reversed phase liquid chromatographic methods using pentafluorophenyl (PFP) stationary phases were developed for determination of paclitaxel and related taxanes in bulk drug and injectable dosage form. Baseline resolution of 15 taxanes including paclitaxel was achieved in less than 20 min on a Whatman PFP column and in 30 min on a Phenomenex Curosil-PFP column, both using an aqueous acetonitrile gradient. Paclitaxel is well resolved from 7-epi-10-deacetyltaxol, cephalomannine, its benzyl analog, and other closely related compounds. The methods developed for the injectable drug form allow good resolution of the taxanes from the excipient Cremophor EL, a polyethoxylated castor oil used with ethanol to solubilize the paclitaxel. The HPLC methods developed are suitable for the determination of potency, content uniformity, and degradation profile of the paclitaxel bulk drug and injectable form. The methods for the bulk drug were fully validated in terms of accuracy, precision, including chromatographic precision and repeatability, and stability in diluent, specificity including forced degradation, limits of detection and quantitation, and linearity and range. The methods for the paclitaxel injectable form were partially validated.

It was demonstrated perfectly that the performance characteristics of the methods meet the requirements for the intended analytical applications. The quantitative HPLC methods are sensitive, selective, accurate, precise, rugged, and stability-indicating. The methods are specific for paclitaxel in the presence of forced degradation products in the bulk drug form, and from these compounds and excipients in the injectable dosage form.

The elution order of taxanes is apparently related to molecular size, the number of acetylated hydroxyl groups, and the substitution of a xylosyl group at the carbon -7 position.

An analysis of variance calculation using SAS for the data for all 13 taxanes indicates the starting composition and gradient rate have a statistically significant effect on k' and resolution as suggested by ANOVA.

Thermodynamics of the separation were studied over the temperature range from 30 °C to 70 °C and enthalpies of transfer, $\Delta H°$, determined. Conversion of a hydroxyl group to an acetyl group, which can interact more strongly with the PFP stationary phase, has a large effect on the $\Delta H°$, as does

the addition of a xylosyl derivative to the 7-hydroxy. For the later-eluting taxanes (#10-15), the enthalpies on the Curosil-PFP column are generally larger than those on the TAC-1 column, reflecting weaker solute adsorptive interactions with the latter. The entropy-related quantities are generally similar on both columns.

APPENDIX I

SAS Computer Program to Analyze Retention Time, Capacity Factor, Resolution and Selectivity by Analysis of Variance (ANOVA)

SAS Computer Program to Analyze

Retention Time and Capacity Factor by ANOVA

```
options nocenter linesize = 256;
data ls;
 do peak = 1 to 13;
      do start = 1 to 3;
           do rate = 1 to 3;
infile '0603cff.dat';
input y @@;
output;
           end;
     end;
 end;
proc glm;
class  start rate peak;
model y = start rate peak;
means  start rate peak/bon;
run;
```

Symbol in Program	Definition
y	Retention time, Capacity factor
Start	Starting Composition
Rate	Gradient Rate
Peak	Taxanes

SAS Computer Program to Analyze

Resolution and Selectivity by ANOVA

```
options nocenter linesize = 256;
data ls;
 do peak = 1 to 12;
     do start = 1 to 3;
         do rate = 1 to 3;
infile '0603 res.dat';
input y @@;
output;
         end;
     end;
 end;
proc glm;
class  start rate peak;
model y = start rate peak;
means  start rate peak/bon;
run;
```

Symbol in Program	Definition
y	Resolution, Selectivity
Start	Starting Composition
Rate	Gradient Rate
Peak	Taxanes

Part II.

Separation of Paclitaxel and Related Taxanes

by Micellar Electrokinetic Capillary Chromatography

Chapter One

Introduction

1.1. The Significance of the Use of Capillary Electrophoresis Techniques for Resolving Various Taxanes

The importance of paclitaxel as a potent new anti-cancer agent has promoted intensive research directed towards development pertinent analytical methods, typically using HPLC [1], as illustrated in Part I of this thesis. In support of studies of various routes for paclitaxel production, pharmacokinetics of paclitaxel and related taxanes and stability research, it is important and timely to develop an analytical procedure that can resolve paclitaxel and related taxanes in a single experiment that is simple, fast, economical, requires small amounts of sample and does not produce large amounts of organic solvent waste. Capillary electrophoresis is a very attractive candidate, because of its high efficiency, short analysis time, small sample requirements, minimal organic solvent waste and low cost.

1.2 Introduction to Capillary Electrophoresis

Chromatography and electrophoresis are the most common analytical techniques available for the separation of mixtures of compounds into individual components. In chromatography, the driving force for the movement of molecules is a liquid or gas (the mobile phase) flowing through a column packed with a finely divided sorbent (the stationary phase) or a capillary with the stationary phase on the wall. The differential partitioning of solutes between the moving phase and stationary phase, that is, differences in the free energy of distribution of solutes between the two phases leads to resolution or separation. The separation of a mixture of compounds is influenced by a combination of kinetic and thermodynamic factors such as the composition, particle size and film thickness of the stationary phase, the composition and flow rate of the mobile phase, and the column dimensions and column temperature.

Electrophoresis is the transport of electrically charged species by an electric field. Because the electric field is the sole driving force in electrophoresis, the voltages needed are usually a few of kilovolts, a

substantial amount of Joule heat is generated in the system and separation efficiency in free solution is limited by thermal diffusion and convection. For this reason, electrophoresis has been conventionally achieved in anti-convective supporting media, such as polyacrylamide, agarose gels, cellulose acetate and starch.

The use of narrow-bore fused silica capillaries for the high-performance electrophoretic separation of complex mixtures developed by Jorgenson and Lukas [2,3] is an area currently gaining increased significance and is under rapid development. Compared to slab-gel electrophoresis, the narrow diameter (normally between 20 and 100 μm) of the fused silica capillaries allows efficient heat dissipation due to its large surface area to volume ratio. This permits free zone electrophoresis without the gel medium and the use of high voltage to drive the separation. Since the speed and resolution of electrophoresis are directly proportional to the field strength, separations by capillary zone electrophoresis (CZE) are faster and much more efficient than those in slab-gels. The recent development of CZE has presented the possibility of separation of a wide variety of analytes, from macromolecules such as proteins and nucleic acids to small molecules such as

inorganic and organic ions, amino acids, peptides and oligonucleotides. The formidable task of automation for the slab-gel format is also solved with CZE. In addition to high efficiency, CZE offers the capability to perform rapid separations and requires very small sample volumes.

Capillary electrophoresis can be performed using an apparatus similar to the one shown in Figure 1.1. The two ends of the capillary are immersed into identical buffer solutions on both sides. Two electrodes, one the cathode and the other anode, are also submerged into the two buffer containers which are connected to the negative and positive polarity of a high voltage power supply, respectively. The driving force for the movement of charged molecules is an electric field applied across the capillary. Unlike HPLC, in which the mobile phase velocities of cationic, neutral, and anionic compounds are equal, the mobile phase velocities of cations and anions in CZE are different due to the nature of the electrophoretic velocities of these ions under the influence of the electric field. The separation of a mixture of charged ions or molecules is achieved by the difference in electrophoretic velocity (a kinetic phenomena). Conventional off-column detection technique is not applicable in CE because smaller inner diameters of capillary results small

zone volumes, and off-column detection causes zone dispersion in the joints, fittings and connectors. The optical properties of fused silica capillaries have allowed the use of on-column UV absorption and fluorescence detection. Glass capillaries have a UV cutoff of approximately 300 nm, making this material unsuitable for UV detection for most compounds. Fused silica has a UV cutoff near 170 nm and is suitable for UV detection of most compounds.

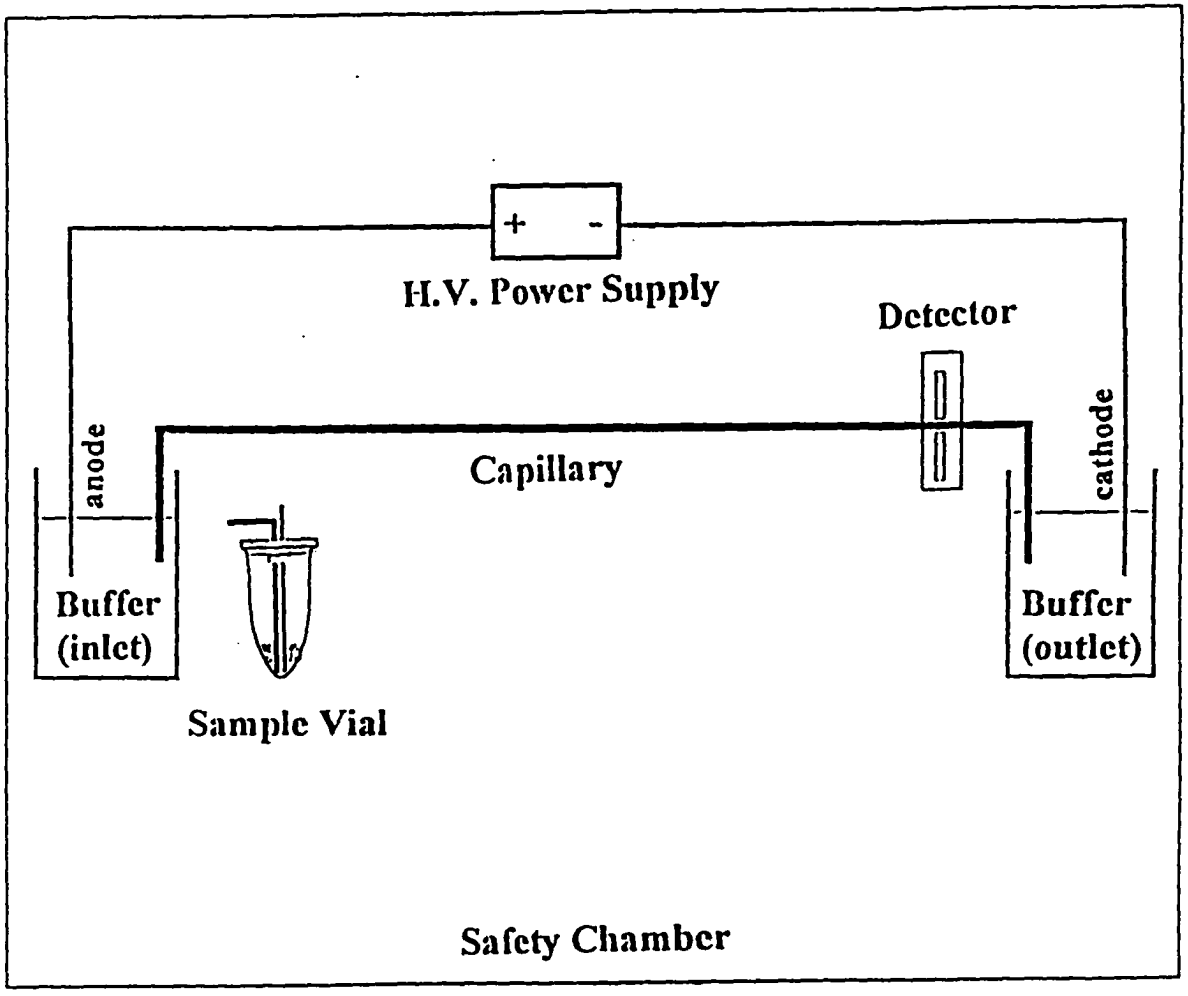

Figure 1.1 Schematic Diagram of a Capillary Electrophoresis Apparatus

1.3 Basic Theory of Capillary Electrophoresis

1.3.1 Electrical Double Layer and Zeta Potential

At any interface there is always an unequal distribution of electrical charges. This unequal distribution causes one side of the interface to acquire a net charge of a particular sign and the other side to acquire a net charge of the opposite sign, yielding a potential across the interface and an electrical double layer. In the case of capillary electrophoresis, an electric double layer is created at the interface between the solid and liquid phases. The zeta potential is the potential of charged surface at the plane of shear between the particle and the surrounding solution side of the rigid layer, in which solvent molecules, which are located close to the wall within the surface of shear, will not move under the influence of an electric field.

1.3.2 Electrophoretic Mobility

Electrophoretic separation of a mixture of charged ions or molecules is achieved by the differences in their electrophoretic velocities. The migration velocity, $v_{ep,}$ of a charged solute is proportional to the applied electric field strength E as given by the following equation:

$$v_{ep} = \mu_{ep}E \qquad (1.1)$$

where μ_{ep} is the electrophoretic mobility, which can be shown to be related to the charge and size of the ion by the following equation:

$$\mu_{ep} = q/6\pi\eta r \qquad (1.2)$$

where q is the net charge of the analyte, r is its ionic radius and η is the buffer viscosity. Electrophoretic mobility μ_{ep}, the rate of movement of ions toward the electrode of opposite polarity, is a fundamental characteristic of a ionic solute in a given buffer. It is determined by the charge density (charge to size ratio) of the ions and the viscosity of the medium.

1.3.3 Electroosmosis

Electroosmosis is the flow of bulk electrolyte in the capillary under the influence of the applied electric field. The electroosmotic flow velocity was defined by von Smoluchowski [4] in 1903 is given by

$$v_{eo} = (\varepsilon \zeta / 4\pi\eta) E \qquad (1.3)$$

Where ε is the dielectric constant, η is the viscosity of the buffer, ζ is the zeta potential of the liquid-solid interface, and E is the applied field strength. The electroosmotic flow depends on the field strengths; temperature; the buffer composition, pH, ionic strength, and viscosity; and the capillary's surface characteristics.

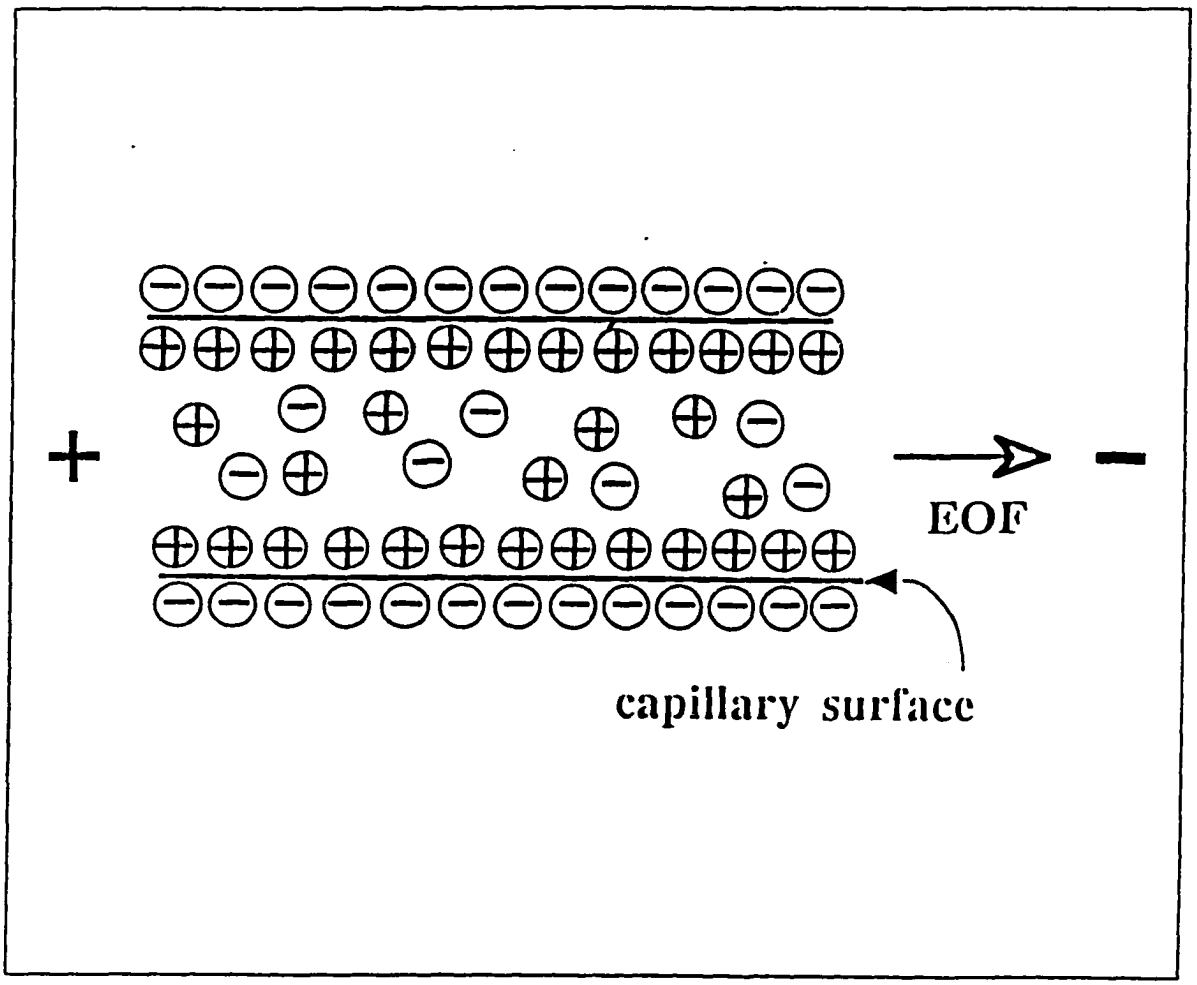

Figure 1.2 Schematic Diagram of Electroosmotic Flow

As is shown in Figure 1.2, electroosmotic flow in a fused silica capillary results from the ionization of the surface silanol (Si-OH) groups to negatively charged silanoate ($Si-O^-$) groups. Because the inner wall of the fused-silica capillary is negatively charged, positive counterions to these anions buildup in the solution adjacent to the capillary wall. When an electric field is applied, the layer of mobile positive charge is drawn toward the negative electrode, since ions are solvated by water, the fluid in the buffer is mobilized as well, resulting in the bulk flow of liquid toward that electrode. Since the capillary diameter is very small, the EOF is uniformly created across the capillary, resulting a flat flow profile in contrast to a laminar flow profile in HPLC, as is shown in Figure 1.3. This is one of the main reasons why CE is more efficient than HPLC.

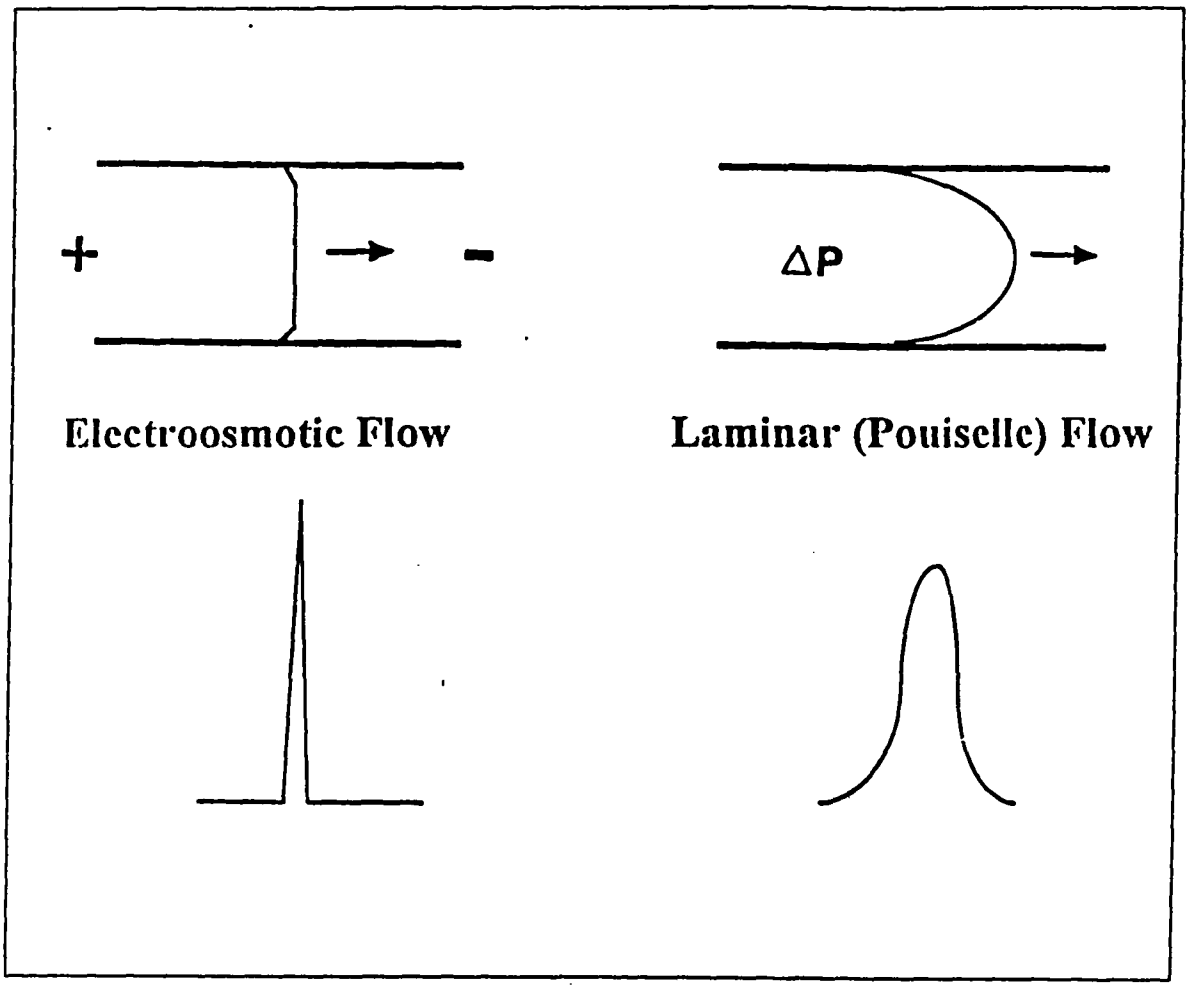

Figure 1.3 Comparison of the Flow Profile of (a) CE and (b) HPLC

In Figure 1.4 is shown the mobility vectors of EOF, cations, neutral solutes and anions. Anions and cations migrate electrophoretically in opposite directions while neutral solutes do not migrate. The net mobilities for cations are the summations of the mobility of EOF and that of the cations. The net mobilities for the neutral solutes are equivalent to the mobility of the electroosmotic flow. The net mobilities of the anions are the difference between the mobility of the EOF and the mobility of the anions. Under normal conditions, the magnitude of electroosmotic flow is greater than that of the electrophoretic mobility of the ions, so the net effect is it carries all molecules, including negatively charged and neutral ones, toward the cathode. Separation of ionic solutes is based on the combination of electroosmotic flow and differential electrophoretic migration, and therefore neutral solutes are not separated in CZE.

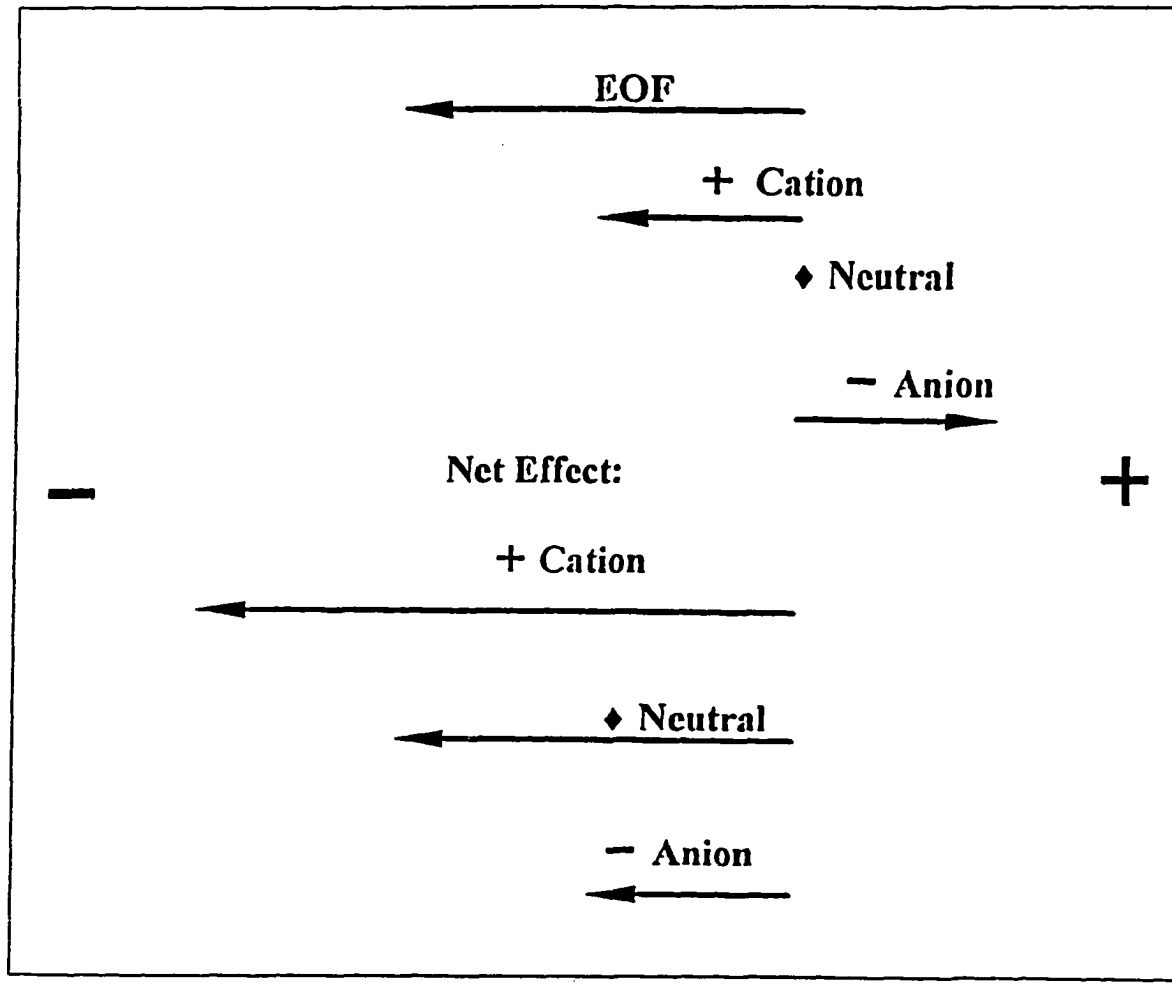

Figure 1.4 Illustration of Mobility Vectors of Cations (+), Neutral Species (◆), and Anions (−) Under the Influence of Electroosmotic Flow

1.3.4 Micellar Electrokinetic Capillary Chromatography (MECC)

A primary limitation of CZE is that neutral molecules cannot be separated because they have zero electrophoretic mobility. An important advance for the separation of neutral molecules by capillary electrophoresis was made by Terabe and coworkers [5,6], who added surfactant to the background electrolyte. An illustration of separation using MECC is given in Figure 1.5. It is assumed that anionic micelles are present at the pH of the buffer, and the sample molecules have net charge of zero. At critical micelle concentration CMC in solution, surfactant molecules aggregate to form micelles, with the hydrophobic tail groups towards inside and the charged hydrophilic head at the surface. Sodium dodecyl sulfate (SDS) is the most widely used anionic surfactant applied in MECC. When a potential field is applied across the capillary, negatively charged micelles migrate toward the anode, while the strong electroosmotic flow brings the micelles to the cathode. These micelles function as a moving "pseudo stationary phase", which is transported through the capillary by a combination of electroosmotic flow and micelle electrophoretic migration.

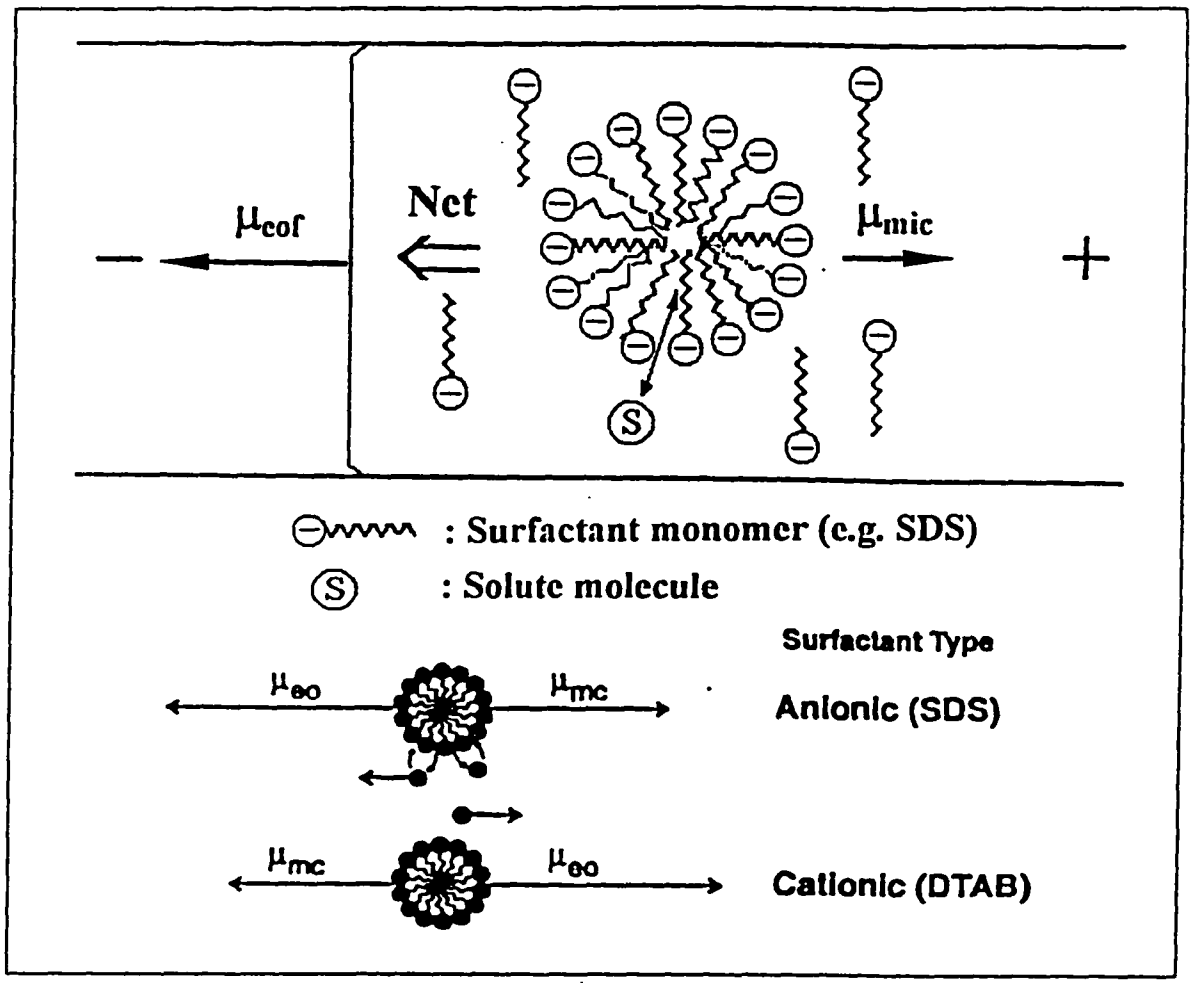

Figure 1.5 Schematic Diagram of the Separation Mechanism of Micellar Electrokinetic Capillary Chromatography

Neutral solutes are separated based on their differential partitioning between the moving micelle phase and the aqueous mobile phase. Charged species, on the other hand, migrate under the influence of electric field. This separation technique combines many of the operational principles of micellar liquid chromatography and capillary zone electrophoresis and is dubbed "Micellar Electrokinetic Capillary Chromatography" (MECC). MECC is the only operational mode of CE which can separate both ionic and nonionic solutes simultaneously.

1.4 Background of Separation of Paclitaxel and Related Taxanes by CE and the Objective of this Research

Taxanes are uncharged compounds with zero electrophoretic mobility so that they migrate with the EOF in the background electrolyte, and can not be separated by CZE. MECC with aqueous electrolytes is ideally suited to the separation of small neutral molecules [5, 6]. However, taxanes are highly hydrophobic, neutral species that are impossible to separate using purely aqueous MECC. There are only two reports in the literature on the separation of members of this class of compounds using capillary electrophoresis (CE). Chan et al. used MECC to separate seven taxanes [7] and applied the method to extracts of *Taxus* bark and needles [8]. There are no reports on the literature concerned with the CE separation of the excipient-containing dosage form of paclitaxel.

The major goal in this part of the thesis research was to explore the MECC separation of taxol A, taxol B, taxol C, xylosyl taxol, taxinine M and their derivatives in less than 15 minutes using ng amounts of sample and a few

microliters of solvent per run to minimize solvent waste. The second goal was to explore the possibility of using MECC to resolve paclitaxel and its excipient Cremophor EL in the paclitaxel injectable form. The use of this approach is potentially beneficial both from the standpoint of new science and from the use of our techniques to solve practical problems, given the high resolving power, short analysis time and low sample size requirements of CE.

Chapter Two

Experimental

2.1 Instrument

Capillary electrophoresis experiments were carried out using either an Applied Biosystems 270A-HT Capillary Electrophoresis System (Perkin-Elmer Corp.) or an Isco Model 3850 Electropherograph. Unless otherwise specified, 50 μm i.d × 375 μm o.d. fused silica capillaries were used. Capillary length was typically 72 cm total and 50 cm from injector to detector. Vacuum injection was applied to introduce sample into the capillary in both systems. With the ABS 270A-HT CE, sample injection was accomplished by applying a highly regulated vacuum (5" Hg) to the outlet of the capillary for a controlled period of time, typically one second. With the Isco Model 3850 CE, sample injection was carried out by applying a vacuum at the outlet buffer beaker for a controlled period of time, typically one to two seconds. The temperature in 270A-HT unit was controlled by the instrument via thermostated air circulation. The instrument is equipped with an autosampler and a spectrophotometric UV detector, which was used at 230 nm for the taxanes. A computer was connected to 270A-HT CE through RS232C interface. The software used for instrument control and data collection and analysis was PE Nelson TurboChrom 4.1.1 (Perkin-Elmer Corp.). With the

Isco 3850 CE, the electropherograms were recorded on a Spectra-Physics SP-4600 integrator.

2.2 Chemicals and Materials

Paclitaxel, other pure taxane standards, and a 13-taxane mixture were donated by Hauser Chemical Research Co. (Boulder, CO). Cremophor EL was obtained from BASF Co. (Mount Olive, NJ). The Taxol injectable dosage form was donated by Bristol-Myers Squibb Co.(BMS) (Princeton,NJ). Sodium dodecyl sulfate (SDS), electrophoresis purity grade, was obtained from Bio-Rad Laboratories (Richmond, CA). Sodium dodecylbenzene sulfonate, Trizma (2-amino-2-hydroxylmethyl-1,3-propanediol·HCl), and urea were obtained from Sigma Chemical Co. (St. Louis, MO). Fisher HPLC grade acetonitrile (ACN), methanol (MeOH) and Baker Analyzed glacial acetic acid were obtained from Fisher Scientific (Springfield, NJ). Water was glass distilled and passed through a Milli-Q system (Millipore Corp., Bedford, MA). Methanol was the marker of electroosmotic flow (EOF); the compound often used for this purpose, mesityl oxide, had a small affinity for the micelle phase and migrated more slowly than methanol. The micelle marker compound was sodium dodecylbenzene sulfonate at 0.2 mM in 10 mM SDS, the same concentration of SDS used for the samples, and it was monitored at 226 nm.

Fused silica capillaries were obtained from Polymicro Technologies Inc. (Phoenix, AZ) and Applied Biosystems (Foster City, CA).

2.3. Procedure and Solutions

Before installing each new column, the ends of the capillary were carefully trimmed to the required length using a ceramic cleaving stone. The polyimide coating for on-column UV detection was removed from the area of capillary to be used as the window by applying a low heat flame from a butane lighter. The window area was then cleaned with a Kimwipe moistened with MeOH.

All newly cut capillaries were washed successively with 1M NaOH for 60 min, deionized water for 10 min, and 0.2 M NaOH for 30 min. Before each injection, the capillary was flushed sequentially with deionized water for 0.5 min, 0.2 M NaOH for 2 min, deionized water for 2 min and finally equilibrated with background electrolyte solution for 5 min. All buffer and sample solutions were filtered through 0.2 μm Millipore filter and ultrasonically degassed before use.

Sample solutions were prepared for injection as follows. Hauser 13-taxane standard mixture: 200 μL of the standard supplied (50 μg/mL each

taxane) was dissolved in 200 μL of 20 mM SDS to give a final concentration of 25 μg/mL taxane in 10 mM SDS; individual taxanes: each was dissolved in MeOH and diluted in SDS solution to make a final concentration of 100 μg/mL taxane in 10 mM SDS; paclitaxel injectable solution: 80 μL of the injectable form at 0.48 mg/mL was diluted with 40 μL of 100 mM SDS and 280 μL to give a final concentration for of 96 μg/mL paclitaxel in 10 mM SDS; placebo blank: 80 μL of placebo (2 mL of Cremophor EL and 2 mL of ethanol in 25 mL ACN/water/glacial acetic acid, 70/30/0.1 by volume) was diluted with 40 μL of 100 mM SDS and 280 μL water.

Chapter Three

Results and Discussion

3.1. MECC Separation of the 13-Taxane Mixture

Taxanes are uncharged compounds with zero electrophoretic mobility and hence are not selectively transported electrophoretically but migrate with the EOF. In the presence of an electric field, anionic micelles are subjected to two forces driving in opposite directions. One force is that of the EOF towards the negative electrode. The other force is electrophoretic migration of the anionic micelles in the direction towards the positive electrode. Since the velocity of EOF is usually higher than the electrophoretic velocity of the micelle, the net velocity vector of the micelle is towards the negative electrode, which is set up at the detector end.

3.1.1 Migration Order of Taxanes in MECC

In Figure 3.1.1 is shown the electropherogram of the 13 taxanes in the Hauser standard mixture in 11.5 min. The optimum conditions are given in the legend. The taxane number refers to the taxanes in Figure 1 of Part One of this thesis. Taxanes #3 and 13 were not included in the standard and do not appear in the electropherogram as major peaks (the small impurity peaks between #2 and #5 and between #12 and #15 in the Hauser standard are these compounds). Their migration time was determined using pure standards. The elution order is generally similar to that in reversed phase LC, but different in detail. In HPLC, although there were subtle differences in the retention times of taxanes between the two commercial pentafluorophenyl (PFP) columns used, the elution order was related to the taxane molecular size, the number of acetylated hydroxyl groups, and the presence of a xylosyl group at the 7-position; all else equal, an increase in hydrophobicity led to an increase in retention. With the PFP HPLC columns used, the possibility of selectivity of the stationary phase results from the interaction of the fluorines with electron pairs on the taxane carbonyl oxygens.

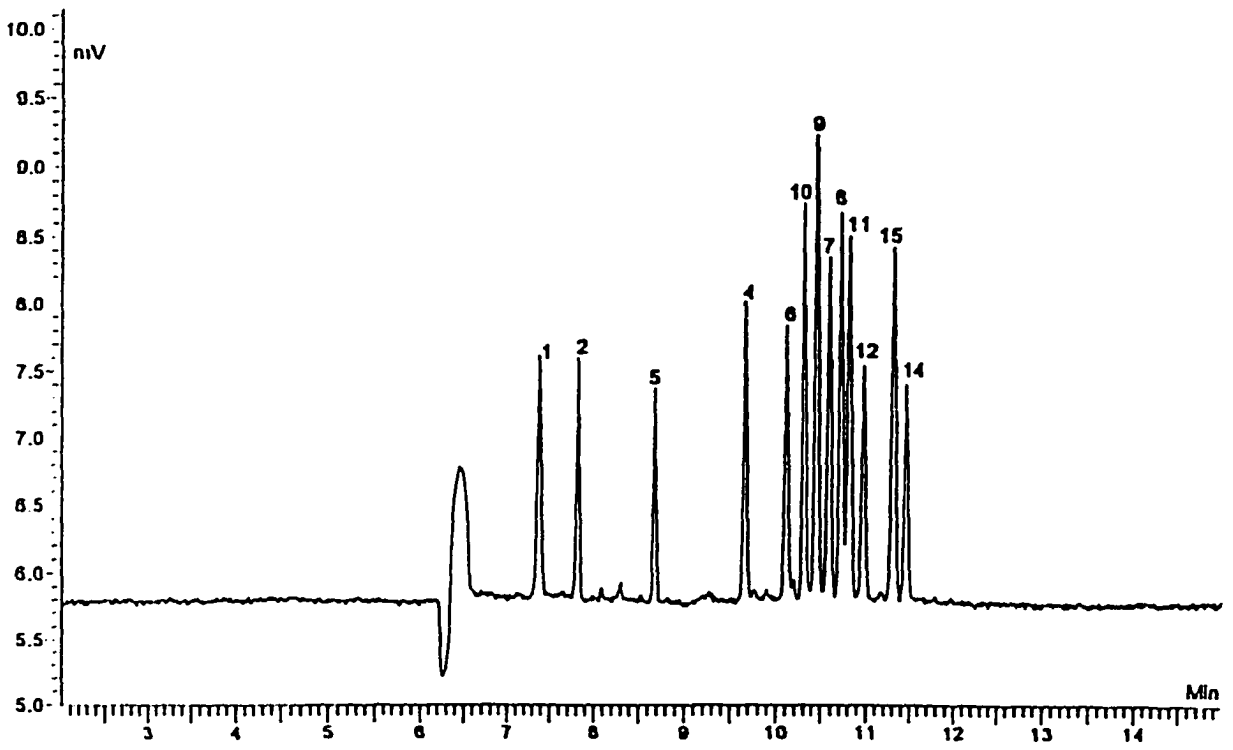

Figure 3.1.1 Electropherogram of 13-Taxanes Mixture

MECC conditions: untreated fused silica capillary, 50 μm i.d. x 375 μm o.d., 50 cm from injector to detector, 72 cm total length; background electrolyte, 25 mM Trizma, pH 9.0, 40 mM SDS, 30 % ACN (v/v), and 10 mM urea; applied voltage, 25 kV; 30 °C; UV detection at 230 nm; sample dissolved in 10 mM SDS; and vacuum sample injection for one second.

In MECC with SDS, one would expect the driving force for solute association with the hydrocarbonaceous core of the micelle to be primarily low solubility in the aqueous buffer combined with dispersive interactions with the core. However, there is not the same possibility for selective interactions. It would consequently be of interest to investigate fluorinated surfactants as MECC buffer additives for the taxanes.

In any case, with SDS surfactant, the direction of electrophoretic migration of the anionic micelle, and thus that of the micelle-taxane complex, is opposite the direction of EOF. The smaller the aqueous phase solubility and/or the stronger the degree of solute association with the micelle, the longer the migration time. Comparison of the MECC taxane separation with that by HPLC, shows the migration order of taxinine M (#5) and 10-deacetyl-7-xylosyl taxol B (#4) is reversed. Indeed, taxanes #1, 2, 3, and 5 lack the 13-side chain, which given the bulk of the rest of the molecule, may be the only part of the taxane molecules which can penetrate into the micelle core. On this basis they should be the taxanes with the shortest migration times, which is observed. In addition, lack of the side chain should increase solubility in the aqueous phase. Cephalomannine (#10) migrates before 10-deacetyl taxol (#9),

and both have shorter migration times than 10-deacetyl-7-xylosyl taxol C (#7) and 7-xylosyl taxol (#8); and 7-epi-taxol (#15) migrates ahead of Taxol C (#14), the last-emerging compound. These could be attributed to the higher affinity of the micelle for a saturated hydrocarbon end of the C-13 side chain than to a phenyl. Alternatively, these differences may be associated with the relative importance of the selective acetyl group/PFP interaction operative in HPLC. In MECC, comparison of the migration orders of #6/#9 and #8/#12 show that the presence of a xylosyl group decreases the migration time, by increasing the aqueous phase solubility. Acetylating a hydroxyl group produces an increase in migration time by decreasing the solubility (and/or increasing the affinity for the micelle), as shown by #1/2, #6/8, #9/12, and #11/15. Simultaneous addition of a xylosyl and acetylation a hydroxyl increases migration time (#4/10, #7/14), indicating the acetylation produces a larger change in affinity for the micelle than addition of the sugar group does to increase aqueous phase solubility. The effect of the hydrocarbon end of the 13-side chain is clear by comparing migration rates of #4/6/7 and also #10/12/14: isobutylene has less affinity for the micelle than phenyl than n-pentyl.

3.1.2 Effect of SDS Concentration

As shown in Figure 3.1.2, no separation of the neutral taxanes is possible in the absence of a charged carrier, e.g. SDS. Increasing the surfactant concentration above the critical micelle concentration (CMC) produces more micelles to interact with the solutes so the migration times and resolution increase. This has been expressed quantitatively in terms of the MECC retention factor k', the ratio of the equilibrium amounts of solute in the micelle and aqueous phases, by [6]

$$k' = K \nu (C_{sds} - CMC) \qquad (3.1)$$

where K is the distribution coefficient of the solute between the two phases, ν is the partial specific volume of the micelle, and C_{sds} is the SDS concentration. Thus k' should increase linearly with C_{sds}, as observed. However, C_{sds} cannot be increased without limit because increasing the SDS concentration increases the current which could lead to undissipatable Joule heating.

Figure 3.1.2 Effect of SDS Concentrations on Separation of Taxanes

MECC conditions: same as Figure 3.1.1 except SDS concentration.

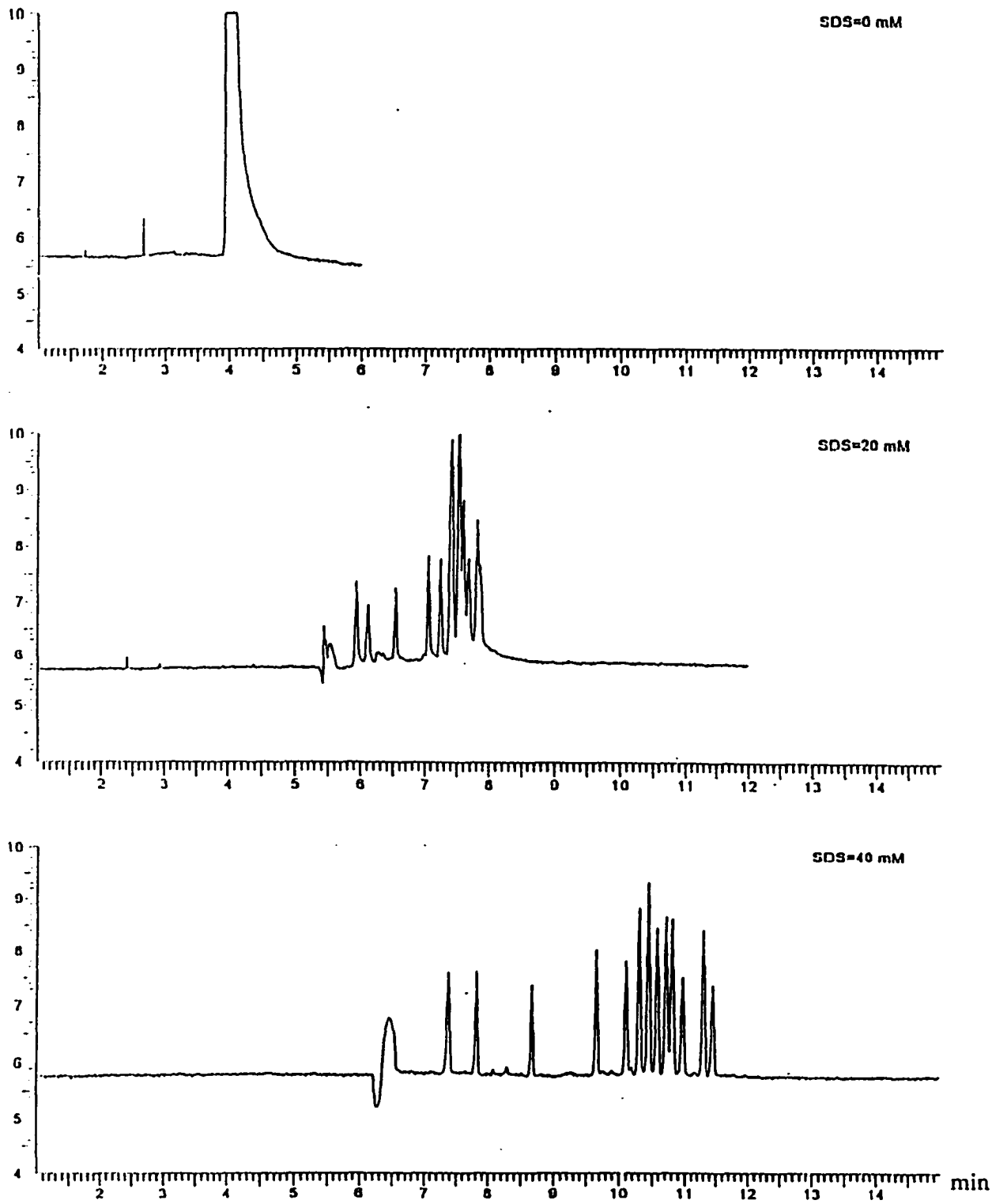

In our buffer the current increased linearly ($r = 0.999$) from 2 to 24 μA as C_{sds} was increased from 0 to 40 mM. Because at 40 mM SDS the separation was good and the Joule heating was not interfering, this concentration was used in subsequent work.

3.1.3 Effect of Organic Additive

Micellar electrokinetic capillary chromatography (MECC) with aqueous electrolytes is ideally suited to the separation of small neutral molecules [5,6]. However, taxanes are highly hydrophobic, neutral species that are impossible to separate using purely aqueous MECC. Taxanes tend to have similar, large partition coefficients in the micelle phase because of their small aqueous solubility. Addition of organic solvent to the background electrolyte increases the solubility of such compounds in the buffer. However, sufficiently high concentrations of organic solvents also produce changes in the size and structure of the micelles [9-14]. This does not necessarily result in the inability of the system to produce electrophoretic separations. Indeed, Walbroehl and Jorgenson [15] described early on the separation of certain polycyclic aromatic hydrocarbons using tetrahexylammonium perchlorate (THAP) in aqueous acetonitrile (ACN); the neutral solutes were said to undergo a "solvophobic association" with the THAP to produce charged species capable of electrophoretic migration. Nashabeh et al. [16] separated recombinant insulin-like growth factor I variants, using a zwitterionic surfactant with up to 60% ACN. Ahuja and

Foley [17] reported no SDS micelles to be present in a pH 7 phosphate buffer containing 50 mM SDS and 50% ACN (v/v), based on the observation that small neutral molecules migrated with the electroosmotic flow (EOF) marker. Nonetheless, under the same conditions, good resolution of hydrophobic C_{20} - C_{24} alkyl aryl ketone homologs was observed. They also achieved good separations of these compounds using what they referred to as "non-micellized" cetyltrimethylammonium bromide (CTAB) in aqueous ACN. On the strength of these successful applications of CE with surfactants in partially aqueous electrolytes, Ahuja and Foley [17] coined the description "hydrophobic interaction electrokinetic capillary chromatography" (HIEKC for short). Fritz and coworkers [18-22] presented examples of excellent separations using a variety of surfactants in the presence of ACN. A "solvophobic interaction" between the aromatic compound solutes (A) and the surfactants (S^-) in the form of an equilibrium displacement was invoked [22] to account for the effect of the ACN,

$$A(ACN)_n + S^- \Leftrightarrow A(S^-) + n\ ACN \qquad (3.2)$$

Palmer et al. [23-25] studied the application in MECC of novel polymers, which are covalently stabilized surfactants having no CMC and whose solvation or solution properties are not affected by organic solvents. They provided separations of hydrophobic compounds superior to those with conventional surfactants. Vindevogel and Sandra [26] discussed the effect of alcohols and ACN on micelle stability. They concluded that sodium dodecylsulfate (SDS) micelles may in fact be stable at high concentrations of ACN in the aqueous buffer, as evidenced by the absence of precipitation of SDS monomers, which are insoluble in ACN. However, they also expressed belief that the existence or nonexistence of micelles in the presence of organic solvents can be established only through physical methods, rather than by inference from methods such as MECC. Indeed, very recently Seifar et al. [27] reported measurements of conductivity of SDS solutions in aqueous ACN as part of a MECC study of certain hydrophobic compounds. The results indicated that even high concentrations (70% v/v) of ACN do not produce complete breakup of the SDS micelles, and that MECC separations result from differential solute partitioning into "micelle-like SDS aggregates". They conclude that the electrokinetic separation of neutral hydrophobic compounds in SDS solutions with up to 30% ACN is still based on the

partition of solutes between the moving SDS micelles and running buffer, because the mobilities observed are too high to be attributed to solvophobic interaction with single, free SDS ions in either a 1:1 or higher order of complexation. Bullock [28] did not find a micelle-indicating break in the plot of conductivity vs. SDS concentration in solutions containing 35% ACN. However, he may not have gone to sufficiently high concentrations of SDS to see such a break, based on the results of Seifar et al.[27].

We conclude that it is not yet entirely clear in precisely what form surfactant molecules exist in the presence of high concentrations of organic solvent, i.e. whether as monomers or associated in clusters smaller than micelles, similar to a "premicelle" conditions, but that separations are achieved that are not possible in the absence of the organic additive. As shown in this section, we have demonstrated the separation of taxanes using SDS in a background electrolyte containing 30% (v/v) ACN. Although we stand ready to be corrected, to simplify the discussion, we refer to our surfactant in organic-aqueous buffers as being in the form of micelles, and retain the description MECC.

The small aqueous solubility of the taxanes except taxanes #1, 2, 3, and to a lesser extent #5 results in large and similar distribution coefficients between the purely aqueous phase and the micelle phase. Without organic modifier added to the bulk electrolyte, the compounds migrate at the same rate as the pseudophase of charged micelles and are not separated, as shown in the top electropherograms in Figures 3.1.3 and 3.1.4. Addition of an organic solvent to the aqueous buffer has five main effects. First, organic solvents decrease the polarity of the mobile phase, increase the solubility of hydrophobic compounds in the aqueous buffer, reduce the distribution coefficients which allows for increased differential solute-micelle interactions, and may improve the selectivity. Second, organic solvents suppress the fused silica capillary wall ζ-potential which reduces the EOF [29-31], and they also decrease the ζ-potential of the micelle head groups which reduces their electrophoretic mobilities. Third, organic solvents are taken up by the micelles either at the interface or interior of the micelle. If small polar organic solvents are adsorbed on the interface of the SDS micelle, the number of ionic head groups per micelle will decrease, causing a reduction of the repulsion between sulfonate groups and decrease in curvature and increase in micelle size. The net result is the decrease of the surface

charge density of the micelle [32-33] and thus decrease their electrophoretic mobilities. If small organic solvents are taken up inside the SDS micelle, the micelle will probably swell, inorder to maintain the same charge density, the surface area of the charged head group has to increase. The net result is unchanged charge density [13-14]. Organic solvents at higher concentrations may thus affect the formation of the micelles such as to cause a decrease in the aggregation number and size [10-13]. Fourth, organic solvent may alter the CMC [12,25], i.e. change the number of monomers and micelles in equilibrium. Common organic solvents such as ACN can interact strongly with the hydrogen-bonding network of water to inhibit micellization, thus raising the CMC. Last, organic solvents may alter the viscosity of the background electrolyte and thus the electrophoretic mobilities may change.

In this work, we evaluated ACN, MeOH, DMSO and 2-propanol. DMSO and 2-propanol did not give useful separations. DMSO did not produce as good resolution as ACN or MeOH did. With 2-propanol as modifier, both the EO mobility and the mobility of the micelles were decreased tremendously, leading to protracted analysis time, so DMSO and 2-propanol were excluded from further study.

As the ACN concentration was increased from 0 % to 20 %, or the MeOH concentration to 30 %, migration times increased and the separation improved, as shown in Figures 3.1.3 and 3.1.4. The increase of the migration time of the micelle is caused by a combination effects of increasing the viscosity (maximum at 20 % ACN) [29] and decreasing the ζ potential of the capillary wall thus lowering the electroosmotic flow mobility [29-31].

Figure 3.1.3 Effect of Acetonitrile on Separation of Taxanes

MECC conditions: same as Figure 3.1.1 except concentration of ACN.

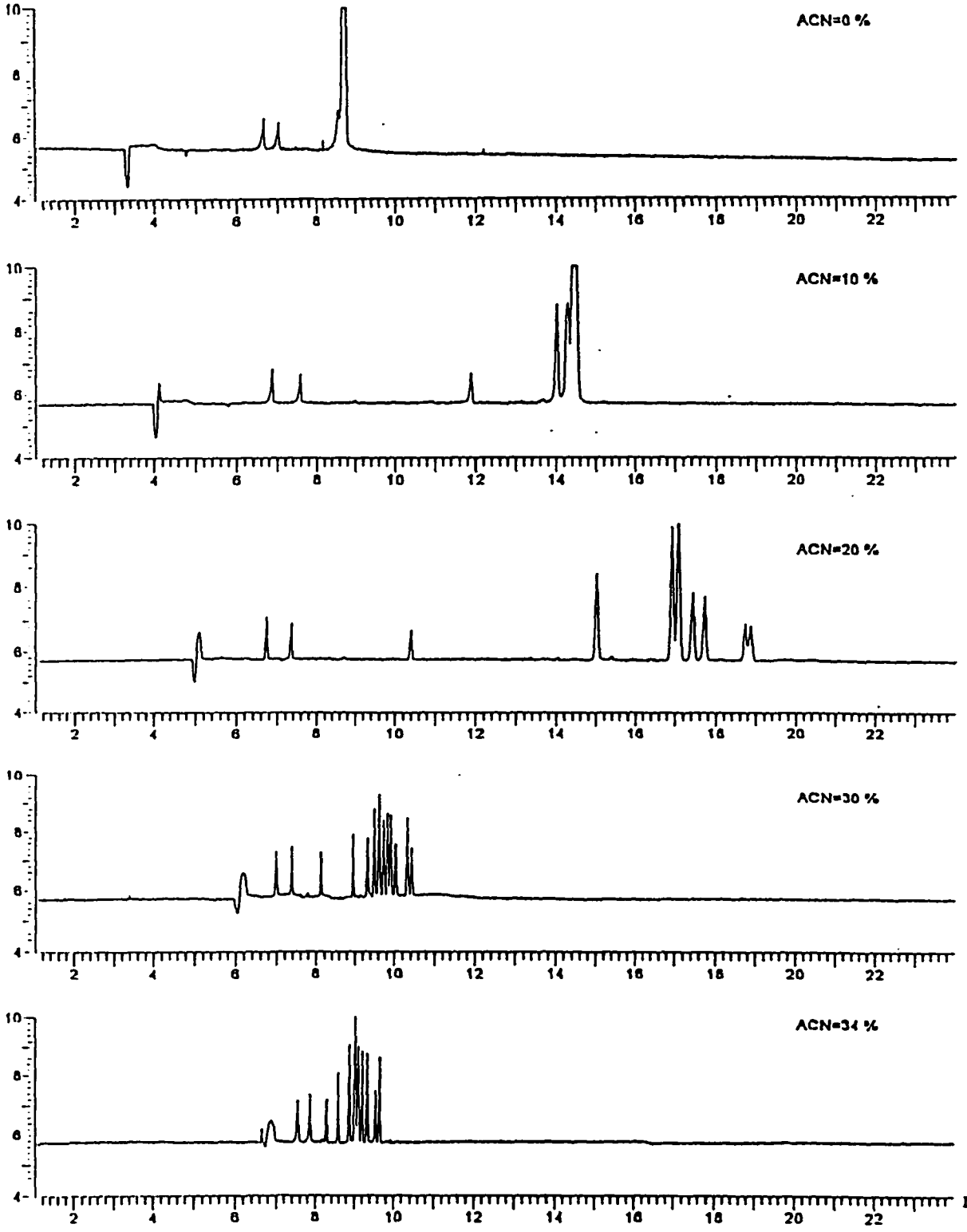

Figure 3.1.4 Effect of Methanol on Separation of Taxanes

MECC conditions: same as Figure 3.1.1 except concentration of MeOH and absence of ACN.

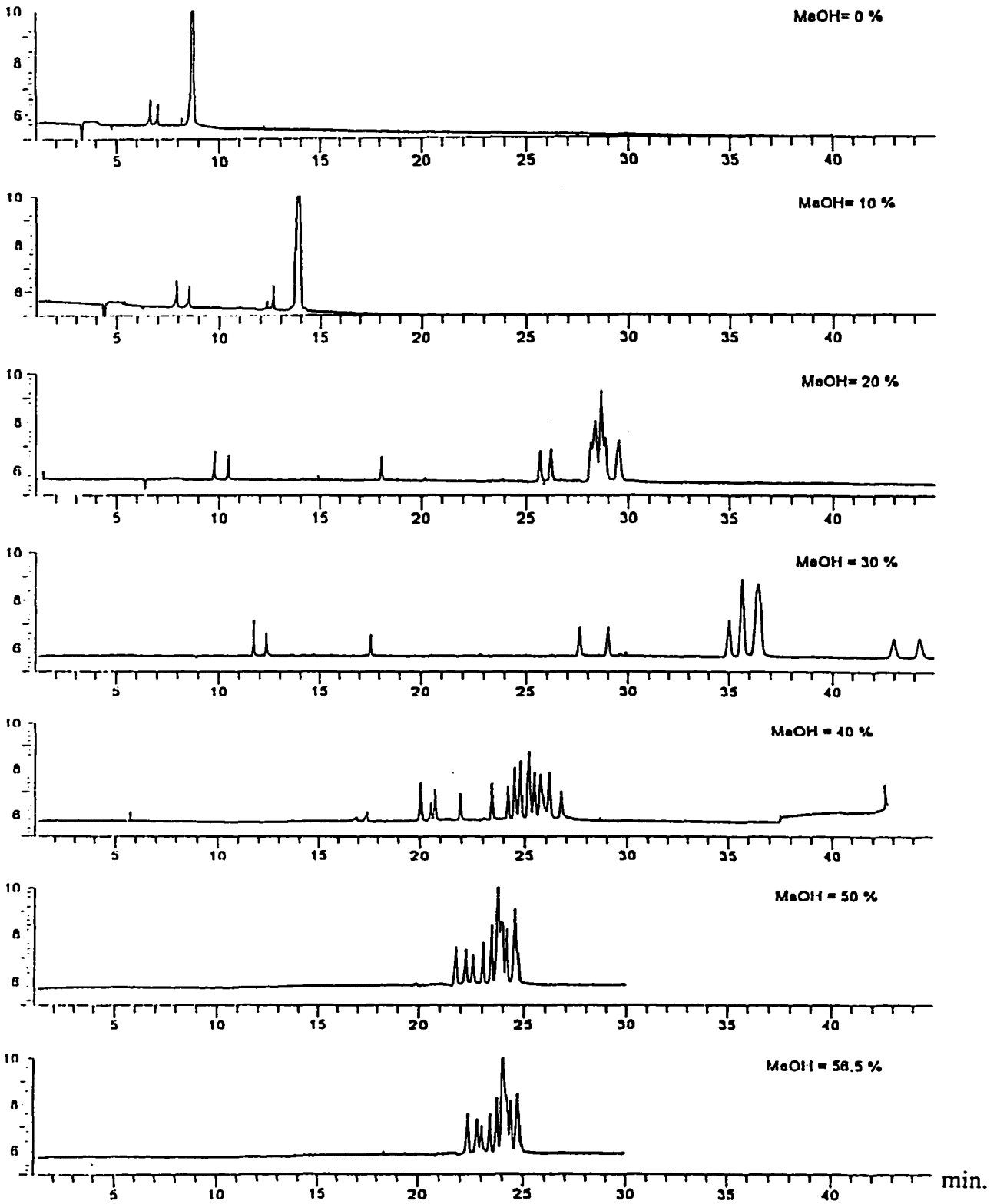

However, except for taxanes #1 and #2, there was a sharp decrease in migration time, or decrease in the electrophoretic mobility of the micelle (see below) between 20 % and 30 % ACN or 30 % and 40 % MeOH. Seifar et al. [27] observed the same behavior for their hydrophobic compounds using ACN. Although migration times continued to decrease as the organic content of the buffer was increased above 30% ACN or 40% MeOH, resolution suffered. ACN gave a better and faster separation than MeOH, and 30% ACN gave the best resolution and shortest analysis times. Thus 30 % ACN was chosen as the optimum. Gorse et al. [34] also found ACN to give faster migration times than MeOH with SDS for various test compounds.

In a given buffer, the electrophoretic mobility of an ionic solute is a characteristic constant determined by its ratio of charge to size and the viscosity of the surrounding buffer. The measurement of mobility is more useful than migration time since mobility of a solute is independent of voltage and capillary length.

In our CE experiment, the electrophoretic mobility of a solute was obtained from a ratio of measured (observed) migration velocity of the solute (L_d/t) to field strength (L_t/V), or a ratio of capillary lengths to measured (observed) migration time and voltage:

$$\mu_{obs} = v_{obs}/E = L_d L_t/tV \qquad (3.6)$$

Where

v_{obs} = the observed (measured) migration velocity of the solute peak (cm/sec).

E = the electrical field strength (V/cm)

L_d = the length of the capillary from the injection end to the detector (cm).

L_t = the total length of the capillary (cm)

t = the observed (measured) migration time of the solute peak (sec)

V = the voltage across the capillary.

In MECC with anionic micelles, the electrophoretic mobilities of the micelles are influenced by two forces, one force is that of EOF towards the negative electrode, the other force is electrophoretic migration of the anionic micelles with μ_{ep} in the direction towards the positive electrode. The observed

electrophoretic mobility, $\mu_{obs,}$ of a neutral solute is the summation of the electroosmotic mobility and the electrophoretic mobility of the micelle. If we define the electroosmotic mobility vector, $\mu_{eof,}$ as positive sign, the electrophoretic mobility vector of the anionic micelle, $\mu_{ep,}$ will have a negative sign, the observed (measured) electrophoretic mobility (μ_{obs}) of the neutral solute which is associated with the micelle is given by

$$\mu_{obs} = \mu_{eof} - \mu_{ep} \qquad (3.4)$$

The true micelle mobility and the mobility of a neutral solute associated with the micelle is:

$$\mu_{ep} = \mu_{eof} - \mu_{obs} \qquad (3.5)$$

When a solute is totally solubilized by the micelle (micelle marker), the observed mobility of the solute is the observed mobility of the micelle. The true micelle mobility is then equal to the observed mobility of the micelle subtracted from the mobility of the electroosmotic flow.

Figure 3.1.5 Effect of Acetonitrile on the Apparent Mobility of Taxanes

MECC conditions: same as Figure 3.1.1 except concentration of ACN.

Taxane number refers to Figure 1, Part I.

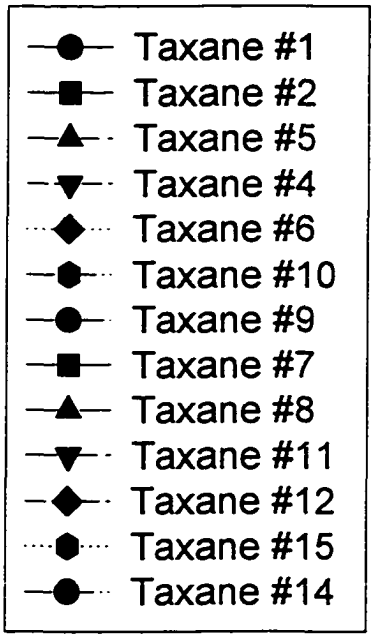

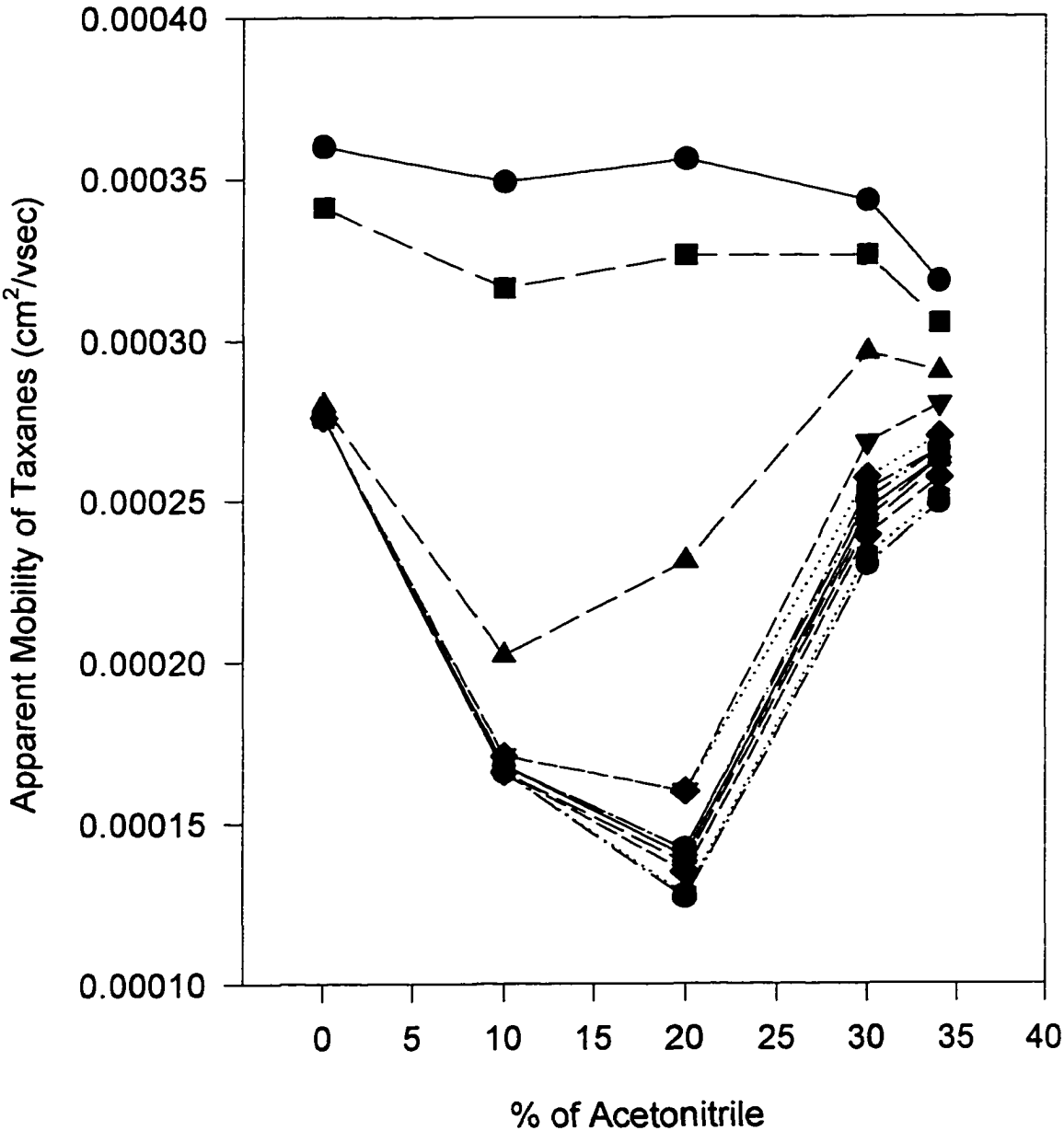

As is shown in Figure 3.1.5, the apparent (observed) mobility of taxanes was decreased (except for taxanes without the 13-side chain (#1, 2, and 5) as ACN concentration in the electrolyte was increased from 0% to 20%. The apparent mobility of taxanes then increased as ACN content was increased from 20 to 34%. The decrease in the apparent mobility of the taxanes resulted from the decreasing ζ-potential of the capillary wall and thus the slowing down of the EO mobility.

A plot of effective mobilities of the taxanes associated with the micelles (Figure 3.1.6) shows that the magnitude of the mobilities decreased as the ACN content in the electrolyte was increased. The effective electrophoretic mobility of nonionic compounds is a result of their association with the electrophoretically migrating SDS micelles and the EOF. A higher concentration of ACN solvates the taxanes in the running buffer more strongly, so taxanes tend to spend more time outside of the micelle, thus their effective mobilities are decreased. Our result is consistent with the findings by Seifar et al.[27].

Figure 3.1.6 Effect of Acetonitrile on the Effective Mobility of Taxanes

MECC conditions: same as Figure 3.1.1 except concentration of ACN.

Taxane number refers to Figure 1, Part I.

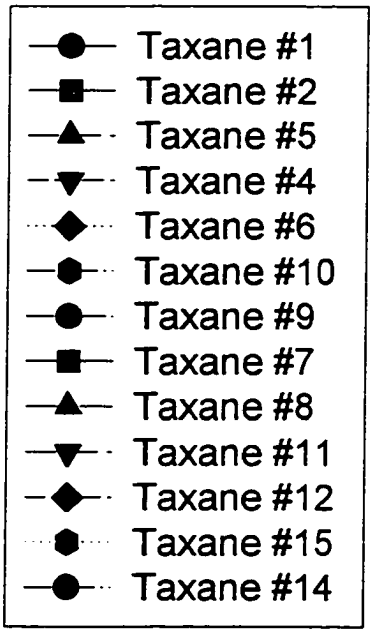

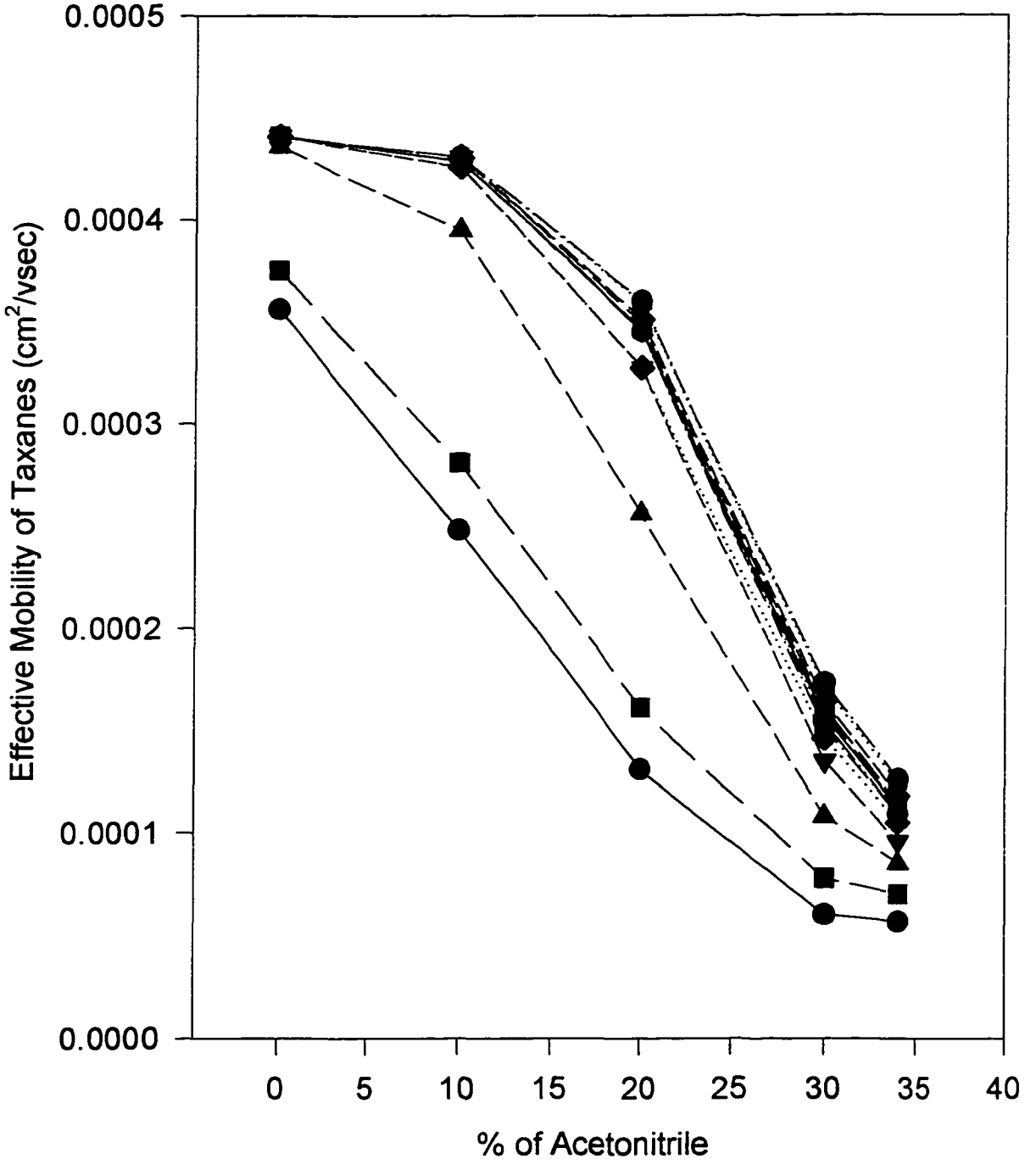

A further look of the true SDS micelle mobility, as shown in Figure 3.1.7, indicates that the micelle mobility decreased gradually as ACN content in the buffer was increased from 0 to 20%. There is a sharp decrease in the true SDS micelle mobility between 20-30 % ACN, which suggests the retention factors or distribution coefficients changed dramatically. The slope of the true SDS micelle mobility is similar to that of the effective taxane mobility, but the true micelle mobility should be the largest and has the longest migration time, which was observed.

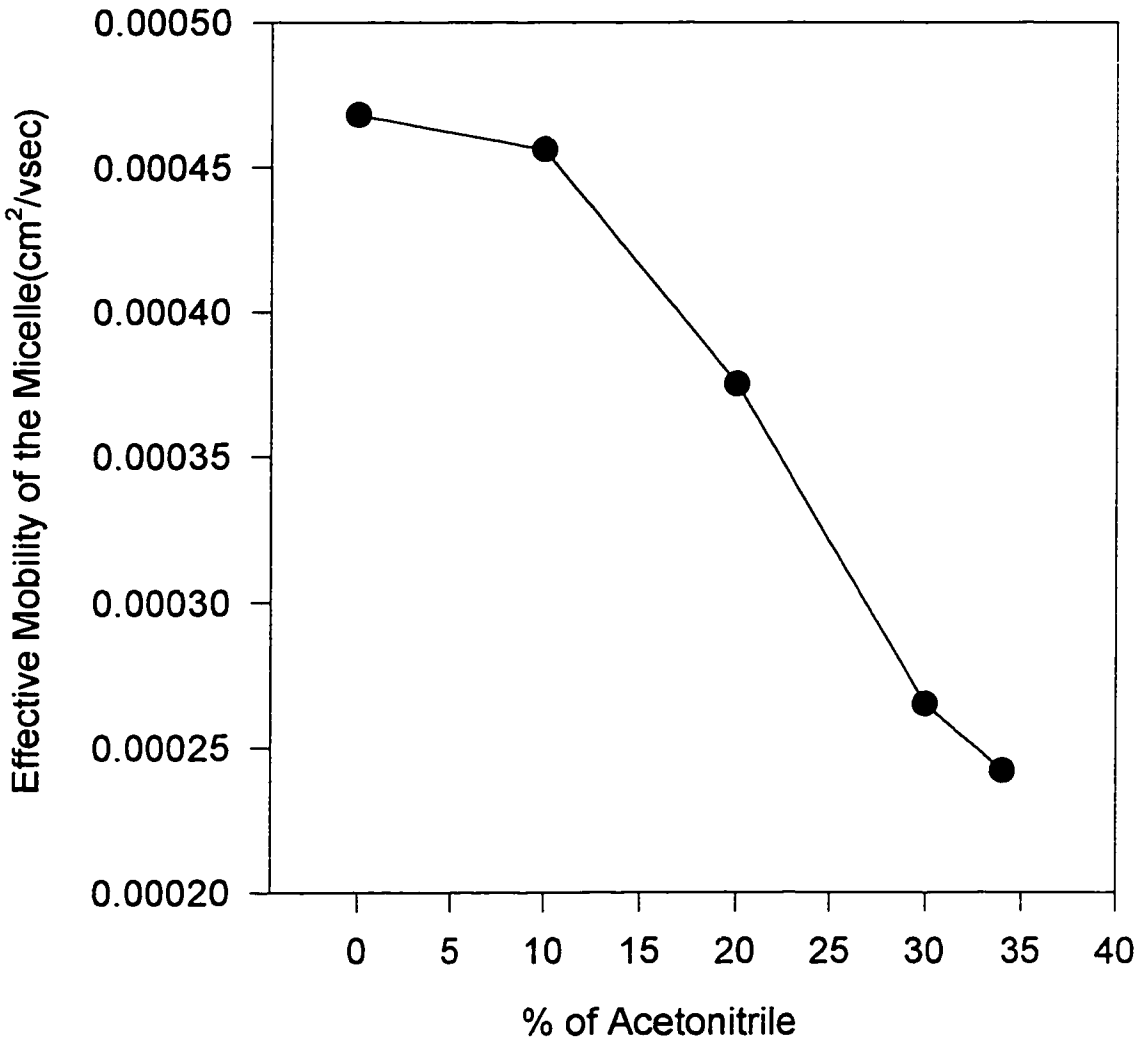

Figure 3.1.7
Effect of Acetonitrile on SDS micelle Mobility

MECC conditions: same as Figure 3.1.1
except concentration of acetonitrile.

Retention factors, k', were determined experimentally from the migration times of the solute, t_R; the MeOH EOF marker, t_{eof}; and the micelle marker, t_{mic}, according to [5]

$$k' = (t_R - t_{eof})/ t_{eof}(1 - t_R/t_{mic}) \qquad (3.7)$$

The k' values are tabulated along with migration times in Table 3.1. We used sodium dodecylbenzene sulfonate as the micelle marker. The often-used [5] micelle marker, Sudan III (obtained from Scientific Resources, Inc.. Eatontown, NJ), gave us problems. The UV absorption spectrum of Sudan III shows λ_{max} at 230 nm, 345nm and 504 nm. Injection of Sudan III saturated in MeOH solvent with detection at 230, 345 and 504 nm did not show any peak at the experimental conditions in our study, so as sudan III dissolved in various MeOH + SDS solution. Injection of 10 mM solution of SDS saturated with Sudan III with detection at 230 nm, as shown in top electropherogram of Figure 3.1.8, gave a noisy baseline and about 10 peaks, which caused by impurities in Sudan III. Detection at 504 nm, which is shown in bottom of Figure 3.1.8, gave a single peak at a time consistent with the

migration time of the micelle, which corresponded to one of the peak in the 230 nm electrophoregram.

Table 3.1 Effect of Acetonitrile on Migration Time and k'

MECC conditions: same as Figure 3.1.1 except ACN concentration

Taxane number refers to Figure 1, Part I

	%ACN									
	0		10		20		30		34	
Taxane #	t	k'	t	k'	t	k'	t	k'	t	k'
1	6.66	3.17	6.87	1.19	6.74	0.54	6.99	0.292	7.54	0.314
2	7.03	4.01	7.59	1.61	7.36	0.75	7.37	0.413	7.87	0.418
5	8.56	13.5	11.9	6.54	10.4	2.16	8.12	0.682	8.28	0.558
4	8.71	15.9	14.0	14.3	15.0	6.81	8.95	1.04	8.59	0.673
6	8.71	15.9	14.0	14.3	15.0	6.81	9.32	1.22	8.88	0.788
10	8.71	15.9	14.3	16.1	16.9	11.5	9.50	1.31	9.03	0.850
9	8.71	15.9	14.3	16.1	16.9	11.5	9.61	1.37	9.03	0.850
7	8.71	15.9	14.3	16.1	17.1	12.1	9.73	1.44	9.11	0.887
8	8.71	15.9	14.3	16.1	17.1	12.1	9.83	1.50	9.11	0.887
11	8.71	15.9	14.5	17.7	17.4	13.5	9.92	1.54	9.21	0.932
12	8.71	15.9	14.5	17.7	17.7	14.8	10.0	1.62	9.34	0.988
15	8.71	15.9	14.5	17.7	18.7	21.9	10.3	1.80	9.55	1.09
14	8.71	15.9	14.5	17.7	18.9	23.3	10.4	1.88	9.65	1.14
t_{eof}	3.35		4.02		4.93		5.95		6.40	
t_{mic}	9.68		17.0		21.5		17.4		18.1	
t_{mic}/t_{eof}	2.89		4.22		4.36		2.93		2.83	

Figure 3.1.8 Electropherogram of Sudan III detection at 230 nm (top) and 504 nm (bottom)

MECC conditions: same as Figure 3.1.1 except Sudan III was dissolved in 10 mM SDS and injected.

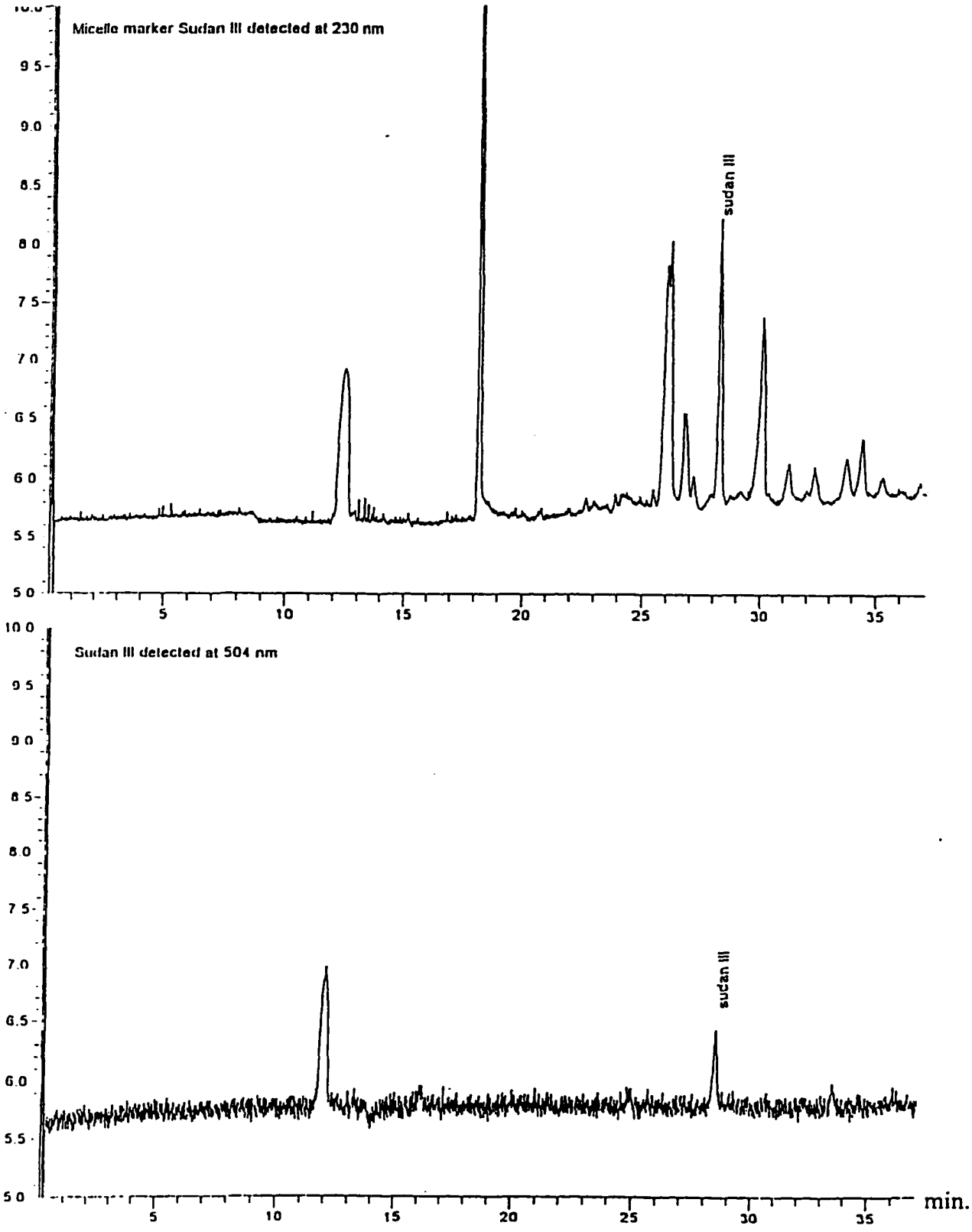

At ACN lower than 20 % in the background electrolyte, injection of Sudan III saturated in 10 mM SDS produced reproducible micelle peak but the migration time of this peak decreased with increasing amounts of ACN, indicating partial solubilization in the aqueous phase, and then disappeared altogether for concentrations of ACN greater than 20%. The problems of small extinction coefficient and the generation of more than one peaks in buffers containing more than 20 % organic solvent, are discussed by several authors [35-36]. Apparently, Sudan III is partially soluble in aqueous phases containing more than 20 % ACN. The dodecylbenzene sulfonate absorbs UV strongly at 226 nm, gave consistent migration times at all ACN concentrations, and is evidently strongly associated with the SDS micelles. Except for taxane #1, #2 and #5, the k' values are essentially same for 0-10 % of ACN and there is a sharp decrease in k' values at about 30% of ACN, where the separation is achieved.

The electroosmotic mobility decreased linearly (r=0.998) with increasing ACN concentration from 0% to 30% by a factor of about 1.8; for MeOH the decrease was a factor of about 2.7. We believe this results from the effect of the organic solvent on the wall-ζ-potential and on the viscosity. The

variation of t_{mic} with ACN shows a maximum value between 10% and 30% ACN, corresponding to the largest MECC 'window" [5], i.e. the largest ratio of t_{mic}/t_{eof}. The increase in t_{mic} can also be attributed to decreasing wall- and micelle-ζ-potentials or decrease in micelle size with increasing ACN.

For the taxanes without the 13-side chain (#1, 2, and 5), the retention factors decrease with increasing ACN. These compounds could be separated without the organic additive, which merely increases their aqueous phase solubility. For the next six taxanes (#4 and 6-10) there is little change in k' between 0 and 10 % ACN and then a sharp reduction above 20 % ACN. The k' values of the most hydrophobic compounds, #14 and 15, go through a maximum; it is not clear why a larger fraction of these compounds should partition into the micelle phase as the ACN concentration is increased up to 20%. Above this, if partial micelle disaggregation and consequent decreased ability to solubilize the taxanes is occurring, the decrease in mobility should be greatest for the most hydrophobic taxanes, which is observed.

The effect on current of the % ACN is shown in Figure 3.1.9. The current increased linearly from 0 to 20% ACN and reached a plateau value

above 30% ACN. The increase in the current indicates increase in the conductivity (reduction in resistance of the buffer), probably because the ACN reduced the size of the micelles, thus increasing the charge to size ratio. Seifar et al. [27] observed the same behavior for the conductivity measurements in SDS and ACN solutions.

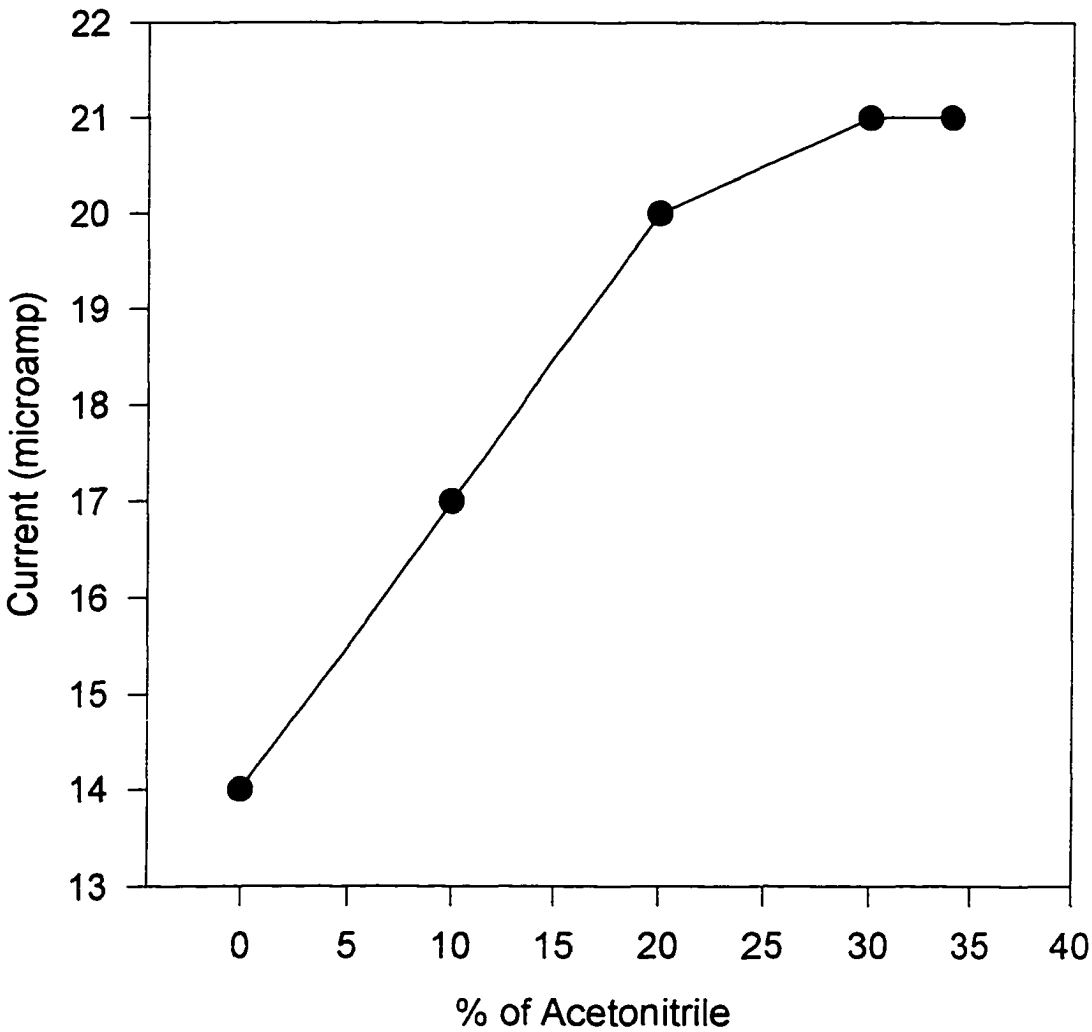

Figure 3.1.9 Effect of Acetonitrile on Current

MECC conditions: same as Figure 3.1.1
except concentration of acetonitrile

3.1.4 Effect of other Buffer Constituents

The function of buffer is to serve as an electrolyte, to carry current and to maintain constant pH in the electrophoretic medium. Tris was used as the buffer compound because it has large and minimally-charged ions, thus its mobility is low which generates a far lower current than a phosphate buffer of the same operational pH (operational because of the presence of ACN). The electroosmotic mobility decreased almost linearly by a factor of 1.3 as the Tris concentration was increased from 10 to 200 mM. The change in EOF also results in change of the separations as is shown in Figure 3.1.10.

Variation of the urea concentration from 0 to 40 mM had little effect on migration rate or resolution of taxanes and is probably not a necessary ingredient of the background electrolyte for the taxanes.

Figure 3.1.10 Effect of Buffer Concentration

MECC conditions: same as Figure 3.1.1 except concentration of Tris.

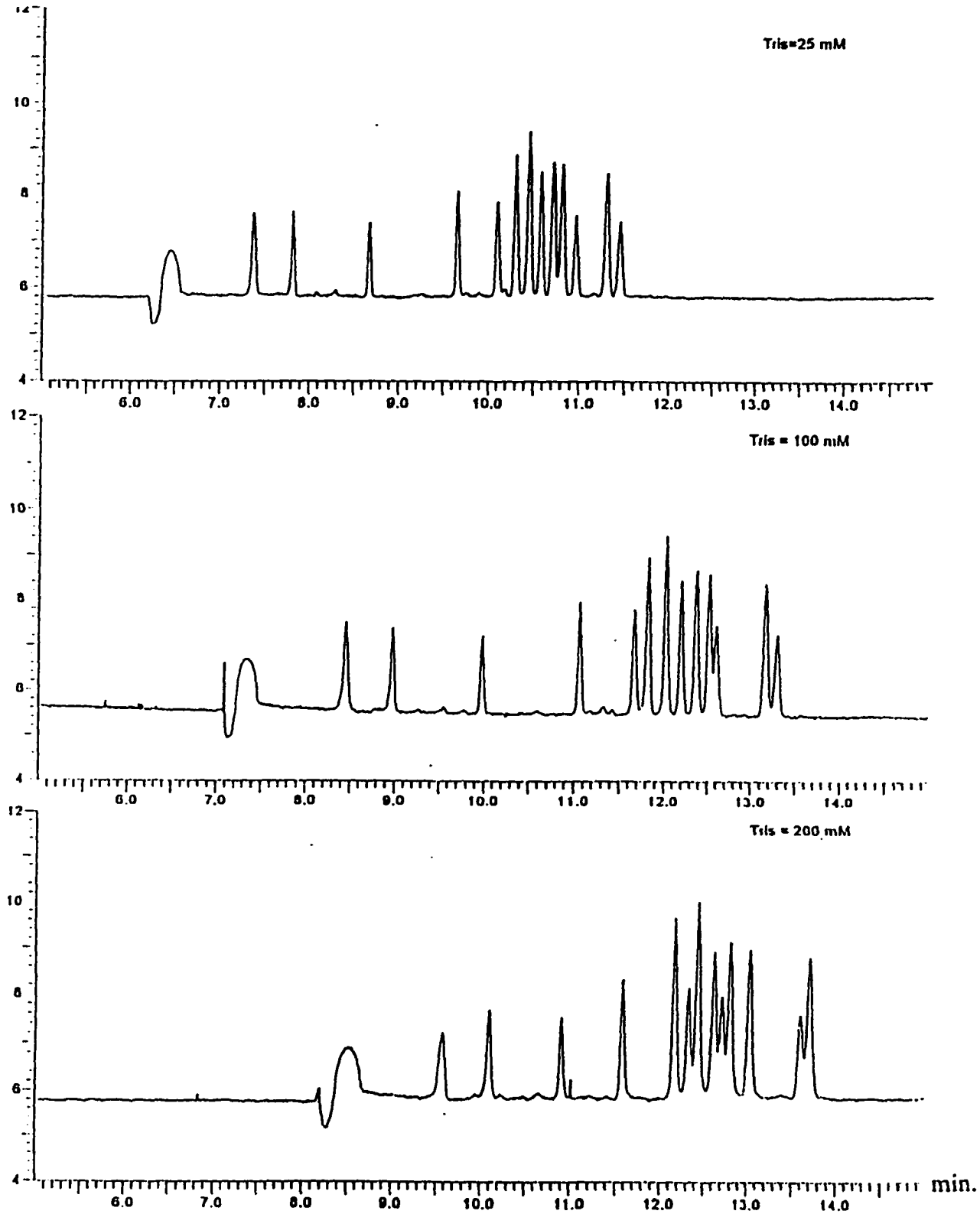

3.1.5 Effect of the Capillary Dimension

The migration velocity, v_{ep}, of a charged solute is given by

$$v_{ep} = \mu_{obs}E = \mu_{obs}V/L_t \quad (3.8)$$

The time, t, for a solute to migrate along the capillary with length L_d is

$$t = L_d/v_{ep} = L_dL_t/\mu_{obs}V \quad (3.9)$$

Diffusion in liquids that lead to broadening of an initially sharp band is described by the Einstein equation [37]:

$$\sigma^2 = 2Dt = 2DL_dL_t/\mu_{obs}V \quad (3.10)$$

Where σ^2 represents the peak variance associated with the Gaussian peak shape, D is the observed diffusion coefficient of the individual solute. The number of theoretical plates, N, is given by:

$$N = L_d L_t / \sigma^2 \qquad (3.11)$$

Substituting equation (3.10) into equation (3.11) gives an expression for the number of theoretical plates,

$$N = \mu_{obs} V/2D \qquad (3.12)$$

From equation (3.12), it can be seen that it is desired to apply a voltage as high as possible to achieve high efficiency. However, the applicable high voltage is often limited by Joule heating. Joule heating is a consequence of the resistance of the buffer to the flow of current, which is proportional to the power (P=VI), producing heat inside the capillary. The heat production can cause temperature gradients across the capillary and temperature changes with time due to ineffective heat dissipation. The amount of heat generated is proportional to the square of the field strength. Decreasing the voltage or increasing the length of the capillary will reduce the joule heating. Since current is inversely proportional to the resistance, while resistance is proportional to the length of the capillary and inversely proportional to the surface area. A capillary with smaller internal diameter or longer length will

significantly reduce the Joule heating. Ohm's law plots for six capillaries with different sizes are given in Figure 3.1.11 and Figure 3.1.12 respectively.

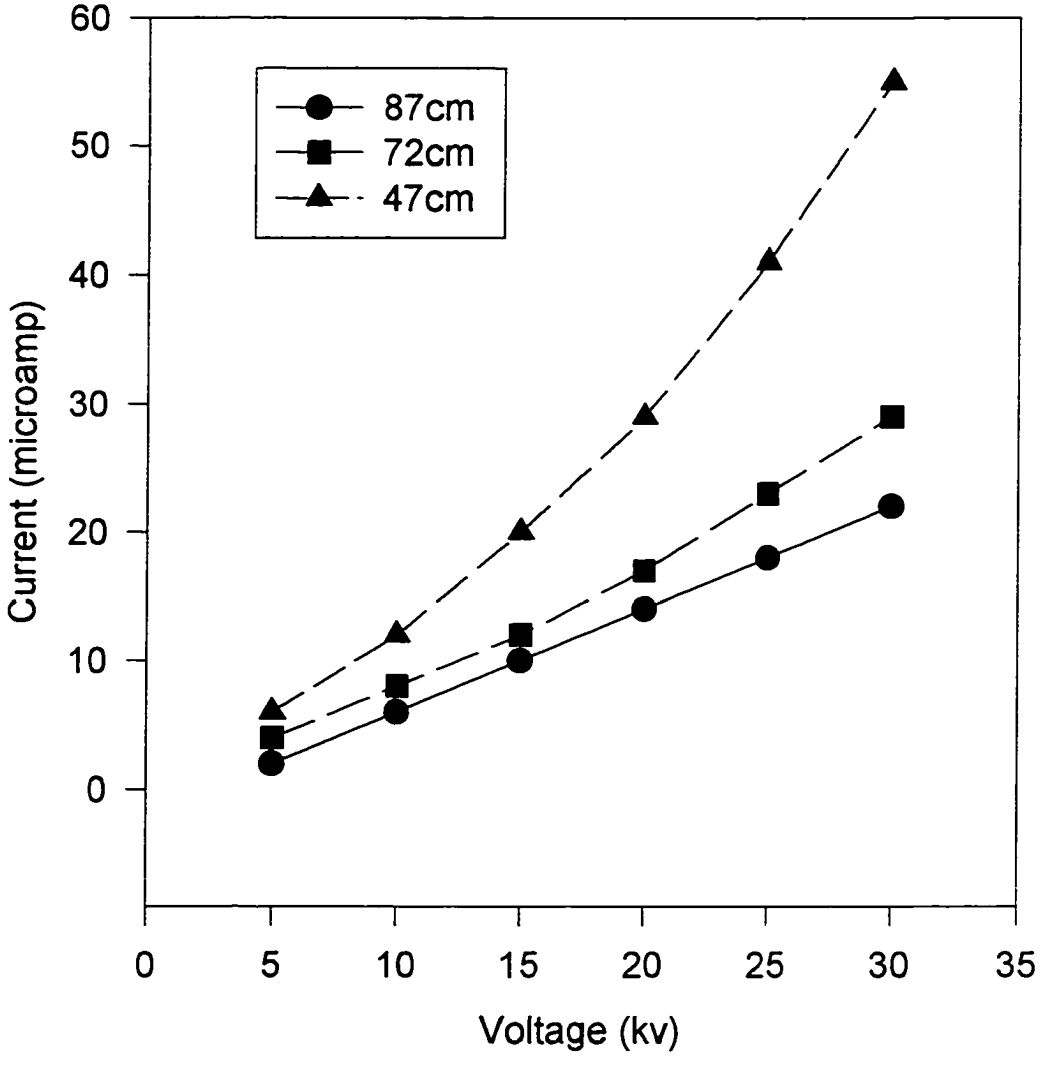

Figure 3.1.11

Ohm's Law Plots for 50 Micrometer Capillaries

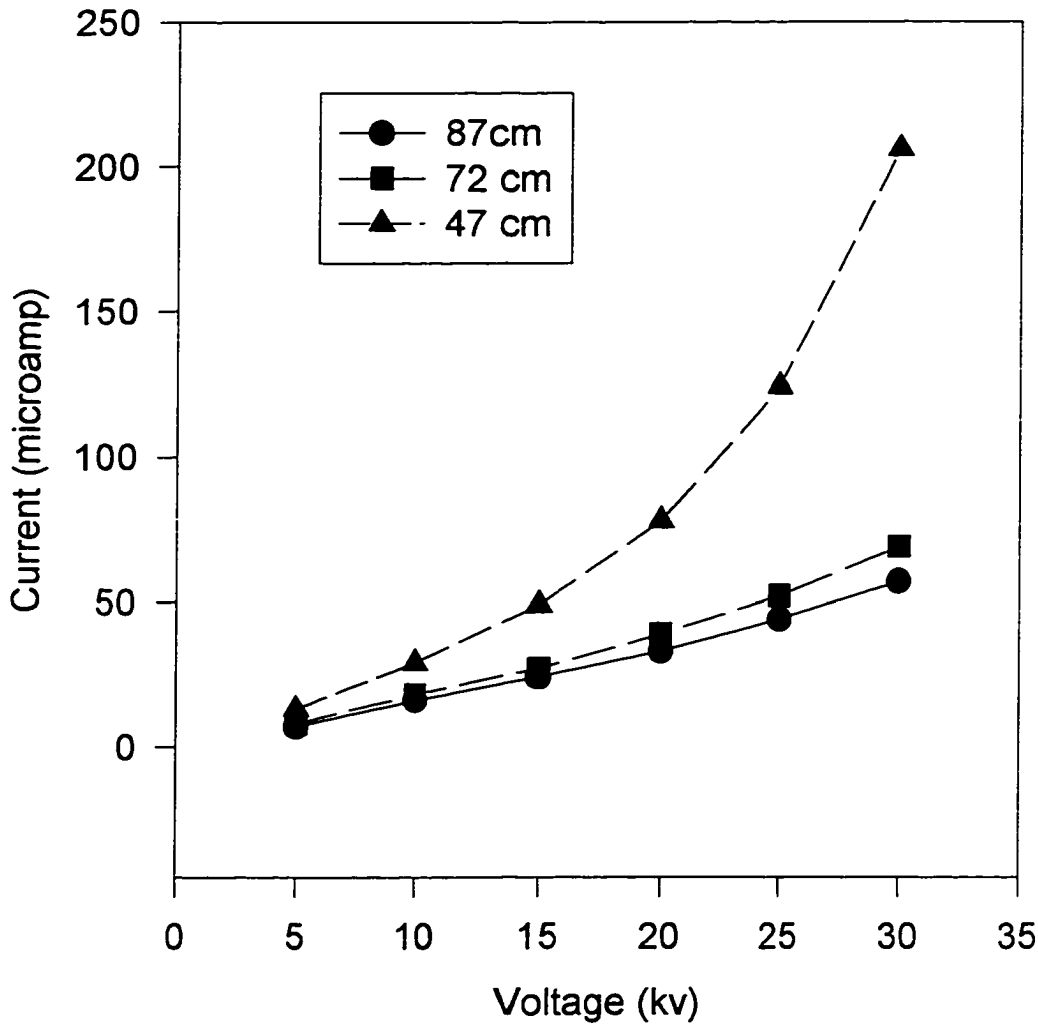

Figure 3.1.12

Ohm's Law Plots for 75 Micrometer Capillaries

For easy comparison, the effect of capillary i.d. (constant capillary length) on Joule heating is shown in Figure 3.1.13. The smaller i.d. capillary dissipates Joule heat more efficiently because of the larger surface area-to-volume ratio. The linear relationship between current and voltage starts to deviate as the capillary i.d. increases, as shown in Figure 3.1.13.

From equation (3.10), it can be seen that high voltages applied to short capillaries would generate the greatest number of theoretical plates.
But shorter capillaries tend to produce more Joule heat, as shown in Figure 3.1.11 and Figure 3.1.12. Thus the optimum capillary internal diameter and length was chosen by taking considerations of various factors such as Joule heat, efficiency, resolution and reasonable migration or analysis time.

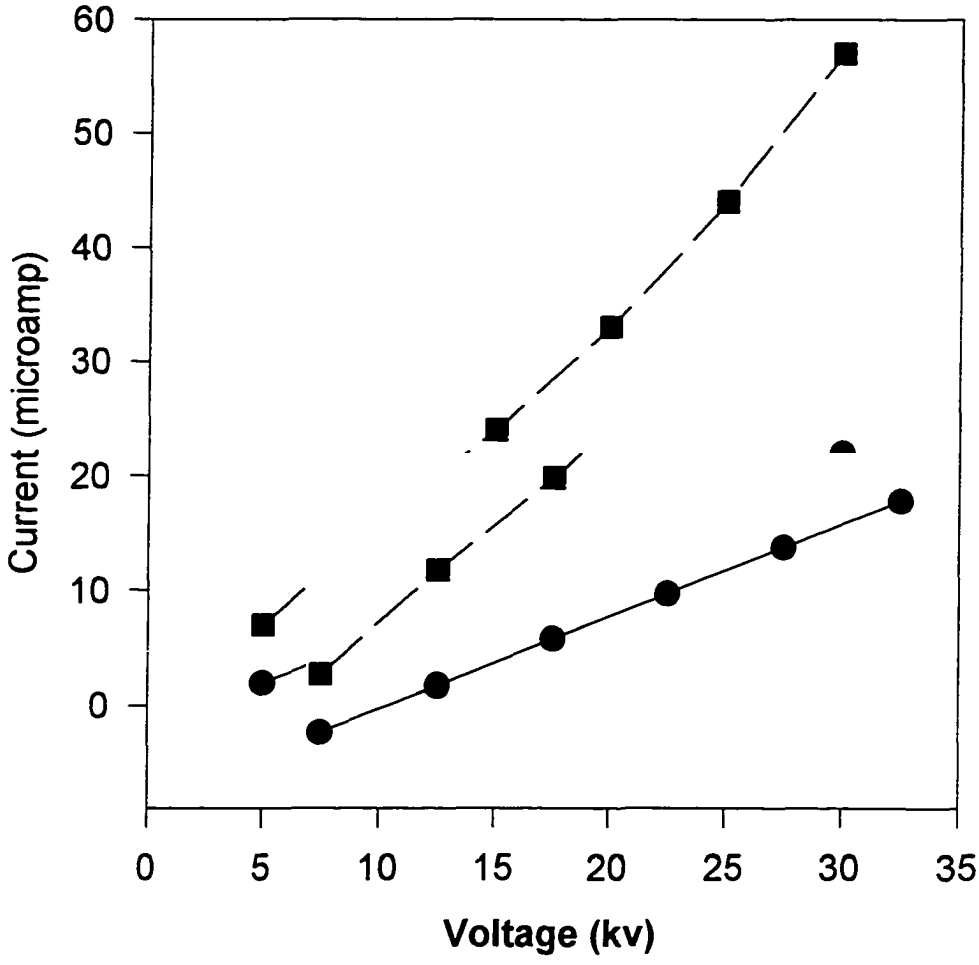

Figure 3.1.13

Effect of Capillary Internal Diameter on Joule Heating

capillaries length: 87 cm

3.1.6 Effect of Sample Matrix

Figure 3.1.14 are electropherograms of the thirteen taxane mixture dissolved in MeOH solvent only (top) and in 10 mM SDS (bottom). The striking difference between the two electropherograms probably results from a stacking effect, as discussed by Liu et al. [38] ; injection of small samples in lower conductivity media containing anionic surfactant above the CMC with normal electrode polarity causes concentration of anionic micelles and thus sample molecules associated with them, at the sample/running buffer interface, resulting in sharp, efficient peaks. In the absence of surfactant, no stacking can occur since the taxanes are neutral.

An alternative explanation for this we considered was mass transfer resistance [39], i.e. a slow rate of transfer of taxanes into the micelles from the injection solution without SDS, vs. injection of already micellized solutes. Plate height, H, was measured as a function of field strength E for baccatin III at 30°C and 60°C for the two sample matrixes. A plot of H vs. E is analogous to a chromatographic van Deemter plot since solute electrophoretic velocity is proportional to E. The data plotted in Figure 3.1.15 and Figure 3.1.16 do not

seem to be consistent with this slow equilibration hypothesis. The plate height for the micellized and stacking-concentrated taxane is low at both temperatures and is essentially independent of E because the micelle diffusion coefficient is small. For the methanol matrix, H initially decreases with E as time available for diffusion decreases, and at the lower temperature, increases at higher field strength possibly because of increased Joule heating [40] at the higher E. At 60°C, a sharp increase is not observed. More important, although there are few reported kinetic studies of solute incorporation into micelles, it seems the first step is rapid adsorption onto the micelle surface followed by slow penetration into the so-called palisade layer of the head groups and finally dissolution in the core [41-45]. Since the solutes are strongly and rapidly adsorptively associated with the micelles, mass transfer rate limitations should not apply. Thus we favor stacking as the source of higher efficiency with the SDS sample medium.

Figure 3.1.14 Effect of Sample Matrix. Sample dissolved in methanol (top) and in 10 mM SDS (bottom)

MECC conditions: same as Figure 3.1.1 except sample solvent.

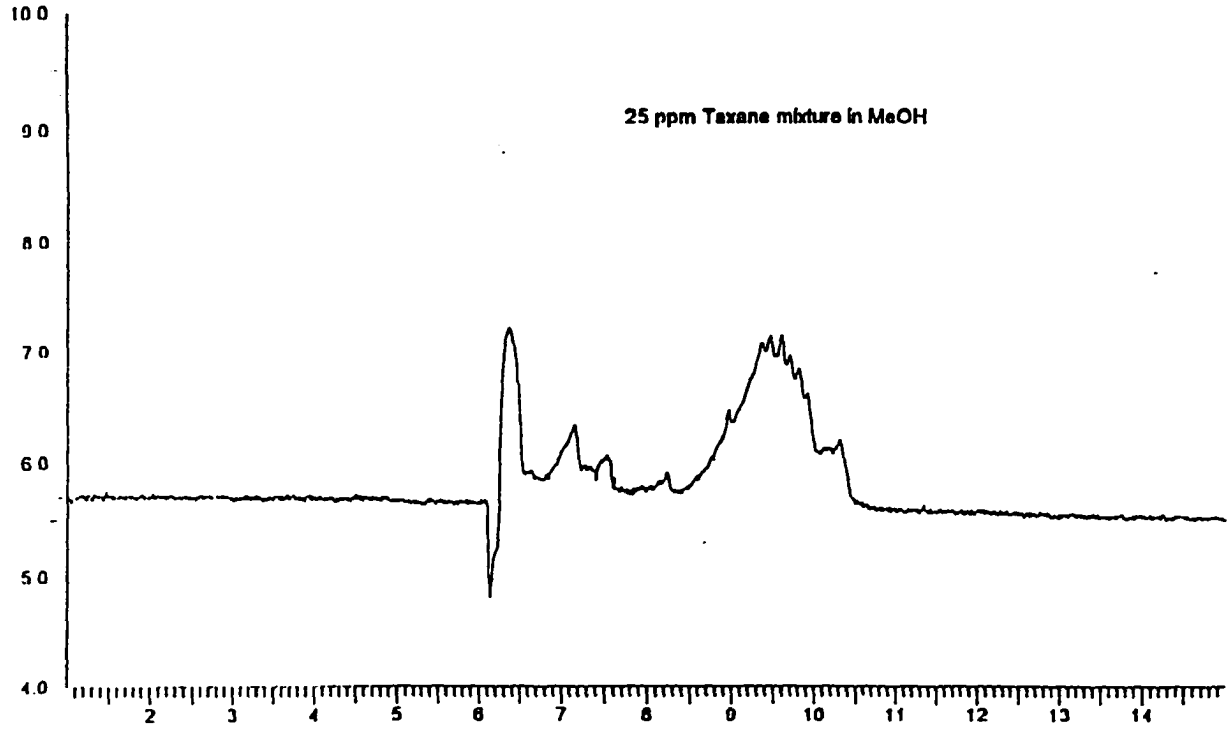

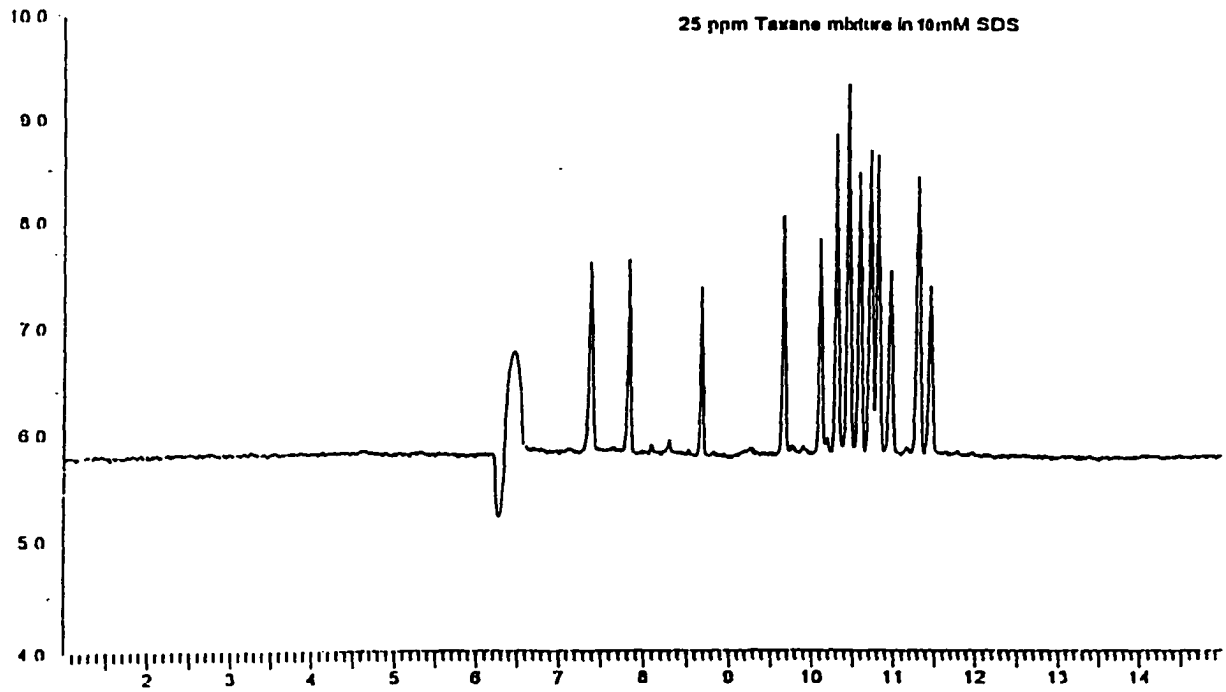

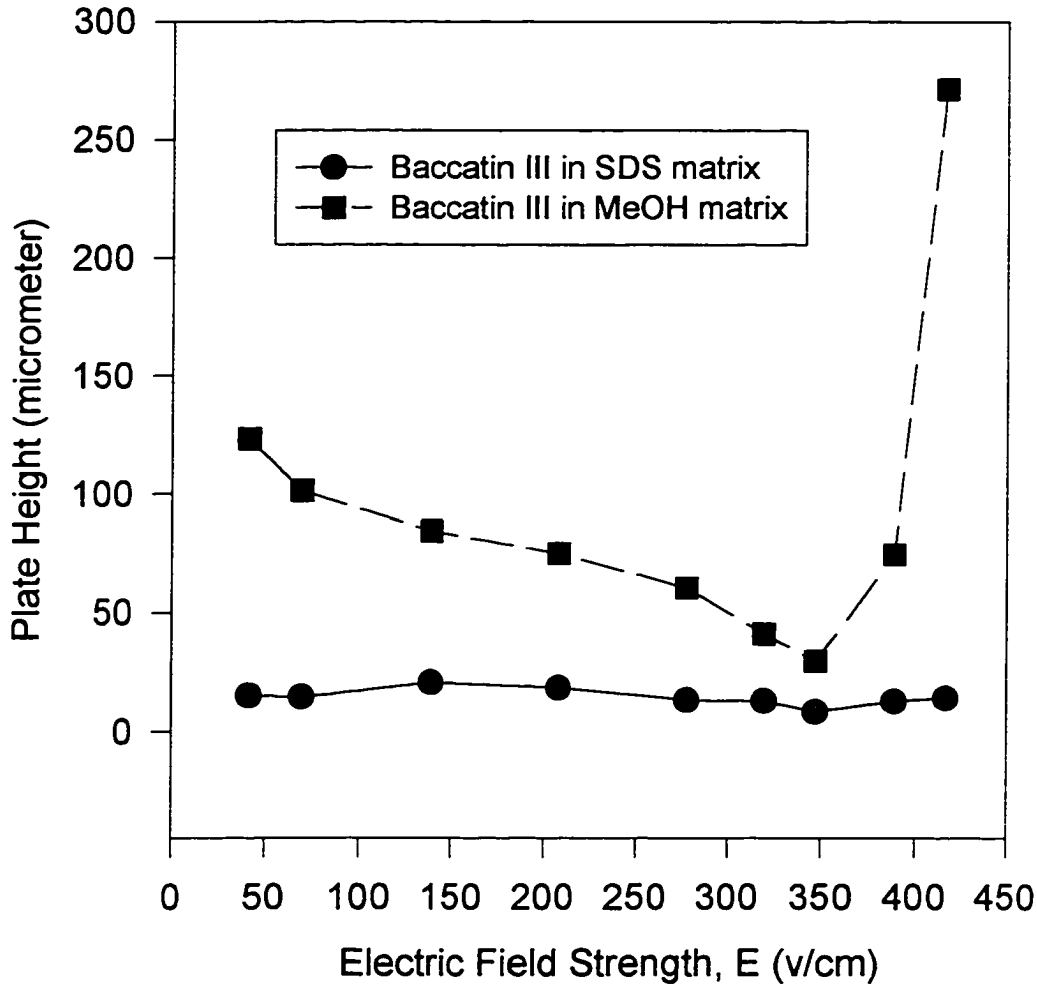

Figure 3.1.15
Plate Height vs. Field Strength at 30 C

MECC conditions: same as Figure 3.1.1
except applied voltage and sample solvent

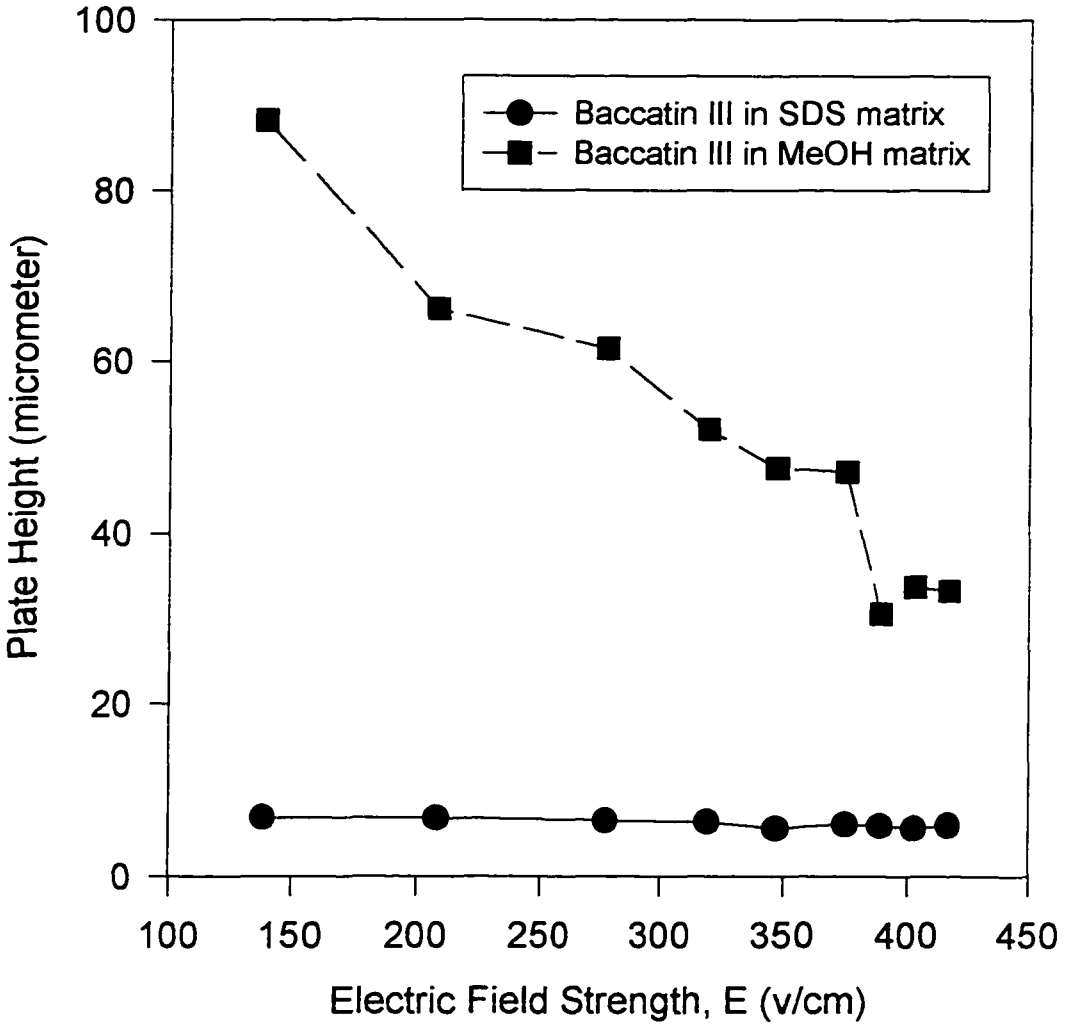

Figure 3.1.16 Plate Height vs. Field Strength at 60 C

MECC conditions: same as Figure 3.1.1 except applied voltage, temperature and sample solvent.

3.1.7 Effect of Temperature

Changes in capillary temperature can cause variations in buffer viscosity, EOF, electrophoretic mobility, CMC, and injection volumes. The temperature has an influence on the separation in MECC in several respects. First, micelles are only formed above critical micelle temperature (Kraft temperature). In general, a temperature increase causes a reduction in the concentration of free micelles due to an increase in CMC. Second, the temperature influences the capacity factor, as the temperature increases, the k' value usually decreases. Because of the dependence of the retention factor on the CMC and the distribution coefficient, temperature effects can be expected to be more serious in MECC than in capillary electrophoresis. Third, the temperature variation influences the buffer viscosity and thus effects the EOF and mobility, since the electrophoretic mobility (Eq.1.2) and the electroosmotic flow velocity (Eq.1.3) expressions both contain a viscosity term in the denominator. As the temperature increases, the viscosity of most fluids decreases, thus, the EOF and electrophoretic mobility increase as well. Fourth, the temperature influences the partition coefficient.

As a further comparison of the taxane separation by MECC and HPLC, migration time measurements for selected taxanes and the marker compounds were made at 10°C increments from 30 to 60°C, using the conditions given in Figure 3.1.1. The ln k' vs. 1/T plots (van't Hoff plots) were linear as shown in Figure 3.1.17. Standard enthalpies and entropies of transfer of solute from aqueous to micelle phase can be determined from the usual relationship,

$$\ln k' = - \Delta H°/RT + \Delta S°/R + \ln V_{mc}/V_{aq} \qquad (3.8)$$

where V_{mc}/V_{aq}, the phase ratio, is the ratio of the volume of micelles in the capillary to the volume of aqueous buffer, and is determined experimentally from [5]

$$V_{mc}/V_{aq} = \nu(C_{sds} - CMC) / [1 - \nu (C_{sds} - CMC)] \qquad (3.9)$$

The CMC of SDS in 30% ACN is certainly greater than the CMC in pure water, 8.1 mM [46]. In addition, values for ν, the partial specific volume of SDS, are given as a function of temperature by Shinoda and Soda [47], in pure water, but not in aqueous acetonitrile. Thus we are in the same quandary

in CE as we were in HPLC in Part I of this thesis; the phase ratio is essentially inaccessible so that the ΔS° can not be reliably determined.

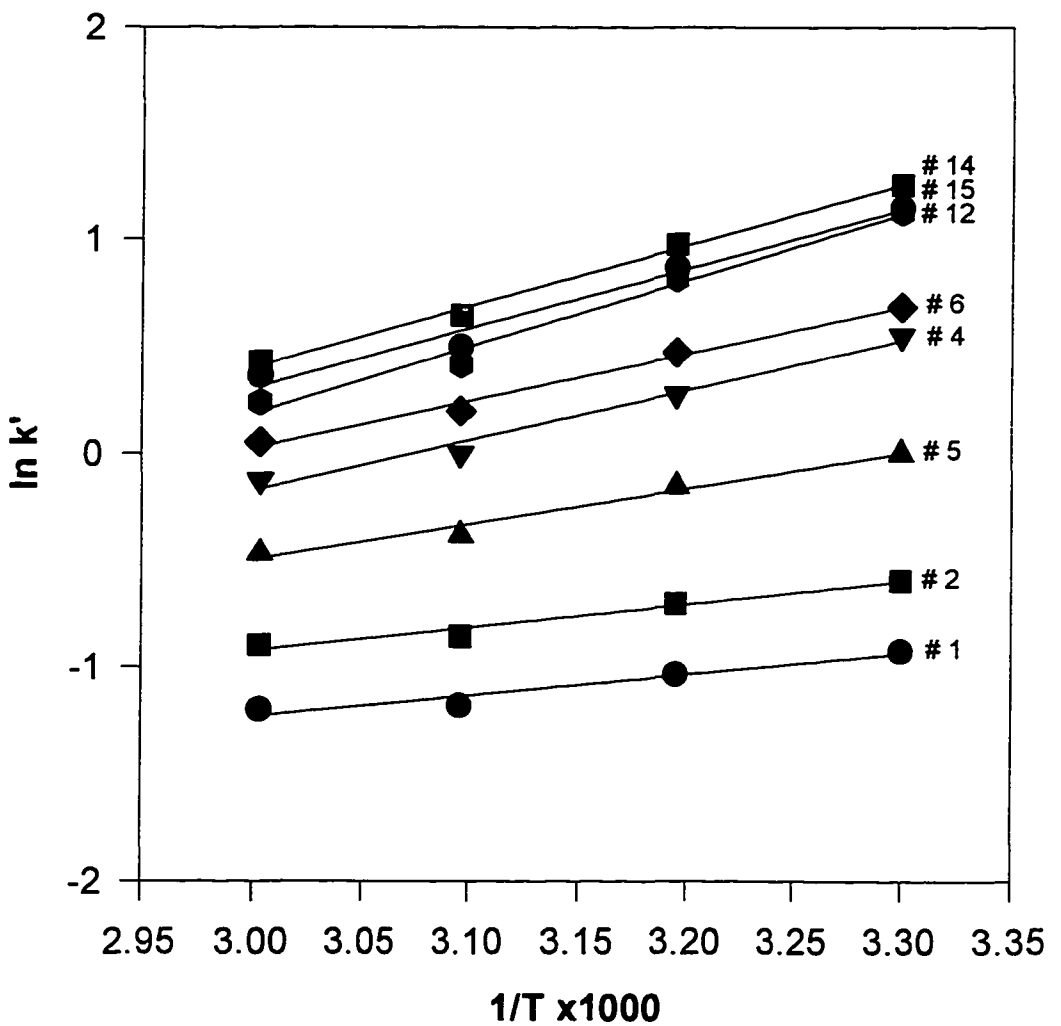

Figure 3.1.17 van't Hoff Plot for Taxanes

MECC conditions: same as Figure 3.1.1 except temperature.

Taxane number refers to Figure 1, Part I.

In Table 3.2 are listed the derived thermodynamic properties. The order of increasingly negative $\Delta H°$ values follows the migration order with the exceptions of #4/#6 and #12/#14. In general, the more hydrophobic the compound, the larger the enthalpy change on association with the micelle. The values of $[\Delta S°/R + \ln V_{mic}/V_{aq}]$ follow the same trend. For simpler aromatic compounds in purely aqueous SDS, Terabe et al. [5] obtained $\Delta H°$ values of approximately the same magnitude. It is interesting to note that "entropy-enthalpy compensation" [48] is observed: a plot of ln k' for the taxanes vs. - $\Delta H°$ is linear ($r^2 = 0.943$).

Table 3.2

Thermodynamic Quantities from the van't Hoff Plot

MECC conditions: same as Figure 3.1.1 except temperature

Taxane number refers to Figure 1, Part I.

Taxane #	$-\Delta H°$ (J/mol)	$-[\Delta S°/R + \ln V_{mic}/V_{aq}]$
1	8.16×10^3	4.17
2	9.03×10^3	4.18
5	1.37×10^4	5.45
6	1.83×10^4	6.58
4	2.33×10^4	7.16
12	2.59×10^4	9.15
15	2.31×10^4	8.03
14	2.37×10^4	8.16

3.1.8 Limit of Detection

There are two means of describing the limits of detection of a system: the concentration limit of detection (CLOD) and the mass limit of detection (MLOD). The CLOD relates to the concentration of the individual sample, whereas the MLOD describes what sample size that the instrument can measure. For example, the CLOD of paclitaxel using HPLC method A is 0.37 μg/mL (see section 3.5.6 of Part I of this thesis). If 15 μL of that compound is injected and detected at three times the baseline noise, the MLOD is 5.55 ng. Another way of describing MLOD is based on the volume of the detector window. If 0.37 μg/mL of paclitaxel solution is aspirated continuously through a column, then for a 0.1 mL detector window, the amount of compound in the window at any given time is 37 ng. Thus MLOD can be manipulated by selecting the size of the detection window.

The narrow capillary diameter in CE allows the use of high field strengths to obtain high efficiency, but it also generates a very short optical pathlength for optical detection, and limits the quantity of analyte that can be introduced into the capillary. The volume of sample required in CE is much

less than that of HPLC, so it is easily concluded that CE has excellent MLODs but poor CLODs comparing to HPLC with optical detection. Under certain conditions, however, CE outperforms HPLC with respect to detectability. Aqueous-based electrolytes (which have low UV absorbance coefficience) are often employed in CE, allowing detection wavelengths such as 200 nm to be routinely employed. Many impurities have poor chromophores making their quantitation at traditional HPLC wavelengths difficult or impossible. Alternatively, the use of low UV wavelengths may be compensate for the inherent poor sensitivity in CE. A number of approaches have been described to improve the concentration sensitivity of UV absorbance detection in CE including extension of the optical pathlength (e.g., with the use of Z-shaped [49], bubble [50], or rectangular capillaries [51]), electrophoretic stacking, [52-55], isotachophoresis, [56-57] and on-line chromatographic reconcentration [58].

The CLOD for paclitaxel by the MECC was determined to be 2.2 μg/mL or 2.5×10^{-6} M. For 50 μm i.d. capillary, an injection using 5" Hg vacuum for 1 second loads about 3.5 nL of aqueous solution [59]. So the MLOD for paclitaxel by MECC was 7.7 pg. As discussed in section 3.5.6 of

Part I of this thesis, the CLOD for paclitaxel was 0.37 μg/mL using HPLC method A and 0.31 μg/mL using HPLC method B. The MLOD for paclitaxel was 5.6 ng for method A and 4.6 ng for method B. Comparing our MECC and HPLC methods, the concentration sensitivity of MECC method was only a factor of ten less than that of HPLC.

3.2 MECC Separation of Paclitaxel from Excipient in Injectable Form

As mentioned in Part I of this thesis, in the Taxol injectable dosage form, paclitaxel is solubilized in an ethanolic solution of the polyethoxylated castor oil-based surfactant, Cremophor EL. This material is used as a parenteral vehicle for a variety of hydrophobic pharmaceuticals. In Figure 3.2.1, in the top electropherogram shows the MECC separation of paclitaxel from excipient in injectable form, and in the bottom diagram shows the interfering ingredient Cremophor EL alone; complete separation between the paclitaxel and Cremophor EL is achieved. Injection of paclitaxel plus an amount of ethanol equivalent to that in the injectable form had no effect on the electrophoregram of the taxane. Apparently, the interaction between Cremophor EL and SDS micelle is stronger than paclitaxel and SDS micelle, so Cremophor EL migrates after paclitaxel. Cremophor EL is a reaction product of castor oil and ethylene oxide and is composed of ricinoleates and glycerin polyglycol ethers, plus esters of ricinoleic acid and polyglycols, as well as, probably, di-esters and higher esters whose hydroxyl groups are esterified with ricinoleic acid [60,61]. The stronger hydrophobic interaction

between SDS micelles and Cremophor EL probably arises from the similar straight chain structures of the both.

Figure 3.2.1 Electrophoregrams of Injectable Paclitaxel (top) and Cremophor EL (bottom)

MECC conditions: same as Figure 3.1.1 except 30 mM SDS.

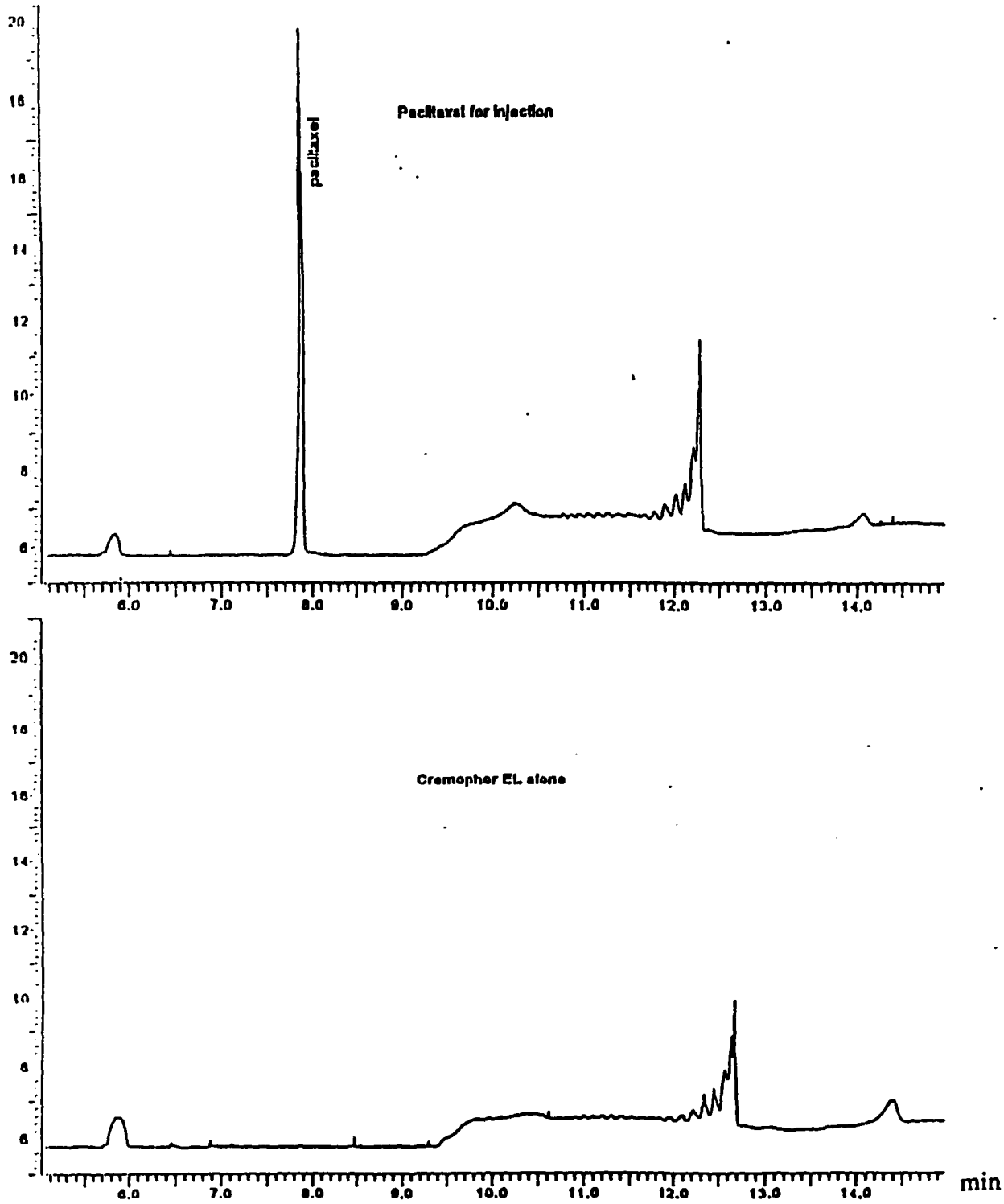

In Figure 3.2.2 is shown the effect of SDS concentration on the separation of Taxol injectable form. Both Cremophor EL and Taxol are nonionic compounds and have zero electrophoretic mobility. In the absence of charged SDS micelle, they migrate with the EOF, so no separation is possible. As the SDS concentration increases, the electrophoretic mobility of SDS micelles increases, as do the net mobilities of paclitaxel and Cremophor EL associated with the micelles. Figure 3.2.3 is shown the effect of SDS concentration on Cremophor EL blank. The Cremophor EL peak does not coelute with the paclitaxel. Because at an SDS concentration of 30 mM, the separation of paclitaxel and Cremophor EL was good and the best peak shape for Cremophor EL was obtained, this concentration was used in the buffer electrolyte. As was observed in HPLC [1], there seems to be some resolution of oligomers of Cremophor EL which may result from the formation of mixed SDS/Cremophor micelles. Bullock [28] obtained excellent separations of oligomers of various surfactants using SDS.

Figure 3.2.2 Effect of SDS Concentration on the Separation of Paclitaxel Injectable Form

MECC conditions: same as Figure 3.1.1 except concentration of SDS.

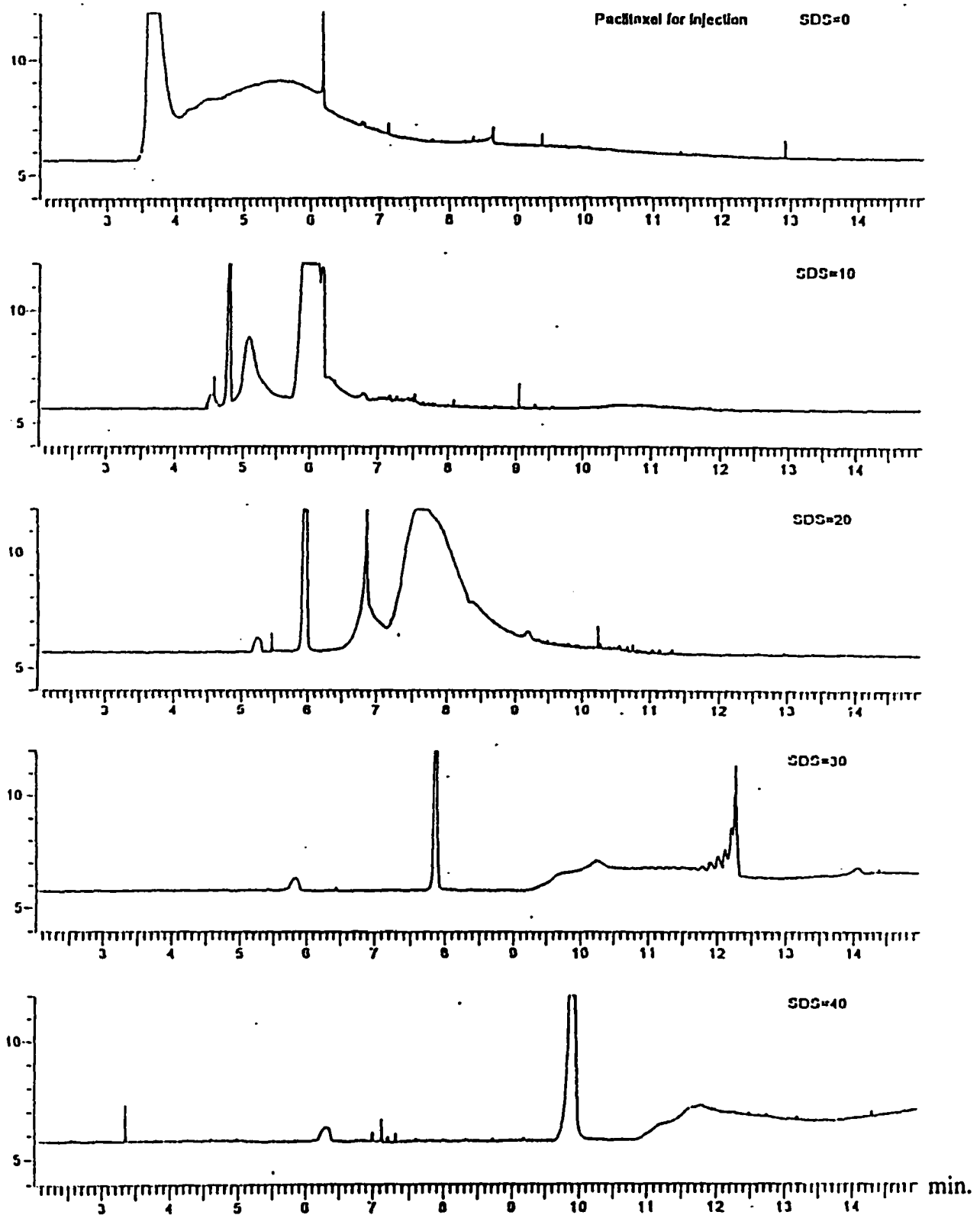

Figure 3.2.3 Effect of SDS Concentration on the Excipient Cremophor EL

MECC conditions: same as Figure 3.1.1 except concentration of SDS.

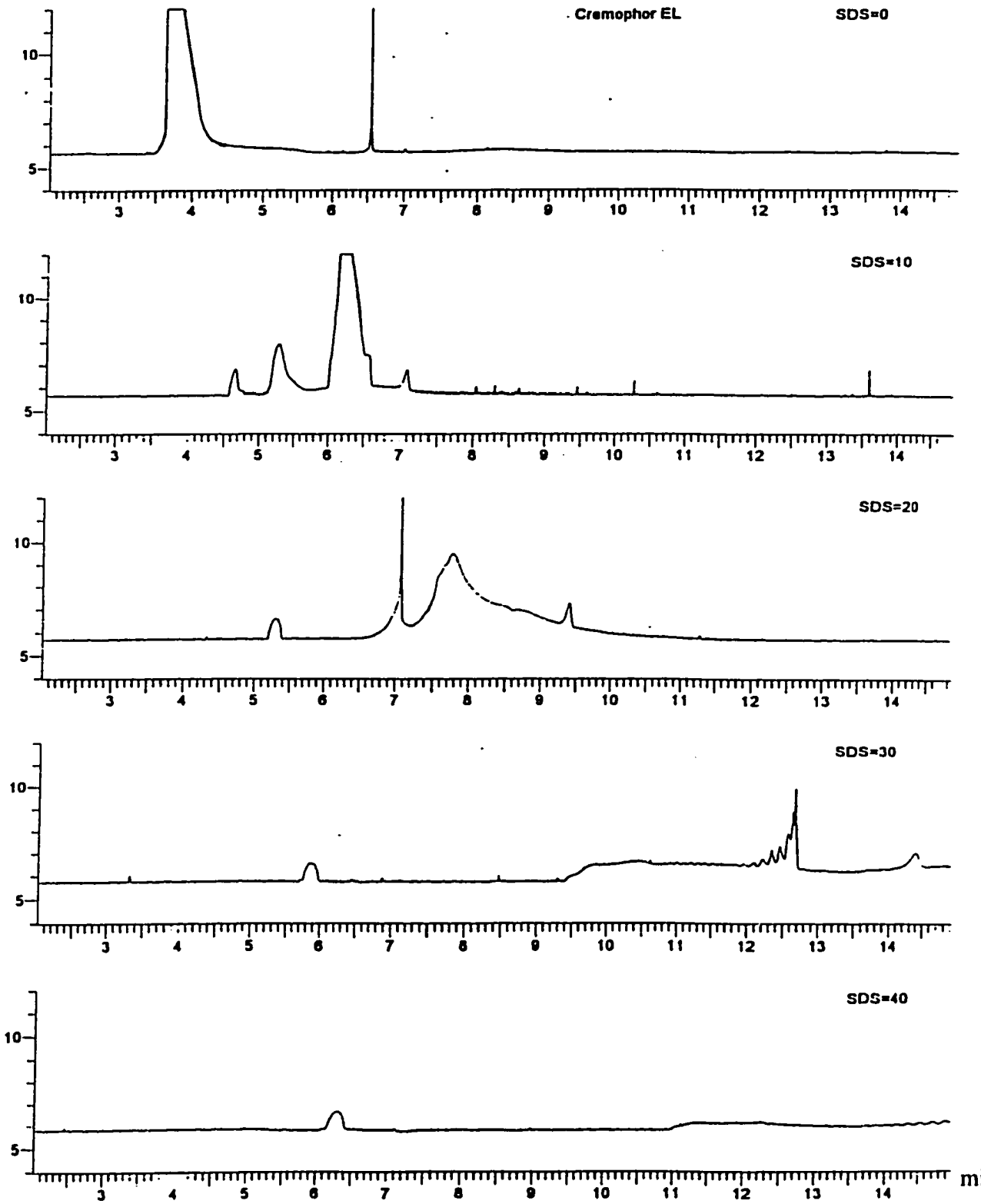

3.3 Conclusions

Micellar electrokinetic capillary chromatography (MECC) is applied to separate paclitaxel and 14 related taxanes in 11.5 min. An aqueous acetonitrile buffer with SDS surfactant allows resolution of the 15 taxanes from each other and from the principal matrix ingredient Cremophor EL (polyethoxylated castor oil) in the injectable dosage form. Although the precise effect of high concentrations of acetonitrile on micelle size and structure is not clear, the separation achieved is not possible in the absence of the organic modifier. The analysis time per injection for separation of 13 taxanes by MECC technique was at least a factor of two less than that of HPLC method. Determination of paclitaxel in its injectable form was achieved in less than eight minutes by MECC method, it saved at least 56 % of the analysis time compared to HPLC methods.

The migration order is apparently that of decreasing aqueous phase solubility, which is related to the presence of a side chain at the carbon-13 position, to the addition of a xylosyl group at the 7-position, and to the

number of acetylated hydroxyl groups; and to the increasing affinity of the taxane side chain for the micellar phase.

The retention factors, k', increase linearly with SDS concentration above the critical micelle concentration (CMC). With increasing concentration of ACN, k' values for taxanes without side chain decrease; for the most hydrophobic taxanes, k' values increase up to 20 % (v/v) ACN and then decrease rapidly at higher concentrations. Similar behavior was observed with methanol but the break in k' occurred between 30% and 40% (v/v).

Resolution was unacceptably poor if the samples dissolved in methanol were injected; samples dissolved in buffer containing SDS were well-behaved, probably because of stacking of the micelles during injection.

van't Hoff plots (ln k' vs. 1/T) were linear and allowed reliable calculations of the $\Delta H°$ of transfer of taxane from aqueous to micelle phase. However, similar to the situation in HPLC, uncertainty in the micelle/aqueous phase ratio precludes reliable determination of the corresponding $\Delta S°$.

References

Part I

[1] Wani, M.C.; Taylor, H.L.; Wall, M.E.; Coggan, P.; McPhail, R.T. *J. Am. Chem. Soc.* **1971**, *93*, 2325-2327.

[2] Spencer, C.M. and Faulds, D. *Drugs* **1994**, *48*, 794-847.

[3] National Cancer Institute Clinical Brochure: Taxol (NSC1259973), NCI, Division of Cancer Treatment, Bethesda, MD, USA, **1983**, 6-12.

[4] Riondel, J.; Jacrot, M.; Picot, F.; Beriel, H.; Mouriquand, C.; Potier, P. *Cancer Chemother. Pharmacol.* **1986**, *17*,137-142.

[5] Jacrot, M.; Riondel, J.; Picot, F.; Leroux, D.; Mouriquand, C; Beriel, H.; Potier, P.; Seances, C.R. *Acad. Sci. Ser.* **1983**, *3*, *247*, 597-600.

[6] McGuire, W.P.; Rowinsky, E.K.; Rosensheim, N.B.; Grumbine, F.C.; Ettinger, D.S.; Armstrong, D.K.; Donehower, R.C. *Ann. Intern. Med.* **1989**, *111*, 273-279.

[7] Thigpen, T.; Blessing, J.; Ball, H.; Hummel, S.; Barret, R. Proc. *Annu. Meet. Am. Soc. Clin. Oncol.* **1990**, *9* (Abstract 604).

[8] Ozols, R.F. *Curr. Probl. Cancer*, **1992**, *16*, 63-126.

[9] Holms, F.A.; Walters, R.S.; Theriault, R.L.; Forman, A.D.; Newton, L.K.; Raber, M.N.; Buzdar, A.U.; Frye, D.H.; Hortobagyi, G.N. *J. Natl. Cancer Inst.* **1991**, *83*,1797-1805.

[10] Murphey, W.K.; Winn, R.J.; Fossella, F.V. et al. *Proc. Annu. Meet. Am. Soc. Clin. Oncol.* **1992**, *11*, 294 (Abstract 985).

[11] Chang, A.; Kim, K.; Glick, J. *ibid.* **1992**, *11*, 293 (Abstract 981).

[12] Sarosy, G.; Kohn, E.; Link, C.; Adamo, D.; Davis, P.;Ognibene,F.; Goldspiel, B.; Cristian, M.;Reed, E. *Proc. Annu. Meet. Am. Soc. Clin. Oncol.* **1992**, *11*, 226 (Abstract 716).

[13] Vidensek, N.; Campbell, A.; Carlson, C. *J. Nat. Prod.* **1990**, *53*, 1609-1610.

[14] Rowinsky, E.K.; Cazenave, L.A.Donehower, R.C. *J. Nati. Cancer Inst.*, **1990**, *82*, 1247-1259.

[15] Pharmacology and Antitumor Effect of Novel Paclitaxel Formulations. *Taxane Anticancer Agents*, ACS symposium series 583. American Chemical Society, Washington, DC **1995**, pp.113.

[16] Witherup, K.M.; Look, S.A.; Stasko, W.M .; Ghiorzi, T.J.; Muschik, G.M.; Cragg, G.M. *J. Nat. Prod.* **1990**, *53*, 1249-1255.

[17] Gueritte-Voegelein, F. *J. Med. Chem.* **1991**, *34*, 992-998.

[18] Christen, A.A.; Bland, J.; Gibson, D. *Proc. Am. Assoc. Cancer Res.* **1989**,*30*, 566.

[19] Cragg, G.M.; Schepartz, S.A.; Suffness, M.; Grever, M.R. *J. Nat. Prod.* **1993**, *56*, 1657-1668.

[20] Gibson, D., Christen, A.; Ketchum, R. *Plant. Physiol.* **1991**, 965, *96*, 19-27.

[21] Stierle,A.; Strobel,G.A.; Stierle D. *Science* **1993**, *260*, 214-216.

[22] Holton, R.A.; Somoza, C.; Kim, S.; Nadizadeh, H.; Suzuki, Y.; Tao, C.;Vu, P.; Tang, S.; Zhang, P.; Murthi, K.K.; Gentile, L.N.; Liu, J.H. *J. Am. Chem. Soc.* **1994**, *116*,1597-1598.

[23] Holton, R.A.; Kim, H.B.; Somoza, C.; Liang, F.; Biediger, R.J.; Boatman, P.D.; Shindo, M.; Smith, C.C.; Kim, S.; Nadizadeh, H.; Suzuki,Y.; Tao, C.; Vu, P.; Tang, S.; Zhang, P.; Murthi, K.K.; Gentile, L.N.; Liu, J.H. *J.Am. Chem. Soc.* **1994**, *116*,1599-1600.

[24] Nicolaou, K.C.; Yang, Z.; Liu, J.J.; Ueno, H.; Nantermet, P.G.; Guy, R.K.; Claiborne, C.F.; Renaud, J.; Couladouros, E.A.; Paulvannan, K.; Sorensen, E.J. *Nature* **1994**, *367*, 630-634.

[25] Nicolaou, K.C.; Nantermet, P.G.; Ueno, H.; Guy, R.K.; Couladourous, E.A.; Sorensen, E. *J. Am. Chem. Soc.* **1995a** , *117*, 624-633.

[26] Nicolaou, K.C.; Liu, J.J.; Yang, Z.; Ueno, H.; Sorensen, E.J.; Claiborne, C.F.; Guy, R.K.; Hwang, C.K.; Nakada, M.; Nantermet, P.G. *J. Am. Chem. Soc.* **1995b**, *117*, 634-644.

[27] Nicolaou, K.C.; Yang, Z.; Liu, J.J.; Ueno, H.; Nantermet, P.G.; Claiborne, C.F.; Renaud, J.; Guy, R.K.; Shibayama, *J. Am. Chem. Soc.* **1995c,** *117*, 645-652.

[28] Nicolaou, K.C.; Ueno, H.; Liu, J.J.; Nantermet, P.G.; Yang, Z.; Renaud, J.; Paulvannan, K.; Chadha, R. *J. Am. Chem. Soc.* **1995d**, *117*, 653-659.

[29] Mattina, M.J.I.; Paiva, A., *J. Environ. Hort.* **1992**, (Dec.), *10* (*4*),187-191.

[30] News, *J. Natl Cancer Inst*, July 3, **1991**.

[31] Huizing, M.T.; Sewbarath Misser, V.H., Pieters, R.C. *Cancer Invest.*, (1994).

[32] Shiff, P.B.; Fant, J.; Horwitz S.B. *Nature*, **1979**, *277*, 665-667.

[33] Manfredi, J.J.; Fant, J.; Horwitz, S.B. *Eur. J. Cell Biol.* **1986**, *42*,126-134.

[34] Shiff, P.B.; Horwitz, S.B. *Proc. Natl Acad. Sci.* **1980**, *77*, 1561-1565.

[35] Kingston, D.G.I. *Pharm. Ther.* **1991**, *52*,1-34.

[36] Kingston, D.G.I, Molinero, A.A.; Rinaldi, J.M. Progr. Chem. Org. Nat. Prod., **1993**, *61*, 1-206, Springer-Verlag.

[37] Kingston, D.G.I. *Trends Biotechnol.* **1994**, *12*, 222-227.

[38] Witherup, K.M.; Look, S.A.; Stasko, M.W.; McCloud, T.G.; Issaq, H.J.; Mushik, G.M. *J. Liq. Chromatogr.* **1989**, *12*, 2117-2132.

[39] Kopycki, W.J.; ElSohly, H.N.; McChesney, J.D. *J. Liq. Chromatogr.* **1994**, *17*, 2569-2591.

[40] Whatman Incorporation Catalog, 1996, Clifton, New Jersey.

[41] Phenomenex Incorporation Catalog, 1996, Torrance, California.

[42] Rizzo, J.; Riley, C.; VonHoff, D.; Kuhn, J.; Phillips, J.; Brown, T. J. *Pharm. Biomed. Anal.* **1990**, *8*, 159-164.

[43] Xu, L.X.; Liu, A.R. *Acta. Pharm. Sinica.* **1991**, *26(7)*, 537-540.

[44] Ketchum, R.E.; Gibson, D.M. *J. Liq. Chromatogr.* **1993**, *16*, 2519-2530.

[45] Chan, K.C.; Alvarado, A.B.; McGuire, M.T.; Muschik, G.M.; Issaq, H.J.; Snader, K.M. *J. Chromatogr. B* **1994**, *657*, 301-306.

[46] Chan, K.C.; Muschik, G.M.; Issaq, H.J.; Snader, K.M. *J. High Resol. Chromatogr.* **1994**, *17*, 51-52.

[47] Mattina, M.J.I.; MacEachern, G.J. *J. Chromatogr. A* **1994**, *679*, 269-275.

[48] Sparreboom, A.; van Tellingen, O.; Nooijen, W.J.; Beijin, J.H. *J. Chromatogr. B* **1995**, *664*, 383-391.

[49] Song, D.; Au, J.L.-S. *J. Chromatogr. B* **1995**, *663*, 337-344.

[50] Huizing, M.T.; Rosing, H.; Koopman, F.; Keung, A.C.F.; Pinedo, H.M.; Beijnen, J.H. *J. Chromatogr. B* **1995**, *664*, 373-382.

[51] Lauren, D.R.; Jensen, D.J.; Douglas, J.A. *J. Chromatogr. A* **1995**, *712*, 303-309.

[52] Vandana, V.; Teja, A.S.; Zalkow, L.H. *Fluid Phase Equilib.* **1996**, *116*, 162-169.

[53] Aboul-Enein, H.Y.; Serignese, V. *Anal. Chim. Acta* , **1996**, *319*, 187-190.

[54] Richheimer, S.L.; Tinnermeier, D.M.; Timmons, D.W. *Anal. Chem.*, **1992**, *64*, 2323-2326.

[55] Yamamoto, F.M.; Rokushika, S.; Hatano, H. *J. Chromatogr. Sci.* **1989**, *27*, 704-709.

[56] Sander, L.C.; Field, L.R. *Anal. Chem.*, **1980**, *52*, 2009-2013.

[57] Hall, P.F. *J. Biol. Chem.* **1979**, *254*, 9080-9084.

[58] Polyoxyethylene Castor Oil Derivatives. *Handbook of Pharmaceutical Excipients*; American Pharmaceutical Association/Pharmaceutical Society of Great Britain: Washington, DC, **1986**; pp 221-224.

[59] Peereboom, D.M.; Donehower, R.C.; Eisnhauer, E.A.; McGuire, W.P.; Onetto, N.; Hubbard, J.L.; Piccart, M.; Gianni, L.; Rowinsky, E.K. *J. Clin. Oncol.*, **1993**, *11*, 885-890.

[60] Clark, M.A.; Shay, J.W. *Endocrinology* **1981**, *109*, 2261-2263.

[61] United States Pharmacopeia, 23rd ed.; section 1225, 'Validation of Compendial Methods.' US Pharmacopeia convention: Rockville, MD, **1995**, 1982-1984.

[62] Debesis, E.; Boehlert, J.P.; Givand, T.E.; Sheridan, J.C. *Pharm. Technol.*, **1982**, (Sept.) 120-137.

[63] Purnell, J.H. Gas Chromatography, John Wiley & Sons, New York, N.Y.,1962.

[64] SAS/STAT User's Guide, Version 6, Forth Edition. SAS Institute Inc., 1989, 1848.

Part II.

[1] Shao, L.K.; Locke, D.C. *Anal. Chem.*, **1997**, *69*, 2008-2016.

[2] Jorgenson, J.; Lukacs, K.D. *Anal. Chem.*, **1981**, *53*, 1298.

[3] Jorgenson, J.; Lukacs, K.D. *Science*, **1983**, *222*, 226-72.

[4] von Smoluchowski, M. *Bull. Int. Acad. Sci. Cracovie* **1903**, 184.

[5] Terabe, S.; Otsuka, K.; Ichikawa, K.; Tsuchiya, A.; Ando, T. *Anal. Chem.*, **1984**, *56*, 111-113.

[6] Terabe, S.; Otsuka, K.; Ando, T. *Anal. Chem.* , **1985**, *57*, 834-841.

[7] Chan, K.C.; Muschik, G.M.; Issaq, H.J.; Snader, K.M. *J. High Res. Chromatogr.*, 1994, *17*, 51-52.

[8] Chan, K.C. Alvarado, A.B.; McGuire, M.T.; Muschik, G.M.; Issaq, H.J.; Snader, K.M. *J. Chromatogr. B: Biomed. Appl.* **1994**, *657*, 301-306.

[9] Shinoda, K. *J. Phys.Chem.*, **1954**, *58*, 1136-1141.

[10] Almgren, M; Swarup, S. *J. Colloid Interface Sci.*, **1983**, *91*, 256-266.

[11] Emerson, M.F.; Holtzer, A. *J. Phys. Chem.*, **1967**, 71, 3320-3330.

[12] Magid, L. Solvent Effects on Amphiphilic Aggregation. In *Solution Chemistry of Surfactants;* Mittal, K., Ed.; Plenum Press: New York, 1979; Vol.1, pp.427-453.

[13] Almgren, M.; Swarup, S. *J. Phys. Chem.* **1985**, *89*, 4621-4626.

[14] Almgren, M.; Swarup, S. *J. Phys. Chem.* **1983**, *87*, 876-881.

[15] Walbroehl, Y; Jorgenson, J.W. *Anal. Chem.*, **1986**, *58*, 479-481.

[16] Nashabeh, W.; Greve, K.F.; Kirby, D.; Foret, F.; Karger, B.L.; Reifsnyder, D.H.; Builder, S.E. *Anal. Chem.* **1994**, *66*, 2148-2154.

[17] Ahuja, E.S.; Foley, J.P. *J. Chromatogr.* A **1994**, *680*, 73-83.

[18] Shi, Y.; Fritz, J.S. *J. High Resolut. Chromatogr.*, **1994**, *17*, 713-718.

[19] Shi, Y.; Fritz, J.S. *Anal. Chem.*, **1995**, 67, 3023-3027.

[20] Li, X.; Fritz, J.S. *Anal. Chem.* **1996**, 68, 4481-4488.

[21] Li, X.; Fritz, J.S. *J. Chromatogr.*A **1996**, *728*, 235-247.

[22] Ding, W.; Fritz, J.S. *Anal.Chem.* **1997**, *69*, 1593-1597.

[23] Palmer, C.P.; McNair, H.M. *J. Microcolumn Sep.* **1992**, *4*, 509-514.

[24] Palmer, C.P.; Khaled, M.Y.; McNair, H.M. *J. High Resolut. Chromatogr.* **1992**, *15*, 756-762.

[25] Palmer, C.P.; Terabe, S. *Anal. Chem.* **1997**, 69,1852-1860.

[26] Vindevogel, J.; Sandra, P. *Anal. Chem.* **1991**, *63*, 1530-1536.

[27] Seifar, R.M.; Kraak, J.C.; Kok, W.Th. *Anal. Chem.* **1997**, *69*, 2772- 2778.

[28] Bullock, J. *J. Chromatogr.* **1993**, *645*, 169-177.

[29] Schwer, C.; Kenndler, E. *Anal. Chem.*, **1991**, *63*, 1801-1807.

[30] Masselter, S.M.; Zemann, A.J. *Anal. Chem.*, **1995**, *67*,1047-1053.

[31] Reijenga, J.C.; Aben, G.V.A.; Verheggen, Th.P.E.M.; Everaerts, F.M. *J. Chromatogr.*, **1983,** *260*, 241-254.

[32] Sepaniak, M.J.; Burton, D.E.; Maskarinec, M.P. *American Chem. Soc.* Symp. Ser., **1987**, *342* (Ordered Media Chem. Sep.), 142-51.

[33] Almgren, M. Swarup, S. *Surfactants in Solution,* Mittal, K.L.; Lindman, B. Eds. Plenum Press: New York, 1984, 613-625.

[34] Gorse, J.; Balchunas, A.T.; Swaile, D.F.; Sepaniak, M.J. *J. High Resol. Chromatogr. & Chromatogr. Commun.*, **1988,** *11*, 554-559.

[35] Takeda, S.; Wakida, S.; Yamane, M.; Kawahara, A.; Higashi, K. *Anal. Chem.***1993**, *65*, 2489-2492.

[36] Burton, D.E.; Sepaniak, M.J. *J. Chromatogr. Science*, Nov. **1987**, vol.25.

[37] Weinberger, R. *Practical Capillary Electrophoresis,* Academic Press: San Diego, 1993; pp.27.

[38] Liu, Z.; Sam, P.; Sirimanne, S.R.; McClure, P.C.; Grainger, J.; Patterson, D.G. J. *Chromatogr.* A, **1994,** *673,* 125-132.

[39] Sepaniak, M.J.; Powell, A.C.; Swaile, D.F.; Cole, R.O. Fundamentals of Micellar Electrokinetic Capillary Chromatography. In *Capillary Electrophoresis, Theory and Practice*; Grossman, P.D.; Colbum, J.C., Eds.; Academic Press: New York,1992, pp 159-189.

[40] Yu, L.; Seals, T.H.; Davis, J.M. *Anal. Chem.* **1996,** *68*, 4270-4280.

[41] Kubota, Y.; Omura, N.; Murakami, K. *Bull. Chem. Soc. Japan,* **1991,** *64*, 814-820.

[42] Goto, A.; Endo, F. *J. Colloid Interface Sci.,* **1979,** *68*, 163-172.

[43] Miyashita, Y.; Hayano, S. *Bull. Chem. Soc. Japan,* **1981,** *54*, 3249-3252.

[44] James, A.D.; Robinson, B.H.; White, N.C. *J. Colloid Interface Sci.,* **1977,** *59*, 328-336.

[45] Robinson, B.H.; White, N.C.; Mateo, C. *Adv. Molec. Relaxn. Proc.,* **1975,** *7*, 321- 338.

[46] Rosen, M.J. *Surfactants and Interfacial Phenomena, 2nd ed.;* John Wiley: New York; 1989.

[47] Shinoda, K; Soda, T. *J. Phys. Chem.,* **1963,** *67*, 2072-2074.

[48] Melander, W.; Campbell, D.E.; Horvàth, C. *J. Chromatogr. 158,* 215-225.

[49] Chervet, J.P.; van Soest REJ, Ursem M. *J. Chromatogr.* **1991**, *543*, 439-449.

[50] Heiger D.N.; Sensitivity improvements in HPCE. Presented at HPCE'93, Orlando, FL, Feb.1993.

[51] Tsuda, T.; Sweedler, J.V.; Zare, R.N. Anal. Chem. **1990**, *8*, 34-39.

[52] Aebersold, R.; Morrison H.D. *J. Chromatogr.* **1990**, *516*, 79-88.

[53] Chien R.L.; Burgi D.S. *Anal. Chem.* **1992**, *64*, 489A-96A.

[54] Chien R.L.; Burgi D.S. *Anal. Chem.* **1992**, *64*, 1046.

[55] Schwer C.; Lottspeich, F. *J. Chromatogr.* **1992**, *623*, 345-355.

[56] Stegehius, D.S.; Irth, H.; Tjaden, U.R.; van der Greef, J. *J.Chromatogr.* **1992**, *538*, 393-402.

[57] Foret, F.; Sustacek, V.; Bocek, P. *J. Microcol Sep.* **1990**, *2*, 229-233.

[58] Swartz, M.E.; Merion, M. *J. Chromatogr.* **1993**, *632*, 209-213.

[59] Applied Biosystems 270A-HT Capillary Electrophoresis System User's manual, 1993, User Bulletin pp.7.

[60] Polyoxyethylene Castor Oil Derivatives. *Handbook of Pharmaceutical Excipients;* American Pharmaceutical Association / Pharmaceutical Society of Great Britain:Washington, D.C., London, 1986; pp. 221-224.

[61] Peereboom, D.M.; Donehower, R.C.; Eisnhauer, E.A.; McGuire, W.P.; Onetto, N.; Hubbard, J.L.; Piccart, M.; Gianni, L.; Rowinsky, E.K. J.Clin. Oncol. **1993**, *11*, 885-890.

IMAGE EVALUATION TEST TARGET (QA-3)

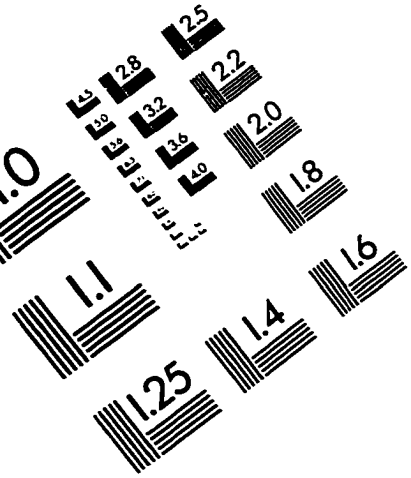

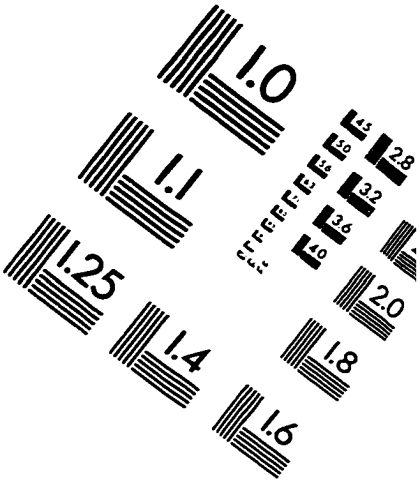

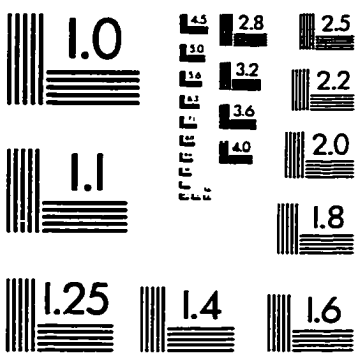

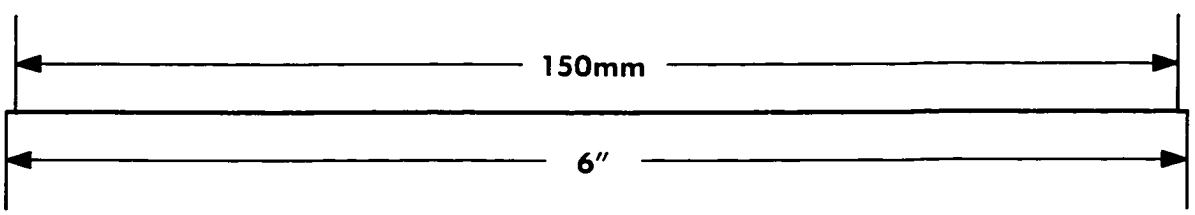

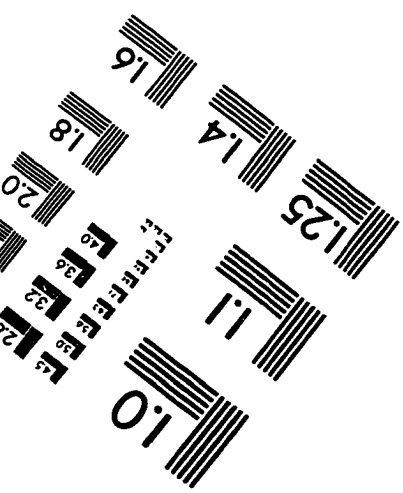

APPLIED IMAGE, Inc
1653 East Main Street
Rochester, NY 14609 USA
Phone: 716/482-0300
Fax: 716/288-5989